

# **Application of new measurement techniques and strategies to measure ammonia emissions from agricultural activities**

J. Mosquera<sup>1</sup>  
P. Hofschreuder<sup>1</sup>  
A. Hensen<sup>2</sup>

IMAG Rapport 2002-11  
December 2002  
€ 19,00

---

<sup>1</sup> IMAG

<sup>2</sup> ECN

## **CIP-GEGEVENS KONINKLIJK BIBLIOTHEEK, DEN HAAG**

Application of new measurement techniques and strategies to measure ammonia emissions from agricultural activities./J. Mosquera, P. Hofschreuder and A. Hensen -Wageningen: IMAG -(Rapport 2002-11/ Wageningen-UR, Instituut voor Milieu- en Agritechniek; 2002)

ISBN 90-5406-215-0

NUGI 849

Trefwoorden: new measurement techniques and strategies, ammonia, agriculture, field application of slurry, animal houses, passive flux samplers, Willems badges, denuders, NO<sub>x</sub> monitor, AMANDA, fast response ammonia sensor, gradient, flux frame, plume measurements, Gauss model

© 2002 IMAG, Postbus 43 - 6700 AA Wageningen

Telefoon 0317-476300

Telefax 0317-425670

Alle rechten voorbehouden. Niets uit deze uitgave mag worden verveelvoudigd, opgeslagen in een geautomatiseerd gegevensbestand, openbaar gemaakt, in enigerlei vorm of op enigerlei wijze, hetzij elektronisch, mechanisch, door fotokopieën, opnamen of enig andere manier zonder voorafgaande schriftelijke toestemming van het instituut.

All rights reserved. No part of this publication may be reproduced, stored in a retrieval system of any nature, or transmitted, in any form or by any means, electronic, mechanical, photocopying, recording or otherwise, without the prior permission of the institute.

## Abstract

**J. Mosquera, P. Hofschreuder and A. Hensen. Application of new measurement techniques and strategies to measure ammonia emissions from agricultural activities.**

Agriculture is the main contributor to the ammonia emissions in the Netherlands. In order to comply with the ammonia emission reduction assigned to the Netherlands, new techniques have been implemented to reduce the ammonia emissions from animal houses, and after application of slurry into the field. Fast and accurate measurements are necessary to get new estimates of the ammonia emission from each agricultural category. Keeping this objective in mind, new measurement techniques and strategies were developed and applied for different agricultural activities. This included ammonia emission after field application of manure, from naturally ventilated animal houses and from animal houses with forced ventilation. The different techniques and strategies are compared based on a reference method, and the results reported and discussed in detail. Limitations and future improvements for these techniques are also shown.

*Keywords: new measurement techniques and strategies, ammonia, agriculture, field application of slurry, animal houses, passive flux samplers, Willems badges, denuders, NO<sub>x</sub> monitor, AMANDA, fast response ammonia sensor, gradient, flux frame, plume measurements, Gauss model*



# Contents

Abstract	3
Contents	5
1 Introduction	7
2 Measurement techniques	13
2.1 Aerodynamic gradient method	14
2.2 Passive flux samplers in a gradient approach	15
2.3 Flux frame approach	17
2.4 Plume dispersion modelling	18
2.5 Passive flux samplers in or under a ventilation shaft (animal houses)	20
3 Measurement locations and general set-up	21
3.1 Ammonia emission after field application of slurry	21
3.1.1 Zegveld	21
3.1.2 Wageningen	26
3.2 Ammonia emission from animal houses	30
3.2.1 Kootwijkerbroek (mechanically ventilated animal house)	30
3.2.2 Barneveld (naturally ventilated poultry house)	32
4 Ammonia emissions after field application of manure	35
4.1 Zegveld	35
4.1.1 Meteorological parameters	35
4.1.2 Concentration measurements	37
4.1.3 Horizontal ammonia flux	43
4.1.4 Vertical ammonia flux	45
4.2 Wageningen	47
4.2.1 Meteorological parameters	47
4.2.2 Ammonia concentrations	49
4.2.3 Horizontal Ammonia Flux	57
4.2.4 Vertical Ammonia Flux	59
5 Ammonia emissions from animal houses	63
5.1 Kootwijkerbroek: mechanically ventilated animal house	63
5.2 Barneveld: naturally ventilated poultry house	67
6 Conclusions and recommendations	71
6.1 Ammonia emission after application of slurry into the field	71

6.2	Ammonia emission from mechanically ventilated animal houses	73
6.3	Ammonia emission from naturally ventilated animal houses	74
	References	75
	Summary	83
	Appendix A: aerodynamic gradient method	85
	Appendix B: denuders	91
	Appendix C: Willems badges	93
	Appendix D: chemiluminescence (NO <sub>x</sub> monitor)	97
	Appendix E: passive flux samplers	99
	Appendix F: AMANDA and fast sensor	107
	List of figures	109
	List of tables	113

# 1 Introduction

Ammonia ( $\text{NH}_3$ ) concentrations in air are generally far too low to cause acute toxic effects, except close to farms. However, in areas with intensive agricultural activities, deposition of ammonia and ammonium ( $\text{NH}_4^+$ ) can cause a wide range of long-term damage effects to ecosystems and to materials and monuments. In the soil  $\text{NH}_x$  (where  $\text{NH}_x = \text{NH}_3 + \text{NH}_4^+$ ) is produced during the microbiologic mineralisation of organic matter and supplemented by the deposition of  $\text{NH}_x$ . During this process, organic nitrogen is first transformed into (mainly)  $\text{NH}_4^+$ . This process is usually followed by oxidation to nitrate by other micro-organisms (nitrification), and therefore generally emissions into the atmosphere as ammonia resulting from this process are limited. However, in the metabolism of animals large amounts of  $\text{NH}_x$  are produced (mainly in the form of urea), because the food contains more nitrogen than is used by the animal for production of animal proteins (meat, milk). This is especially the case for livestock: about 81% of the nitrogen taken up by dairy cows is not used (Tamminga, 1992). The excess nitrogen is excreted mainly as urea, which after decomposition produces  $\text{NH}_4^+$ , which is emitted partly as  $\text{NH}_3$  to the atmosphere. As numbers of livestock have increased dramatically in the last century,  $\text{NH}_3$  emissions have risen accordingly (Sutton *et al.*, 1993).

Atmospheric  $\text{NH}_3$  readily reacts with atmospheric acids to form ammonium ( $\text{NH}_4^+$ ), which is an important constituent in aerosols and precipitation. Via its role as the most important base in the atmosphere,  $\text{NH}_3$  is therefore important in determining the level of atmospheric acidity (Allen *et al.*, 1988; Erisman *et al.*, 1988). Once emitted to the atmosphere, ammonia may be removed by dry and wet deposition or atmospheric reaction. After  $\text{NH}_x$  is deposited, it may cause soil acidification because of nitrification processes (van Breemen *et al.*, 1982), although this depends (Galloway, 1995) upon the biological and chemical status of the soil on which it is deposited, and upon the form of  $\text{NH}_x$ . In the Netherlands, with the greatest  $\text{NH}_3$  emission per  $\text{km}^2$  in Europe (Asman, 1995), 46% (Erisman and Bleeker, 1997) of the acidification of forest, heath lands and fresh water ecosystems is caused by the deposition of  $\text{NH}_3$ , mainly originating from agricultural activities (Heij and Schneider, 1995; Anonymous, 1996).

Furthermore, inputs of  $\text{NH}_x$  from the atmosphere may cause eutrophication, as well as nitrogen leaching (Binkley and Richter, 1987; van Breemen and van Dijk, 1988; Schulze *et al.*, 1989). Deposition of  $\text{NH}_3$  and its reaction product  $\text{NH}_4^+$  to nitrogen deficient terrestrial ecosystems represents a significant perturbation to ecosystem stability and biodiversity, causing replacement of slow growing plant species with fast growing grass species (van Dam *et al.*, 1986; Heil and Bruggink, 1987; Bobbink *et al.*, 1992). Nitrification of deposited ammonium enhances soil acidification. Deposition of  $\text{NH}_3$  and  $\text{NH}_4^+$  may also be involved in die-back of coniferous forest trees by causing severe nitrogen overload (van Dijk and Roelofs, 1988; Pearson and Stewart, 1993; Pérez-Soba *et al.*, 1994). Quantifying emission

and deposition fluxes of NH<sub>3</sub> between ecosystems and the atmosphere is essential to modelling of atmospheric ammonia pollution as well as of ecological effects of ammonia deposition.

In the Netherlands, approximately 94% of the Dutch ammonia emissions (157 kton in the year 2000) originate from agricultural activities (RIVM and CBS, 2001). Livestock buildings, and application of manure/slurry into the field, are the most important sources of ammonia emissions from agriculture (table 1.1). In the past, field application of manure/fertilizer was the most important source of ammonia emissions. However, the introduction of new application techniques, aimed to reduce the ammonia emission after manure application into the field, has increased relatively the contribution of emissions from animal houses. The aim of the Dutch government is to reduce in 2010 the total ammonia emission to approximately 70% (100 kton) compared with the year 2000 (Sliggers, 2001). Besides, the contribution from Dutch agriculture to the total ammonia emission should be reduced to 86% (86 kton) in 2010.

**Table 1.1** NH<sub>3</sub> emissions from animal husbandry in the Netherlands in the year 2000, expressed in % (Sliggers, 2001).

Animal houses	46
Manure/slurry application	41
Grazing	9
Storage outside housing	3

Ammonia emissions from animal houses (46% of total ammonia emissions from agriculture in 1997) are an important environmental issue in the Netherlands. The Dutch government uses ammonia emission factors as one of the tools to calculate ammonia emission and deposition, and to use this information to design ways to control agricultural ammonia emission. The most important emission factors are ammonia emissions of animal housing system categorised by species (Van der Hoek, 1994). When possible these factors are determined by measuring the ammonia emissions from a specific animal housing system (<http://www.stalemissies.nl>). Emissions are continuously measured over several months during winter and summer periods. Costs of these measurements on equipment, maintenance and labour are high. Due to these high costs the number of animal houses measured is relatively small. During campaigns to measure emissions from animal houses, it became clear that management is an important factor in determining the emission level. Differences between animal houses of the same type and kind of animal may differ more, than the variation in time and season within one animal house. These management related differences in emission factors point at the need to measure more animal houses during a shorter period. This stresses the need for development of flexible methods to be used in short term measurements, which allows monitoring the ammonia emission from a larger number of animal buildings per year. Ammonia emissions from animal houses depend on many factors, including:

- The species, age and weight of the animal.
- The housing system of the animal, including storage of the wastes inside the building.
- Indoor temperature will modify other parameters (ventilation rate, air speed) and animal behaviour (soiled animals, higher water consumption, less meat production, variation in the food intake, variation in the food conversion ratio), which influence ammonia emissions.
- The nitrogen content of the food and the relative share of different amino acids.
- The conversion of nitrogen in food to nitrogen in meat, milk and eggs, and hence the amount of nitrogen in the animal wastes.

Ammonia gas ( $\text{NH}_3$ ) is often emitted into the atmosphere following the surface application of nitrogenous fertilizers and various ammoniacal wastes to soil (Black *et al.*, 1989; Brunke *et al.*, 1988; Hoff *et al.*, 1981; Schimel *et al.*, 1986; Vertregt and Rutgers, 1988). A high proportion of the total emission occurs during the first few hours after spreading, although emission may continue for over 15 days. This leads to a number of different environmental problems, both on local, regional and global scales. Ammonia can be re-deposited nearby, or can react with acidic gases to form ammonium salts that may be transported over long distances. This not only represents a significant loss of nitrogen from animal production systems but can also have severe effects on natural and semi-natural ecosystems. Emission after manure spreading depends on:

- Meteorological/climatological conditions. The emission generally increases with temperature and turbulence, but decreases with air humidity and during precipitation periods.
- Amount applied per ha. The fraction of N in manure that evaporates increases with the amount applied per ha.
- The way of applying the manure. If the manure is injected in the ground a much lower emission results, compared to surface application.
- Properties of the manure. The emission generally increases with pH, viscosity and content of dry matter. A high viscosity prevents the manure or fertilizer from entering the soil.
- Properties of the soil. The emission generally increases with pH, calcium content and porosity, but decreases with buffer capacity and water content.
- Time between spreading and soil tillage (e.g. ploughing for arable land). The emission is generally most pronounced during the first hours after spreading.

Grazed pastures can contribute to the emissions not only by animal wastes deposited of during grazing, but also via application to the land of wastes excreted in the animal houses and via fertiliser application. In this way, they can be important sources of ammonia in periods during and after these treatments. When animals are in the house, volatilisation of ammonia to the atmosphere is the only loss process. If the animals are grazing in the meadows, the manure is not stored, but is deposited directly. After deposition it is immediately exposed to other loss processes than volatilisation of  $\text{NH}_3$  to the atmosphere (i.e. leaching). For that reason, the emission to the atmosphere during the grazing is less than that during the period in the animal house (including losses due to storage and spreading).

Another important point to be considered is the new situation where animals are not confined all the time in the buildings, but have access to walking areas outside the barns (i.e. for pigs and poultry). This new complex situation is especially important for organic farming systems, which has not been so far studied in detail.

With increasing concern about the potential environmental damage caused by atmospheric transport and subsequent deposition of  $\text{NH}_3$ , it is important to have reliable measurements of emission sources both for development and evaluation of potential abatement strategies and compiling national emission inventories. Estimates of surface emissions (grazing animals, manure spreading), as well as emissions from naturally ventilated buildings, are not so simple to obtain as in mechanically ventilated buildings. In the last case, ammonia emission estimates can be obtained by measuring the ventilation rate and the ammonia concentrations at the outlets of the building. For surface emissions, various strategies and techniques have been developed and described in detail in van Ouwerkerk (1993), Mosquera *et al.* (2002) and Hofschreuder (2002). The flux of  $\text{NH}_3$  from naturally ventilated animal houses is difficult to determine, as the ventilation rate (the number of air mass exchanges per unit time) varies according to temperature, wind speed, building design, orientation to the wind and animal occupancy. Estimating emissions from waste stores also presents considerable difficulties: stores are covered by a lid or tent, as forced by regulations in the Netherlands. The natural ventilation rate is therefore low and mixing within the air space of the tank is bad. Moreover gas production by bacteria contributes significantly to the ventilation of the tank. When we consider a farm as one ensemble of emission sources, which turns even more complex when walking areas outside the animal houses are present, there is no physical border to the emission source from which measurements or samples can be taken. For walking areas outside barns, new methods and strategies should be developed and tested for future measurements.

The overall aim of this study is to investigate and compare new methods for estimating the emission of ammonia in agricultural applications (emissions after field application of manure, emissions from animal houses). The basis for the selection of available methods is supplied by van Ouwerkerk (1993), Mosquera *et al.* (2002) and Hofschreuder (2002). To

calibrate the suitability of the selected methods in terms of accuracy, costs, ease of use in the field, and capability for short- or long-term purposes, a reference method is used. The following techniques and strategies are selected:

1. Gradient technique.
  - Denuders (concentration measurements).
  - Willems badges (concentration measurements).
  - NH<sub>3</sub> to NO converters and a NO<sub>x</sub>-chemiluminescent monitor (concentration measurements).
  - Passive flux samplers (flux measurements).
2. Passive flux samplers attached to a wind vane (flux measurements).
3. Flux frame method/Plume measurements.
  - Denuders (concentration measurements).
  - Willems badges (concentration measurements).
  - Passive flux samplers (flux measurements).
4. Passive flux samplers in a ventilation shaft (flux measurements).
5. Plume measurements.
  - NH<sub>3</sub> fast sensor (ECN) + AMANDA (ECN) (concentration measurements).

In chapter 2, the measurement locations and set-up used in this study, are described in detail. Chapter 3 gives an overview of the measurement techniques and strategies to be used. For further details over a specific technique, the reader is addressed to a particular appendix at the end of the report. Chapter 4 presents the main results of the measurements performed in two locations to determine the ammonia emission after field application of slurry. This includes not only information of the emission estimates, but also a comparison of the different techniques used in each experiment. In chapter 5, results on ammonia emissions from animal houses (mechanically and naturally ventilated animal houses) are reported, and the different measurement techniques compared. In chapter 6, the main conclusions and recommendations from this report are summarised.

The Ministerie van Landbouw, Visserij en Natuurbeheer (LNV) is acknowledged for making this study possible in the framework of programme 309.



## 2 Measurement techniques

Surface exchange of  $\text{NH}_3$  can be quantified by micrometeorological measurements using the *aerodynamic gradient* or the *mass balance method* (Denmead, 1983). The latter is suitable for measuring  $\text{NH}_3$  emissions from small plots, to which experimental treatments resulting in high  $\text{NH}_3$  concentrations and high  $\text{NH}_3$  emissions relative to the surroundings have been applied. The *mass balance* for small plots suffers from some disadvantages. The application of manure in a small round plot may differ from large-scale manure application. The total emissions of the plot are relatively low, making them very soon indistinguishable from background concentrations. Besides, the tail of the decreasing emissions with time is not measurable. For measurements of emissions on field scale, the aerodynamic method is preferred. The *aerodynamic method* is based on frequent and precise measurements of the gradients of  $\text{NH}_3$  concentration, wind speed and temperature over the exchange surface. The method requires large homogeneous surfaces, so that the air flowing over them is in equilibrium with the surface up to a given height above the ground. The principles of the *micrometeorological gradient* approach are best suited for short sampling periods (1 to 2 h) in which large changes in  $\text{NH}_3$  concentrations and wind direction and velocity are not likely. When *gradient* or *mass balance* measurements are performed with continuous monitors, expensive instrumentation and a large labour force are needed, limiting the number of places and the time scale over which the method can be operated. The *flux frame* method can also be used to determine the ammonia emission from surface sources. In this method, the horizontal flux of ammonia through a vertical plane perpendicular to the wind direction upwind and downwind of the source is measured. Another approach is to estimate emissions on the basis of a dispersion model (e.g. the *Gaussian plume model*).

To determine the ammonia emission from an animal house it is necessary to establish the dynamics with time of the emission. The surface under the emission curve will determine the ammonia emission from the animal house. Two possible approaches can be considered:

- a) At regular time intervals, both the ventilation rate and the ammonia concentration in the outgoing air are determined. The emission calculated in this way gives an average value for that particular time interval. From these average emission values, an average emission for the animal building can be obtained. To have reliable results, short time intervals should be considered.
- b) From the air leaving the animal house through the ventilation shafts a proportional sample is taken. The amount of ammonia trapped in the sampler, together with the sampling time and a proportional constant factor (specific for the sampler), can be used to determine the ammonia emission from the animal house.

The current technique to measure ammonia emissions from mechanically ventilated animal houses is based in the approach a). Because the frequency of measurements of ammonia concentrations and ventilation rates is high, the results obtained following this approach are usually precise and reliable. One advantage of using this method is that it is possible to follow the emission processes. One example for this kind of approach is the use of a NH<sub>3</sub> to NO converter and a NO<sub>x</sub> analyser to measure ammonia concentrations, and a ventilator in the shaft to estimate the ventilation rate (Groenestein, 1993; Groenestein *et al.*, 2001; Scholtens, 1993; Phillips *et al.*, 1998a; Groot Koerkamp *et al.*, 1998; Demmers *et al.*, 1999).

For the second approach, one alternative to determine the NH<sub>3</sub> emission from a mechanically ventilated animal house is to use passive flux samplers under the ventilators in the shafts, and to multiply the measured fluxes with the surface area of the ventilation shaft (Michorius and Scholtens, 1995; Monteny *et al.*, 1999). The flux frame method, provided with a number of anemometers and passive (Willems badges, passive flux samplers) or active (denuders) sampling techniques, could be used to measure the ammonia emission from naturally ventilated animal houses (Hofschreuder, 2002).

In this chapter, the measurement techniques and strategies used during this study are discussed. When necessary, more detailed information is provided as an extra annex at the end of this report. The basis for the selected techniques can be found in Ouwerkerk (1993), Mosquera *et al.* (2002) and Hofschreuder (2002).

## 2.1 Aerodynamic gradient method

This technique requires measurement of NH<sub>3</sub> concentration  $c$ , wind speed  $u$  and temperature  $T$  at several heights (appendix A). Ammonia concentration can be measured directly using impingers, denuders (appendix B), Willems badges (appendix C), or after conversion to NO, and detection using a NO<sub>x</sub> monitor (appendix D). The friction velocity  $u_*$  (m s<sup>-1</sup>), can be determined by rearranging the logarithmic wind speed profile given as:

$$u(z) = \frac{u_*}{k} \cdot \left[ \ln\left(\frac{z-d}{z_0}\right) - \psi_m\left(\frac{z-d}{L}\right) + \psi_m\left(\frac{z_0}{L}\right) \right] \quad (2.1)$$

where  $u(z)$  is the wind speed (m s<sup>-1</sup>) at the measurement height  $z$ ,  $k$  the von Karman's constant (0.41),  $d$  the displacement height (m),  $z_0$  the surface roughness (m), and  $\psi_m$  a profile correction for stability, which is a function of the Monin-Obukhov stability length ( $L$ ). Similarly,

$$c(z) = \frac{c_*}{k} \cdot \left[ \ln\left(\frac{z-d}{z_0}\right) - \psi_h\left(\frac{z-d}{L}\right) + \psi_h\left(\frac{z_0}{L}\right) \right] \quad (2.2)$$

where  $c_*$  is the turbulent concentration scale ( $\mu\text{g}\cdot\text{m}^{-3}$ ). Regressing  $u$  and  $c(z)$  against the logarithmic profile yields the slope and therefore  $u_*$  and  $c_*$ . The flux of  $\text{NH}_3$  is equal to the product of  $u_*$  and  $c_*$ :

$$F = u_* \cdot c_* \quad (2.3)$$

## 2.2 Passive flux samplers in a gradient approach

The passive flux samplers collect ammonia in an amount that is proportional to the product of the ammonia concentration and the wind speed passing through the sampler. Three different configurations have been used: a) conventional design (appendix E), fixed into the measurement mast; b) conventional design, attached to a windvane; c) cross design (figure 2.1), fixed into a measurement mast.

For the cross design, the horizontal mean flux can be calculated as (Schjoerring, 1995):

$$F_a(z) = \frac{\sum_{i=1}^{i=4} M_i}{\pi \cdot r^2 \cdot K_s \cdot K_2 \cdot \Delta t} \quad (2.4)$$

where  $z$ (m) is the height above the ground surface,  $M_i$  ( $\mu\text{g}$ ) the amount of ammonia in one of the 4 tubes,  $r$  (m) the radius of the orifice of the stainless-steel disc (0.5 mm),  $\Delta t$  (s) the duration of the measurement period,  $K_s$  a factor correcting for reduced air velocity within the sampler due to turbulence created by the stainless steel disk (appendix E), and  $K_2$  a correction factor taking into account the fact that when the wind direction is not along the axis of a passive flux sampler, the average horizontal flux will be over-estimated because  $\text{NH}_3$  is collected simultaneously in two sampler units. Wind direction information is therefore essential for a correct analysis of the results of the passive samplers in these situations.

During periods with constant wind direction,  $K_2$  can be calculated as (Schjoerring, 1995):

$$K_2 = \cos \alpha + \sin \alpha \quad (2.5)$$

where  $\alpha$  denotes the angular deviation from the axis of a sampler. Therefore maximum and minimum values of  $K_2$  are 1.41 and 1, respectively, for periods with constant wind direction. The mean value of  $K_2$  during periods with changing wind direction is calculated according to (Schjoerring, 1995):

$$\overline{K_2} = \frac{[\sin \alpha]_{\alpha_1}^{\alpha_2} - [\cos \alpha]_{\alpha_1}^{\alpha_2}}{\alpha_2 - \alpha_1} \quad (2.6)$$

When  $\alpha$  varies between 0 and  $\pi/2$ ,  $K_2$  is 1.27 ( $4/\pi$ ), as is also the case when  $\alpha$  varies between 0 and  $\pi$ , between  $\pi/2$  and  $3\pi/4$ , or between 0 and  $2\pi$ .

The following expression has been suggested for the calculation of the horizontal flux using the fixed (cross) design:

$$F_a(z) = \frac{\sum_{i=1}^m M_i}{\pi \cdot r^2 \cdot K_s \cdot \Delta t} \cdot \frac{\bar{u}}{\frac{\sum_{j=1}^n u_j \cdot (\cos \alpha_j + \sin \alpha_j)}{n}} \quad (2.7)$$

where  $M_i$  is the amount of ammonia collected in the tubes facing the wind direction, and  $\alpha_j$  the angle between the axis of a sampler and the wind direction for a particular time interval  $j$  (figure 2.1).

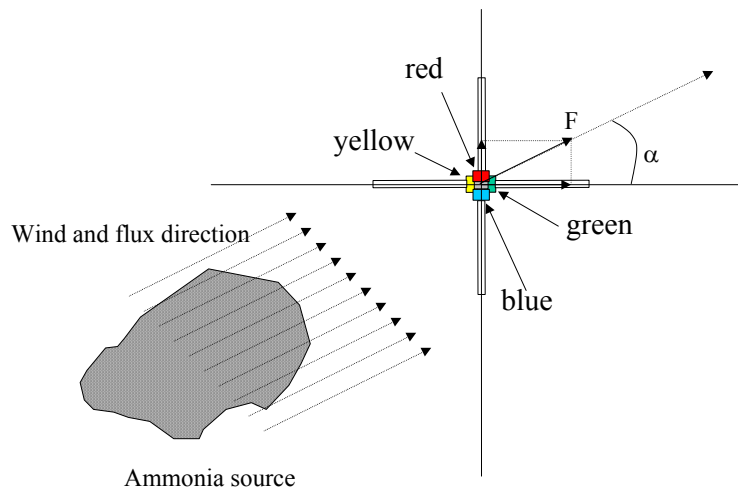


**Figure 2.1** Schematic drawing of a sample arrangement (fixed PFS, cross design) for non point source measurements.

For the conventional design, the horizontal mean flux can be calculated as:

$$F_a(z) = \frac{M}{\pi \cdot r^2 \cdot K_s \cdot \Delta t} \quad (2.8)$$

where  $M(\mu\text{g})$  is the amount of ammonia collected in the tube facing the wind direction.

As in the aerodynamic approach, the slopes of the regression of  $u$  and  $c_a$  against  $\ln(z-d)$  are used to determine  $F_a$ . For this regression,  $c_a$  is determined at each height by dividing the calculated horizontal flux (the amount of  $\text{NH}_3$  collected by the passive sampler divided by the effective area and time) by the wind speed at that level:

$$c_a(z) = \frac{F_a(z)}{u(z)} \quad (2.9)$$

The concentration is wind-weighted because the measurement of horizontal fluxes gives more weight to ammonia concentrations during period of high fluxes (high wind speeds) than at period of low fluxes (low wind speeds). As a consequence, the wind-weighted concentration will differ from the true time-weighted concentration. The estimated vertical flux is expected to differ from the true flux for several reasons: (i) no stability correction is applied, (ii) wind-weighted concentrations are used instead of time-weighted, and (iii) averaging rules due to changing concentrations and wind velocities are neglected. The theory involved in the use of passive flux samplers is described in appendix E.

### 2.3 Flux frame approach

In the flux frame method, the horizontal flux of ammonia through a vertical plane perpendicular to the wind direction upwind of a source (e.g. field, silo, animal houses) is compared with the flux through a vertical plane on the downwind side of the source. The difference between the two gives the net emission from the source. The flux frame method has been applied to determine the ammonia emission from livestock buildings (Michorius *et al.*, 1995) and manure stores (Phillips *et al.*, 1997), and in principle is also suitable for complex sources such as close combinations of livestock buildings and manure stores. The source strength can be determined as:

$$Q = \sum \left( z \cdot \sum d \cdot \bar{u} \cdot (C_{down} - C_{up}) \right) \quad (2.10)$$

where: Q = source strength ( $\mu\text{g}\cdot\text{s}^{-1}$ )  
 $\bar{u}$  = average horizontal wind speed ( $\text{m}\cdot\text{s}^{-1}$ )  
 $C_{up}$  = average concentration on the upwind side ( $\mu\text{g}\cdot\text{m}^{-3}$ )  
 $C_{down}$  = average concentration on the downwind side ( $\mu\text{g}\cdot\text{m}^{-3}$ )  
z = height of the plane for which the measured concentration was representative (m)  
d = distance between two adjacent masts (m)

The procedure is as follows. First the average concentration on the upwind side is subtracted from the average concentrations on the downwind side, and the result is multiplied by the average wind speed. For each height the result of this calculation is multiplied by the distance between two adjacent masts and summed. This summation, which reflects the contribution of the source to the horizontal flux per unit of height ( $\mu\text{g m}^{-2} \text{s}^{-1}$ ), is then multiplied again by the height where the calculated flux is representative.

To use the flux frame method, the following conditions must be satisfied:

- The whole of the plume must pass through the flux frame.

- The flow through the flux frame must suffer minimum interference from obstacles.
- The upwind and downwind fluxes should be measured simultaneously.
- The correct weather conditions should prevail during measurement (suitable wind speed and direction, appropriate stability class and no rain).
- The concentration and wind speed measurements must be sufficiently accurate to reflect the difference between the emission flux on the upwind and downwind sides. The emission flux on the upwind side should preferably be as low and uniform as possible.

The flux frame method present the following limitations:

- When measuring close to an animal house, building effects are important, disturbing the flow pattern between the house and the measuring equipment. This makes it difficult to interpret the measured data.
- Far from the source, a high measuring mast is necessary to be able to capture the whole plume.
- The large number of measurements to be performed.

## 2.4 Plume dispersion modelling

An empirical plume dispersion model can be used, together with measurements of downwind ammonia concentrations, to deduce the strength of the ammonia source. This is the so-called *inverse modelling* approach. In principle, it is sufficient to make measurements at one location, preferably near the centreline of the plume, but there is an advantage in using multiple measurements, because this makes it easier to determine the width of the plume. When determining the vertical dispersion parameter  $\sigma_z$ , a number of measuring points may be positioned on the plume axis at different heights. The background concentration may be determined upwind by direct measurements, or downwind by extending the measuring points until they reach the edges of the plume where the concentration is equal to the background concentration.

The Gaussian plume model is the most common air pollution model. It has been used extensively in the atmospheric sciences to predict atmospheric diffusion (Pasquill, 1971; Ludwig *et al.*, 1977; Pasquill and Smith, 1983; Gryning *et al.*, 1987; Zannetti, 1990; Turner, 1994; Sharan *et al.*, 1995) as well as in agricultural engineering for odour emission problems. The model assumes a Gaussian concentration distribution in horizontal and in the vertical directions downwind from a source. The concentrations are symmetrical about one plume axis and the shape of the concentration curve is the same as that of the normal or Gaussian

distribution. The Gaussian Plume approach calculates the contribution of a plume from a single source to a certain receptor point using:

$$C(x, y, z) = \frac{Q}{2\pi \cdot \sigma_y \cdot \sigma_z} \cdot e^{-y^2/(2\sigma_y)^2} \cdot \left( e^{-(z-H)^2/(2\sigma_z)^2} + e^{-(z+H)^2/(2\sigma_z)^2} \right) \quad (2.11)$$

$$\sigma_y = A \cdot x^B \cdot z_0^{0.2} \cdot T^{0.35}$$

$$\text{where} \quad \sigma_z = C \cdot x^D \cdot (10 \cdot z_0)^{0.53 \cdot E} \quad (2.12)$$

$$E = x^{-0.22}$$

In this equations,  $C(x, y, z)$  is the downwind air concentration due to a continuous source of constant strength  $Q$  (mass per unit time) located at the point  $(0, 0, H)$ , where  $H$  is the height of the emission source (animal house, surface) in meters. The coordinates  $x, y, z$  are oriented, respectively, in the direction of the mean wind  $u$  ( $\text{m}\cdot\text{s}^{-1}$ ), horizontal and normal to  $u$ , and vertical and normal to  $u$ , respectively. The diffusion parameters  $\sigma_y$  and  $\sigma_z$  are the standard deviation of the lateral and vertical concentration distribution (m), and depend on distance to the source, on the degree of turbulence of the atmosphere, the roughness length of the surface  $z_0$ , and on the timescale used for averaging ( $T$ ).  $A, B, C$  and  $D$  are dependent on the stability classes (Pasquill, 1974). The downwind ( $x$ ) and crosswind ( $y$ ) distances are given by:

$$\begin{aligned} x &= -(X(R) - X(S)) \cdot \sin(WD) - (Y(R) - Y(S)) \cdot \cos(WD) \\ y &= (X(R) - X(S)) \cdot \cos(WD) - (Y(R) - Y(S)) \cdot \sin(WD) \end{aligned} \quad (2.13)$$

where  $(X(R), Y(R))$  and  $(X(S), Y(S))$  are the receptor and source coordinates, respectively, and  $WD$  is the measured wind direction. The assumptions underlying the use of the Gaussian plume model are:

- Turbulence is uniform and stationary, i.e. not dependent on time and place.
- The plume is fully reflected onto the ground.
- There is no reduction in or addition to substances through chemical reaction or physical processes.
- The average wind speed is representative for the whole layer where diffusion occurs.
- The wind direction is the same at all levels.
- Dispersion coefficients  $\sigma_y$  and  $\sigma_z$  are not dependent on height.
- The source strength is constant.

The limitations of the Gaussian plume model are:

- The model may only be used for downwind distances for which  $\sigma_y$  and  $\sigma_z$  have been determined experimentally. Extrapolation of values of  $\sigma_y$  and  $\sigma_z$  for distances  $< 100$  m gives only a concentration trend.
- Situations where the wind speed is less than  $1 \text{ m}\cdot\text{s}^{-1}$  cannot be described by the model because the turbulent diffusion in the x direction can no longer be ignored.
- Dispersion coefficients are influenced by buildings.
- Uneven terrain changes the transport of pollution, which is assumed to be strictly horizontal.
- sampling time must be longer than 30 minutes to 1.5 hours to allow the random dispersion characteristics to reach an average Gaussian distribution.

## 2.5 Passive flux samplers in or under a ventilation shaft (animal houses)

The use of passive flux samplers (appendix E) in or under a ventilation shaft of a mechanically ventilated building to measure gaseous ammonia emissions is straightforward because  $\cos(\alpha)=1$ . However, obstructions in the ventilation shaft such as ventilators and valves might disturb the airflow around the sampler, thus leading to erroneous results. Due to the high ammonia flux density in ventilation shafts high acid loads in the absorption chambers are needed, to prevent saturation of the sampler. Acid coated tubular sheaths of glass fibre filter papers were placed inside the chambers of the sampler, which increases the ammonia binding capacity.

## 3 Measurement locations and general set-up

### 3.1 Ammonia emission after field application of slurry

#### 3.1.1 Zegveld

Measurements were performed during the period 3-7 April 2002 near the village of Zegveld about 30 km south of Amsterdam (the Netherlands). The location is part of a region of flat, humid polder land with peat soil. The measurement site was located on the pasture at the experimental husbandry station at Zegveld (ROC-Zegveld, figure 3.1), in an area of intensive livestock breeding (mainly dairy cattle farming). The soil at the experimental station is classified as peat with a high (-0.30 m) to intermediate (-0.70 m) ground water table. Three fields (12-14) of 1.6, 1.6 and 1.34 ha were assigned to the experiment. Slurry accumulated beneath the slatted floor of the farm building housing dairy cattle was applied into the fields on 3 April 2002, and the measurement period lasted for 4 days. Analyses of representative samples for the different fields used in the experiment are presented in table 3.1, and the application rates in table 3.2.

In the present experiments in Zegveld, the performance of different methods for measuring ammonia emission following slurry application to land was investigated and the results compared. The experimental set-up (figure 3.2) includes the following methods:

1. Gradient technique
  - Denuders (concentration measurements, figure 3.3; reference method).
  - Willems badges (concentration measurements, figure 3.3).
  - $\text{NH}_3$  to  $\text{NO}$  converter and a  $\text{NO}_x$ -chemiluminescent monitor (concentration measurements, figure 3.4).
  - Passive flux samplers fixed in a tower at different heights (horizontal flux measurements, figure 3.4).
2. Passive flux samplers attached to a wind vane (horizontal flux measurements, figure 3.5).



Figure 3.1 Experimental station at Zegveld.

**Table 3.1** Slurry analyses (Zegveld).

Field 12	ANALYSIS 1	ANALYSIS 2
	(kg/ ton product)	(kg/ ton product)
Dry matter	58.3	58.3
Ash residuals	14.1	14.1
Organic matter	44.2	44.2
Ammonium-N	1.6	1.6
Organic-N	1.5	1.5
Total N	3.1	3.1
Phosphate (P <sub>2</sub> O <sub>5</sub> )	1.1	1.1
Potassium (K <sub>2</sub> O)	5.3	5.2
C/N ratio	7.0	7.1

Field 13	ANALYSIS 1	ANALYSIS 2
	(kg/ ton product)	(kg/ ton product)
Dry matter	58.6	58.0
Ammonium-N	1.66	1.68
Total N	3.40	3.33
Total P	0.465	0.466

Field 14	ANALYSIS 1	ANALYSIS 2
	(kg/ ton product)	(kg/ ton product)
Dry matter	59.3	58.3
Ash residuals	14.1	14.1
Organic matter	45.2	44.2
Ammonium-N	1.7	1.7
Organic-N	1.5	1.4
Total N	3.2	3.1
Phosphate (P <sub>2</sub> O <sub>5</sub> )	1.1	1.2
Potassium (K <sub>2</sub> O)	5.2	5.2
C/N ratio	7.0	7.1

**Table 3.2** Application rates of cattle slurry to grassland (Zegveld).

Field	Slurry applied (m <sup>3</sup> )	Surface (ha)	Application rate (m <sup>3</sup> .ha <sup>-1</sup> )
12	25.6	1.6	16.00
13	32.0	1.6	20.00
14	23.9	1.34	17.84



**Figure 3.2** Experimental set-up for ammonia concentration/flux measurements (Zegveld).  
A) Left tower: passive flux samplers attached to the wind vane. Right tower: denuders, Willems badges, passive flux samplers (cross), and sample line connected to the  $\text{NH}_3$  to  $\text{NO}$  converter+ $\text{NO}_x$  monitor system. Measurements in the right tower were performed at three heights: 0.5, 1 and 2 m.  
B) Background measurements (10 m height) for the different techniques and meteorological data.

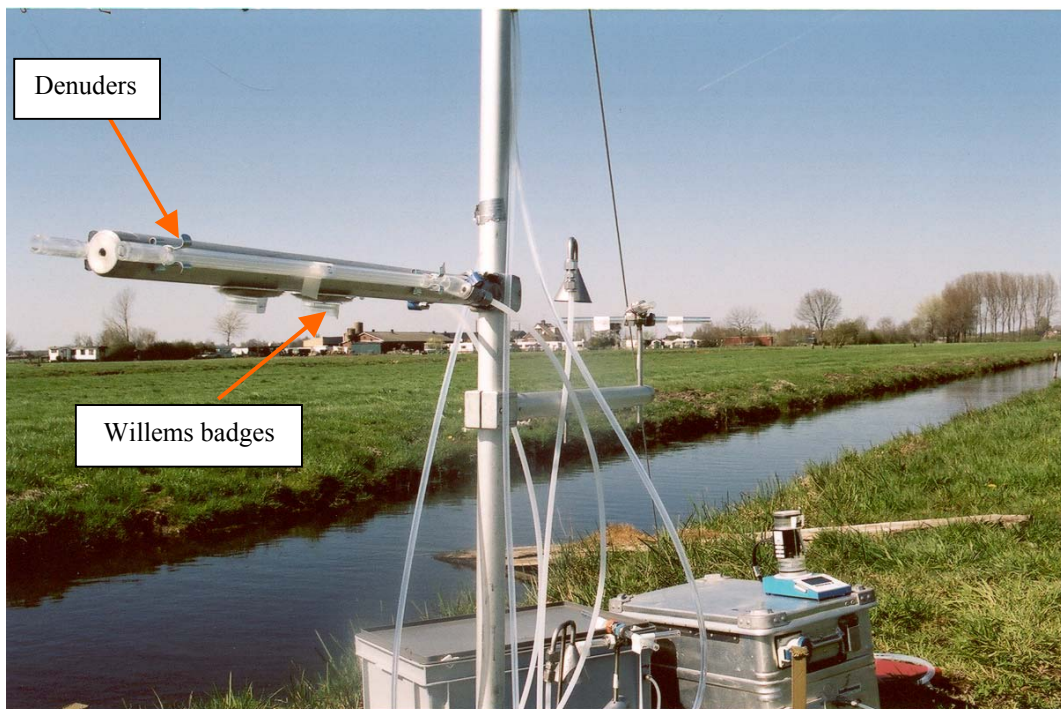


**Figure 3.3** Experimental set-up in Zegveld: denuders and Willem's badges in the right tower.

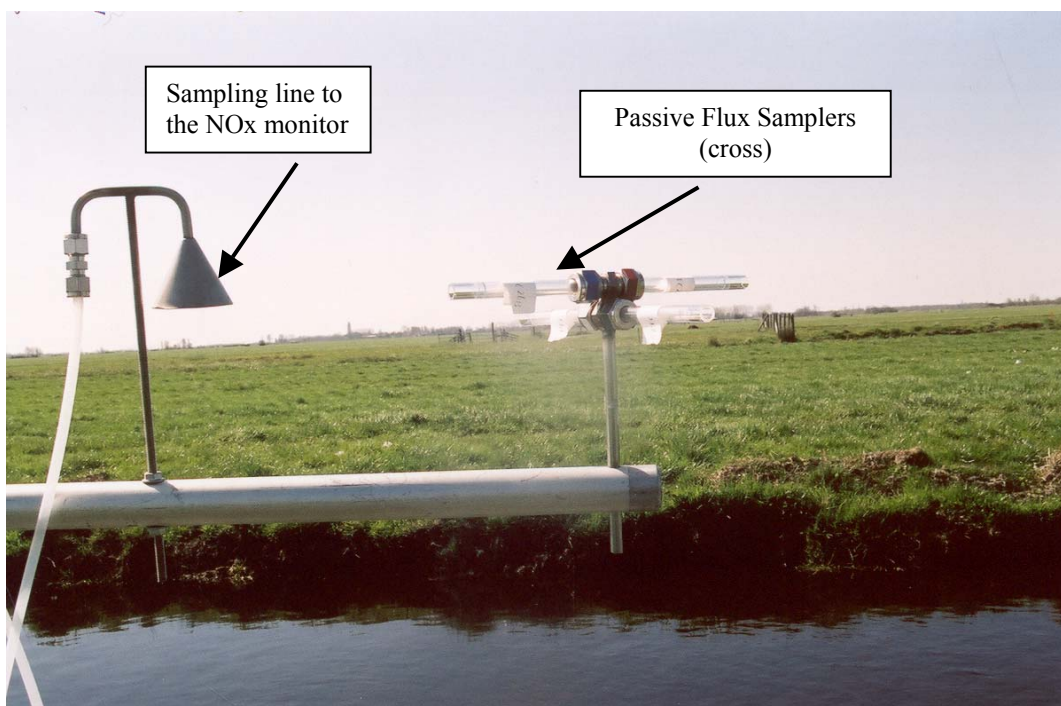


**Figure 3.4** Experimental set-up in Zegveld: ammonia passive flux samplers (cross), and sample line going to the  $\text{NH}_3$  to  $\text{NO}_x$  converter +  $\text{NO}_x$  monitor system, in the right tower.

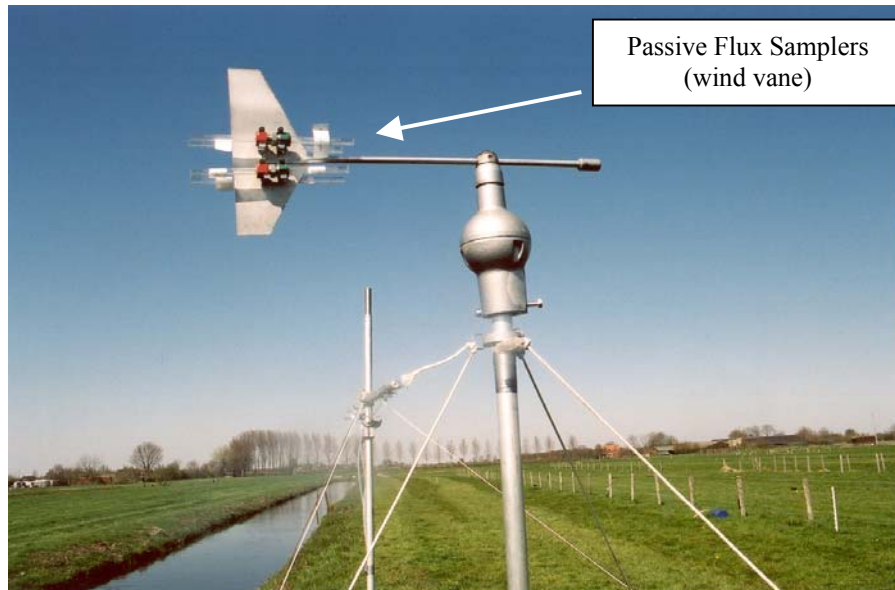


**Figure 3.5** Experimental set-up in Zegveld: ammonia passive flux samplers attached to the wind vane in the left tower.

Denuders, Willems badges and passive flux samplers were changed after pre-determined periods of 1.5, 3, 6, 24 and 48 hours after slurry application and were finally removed at 96 hours, to determine the cumulative losses and rates of loss of ammonia. Ammonia concentrations from the denuders, Willems badges and passive flux samplers were determined using photometry, and were performed at the environmental laboratory of IMAG.

### 3.1.2 Wageningen

A second experiment was performed at the experimental facility at Ossekampen (figure 3.6), northwest from Wageningen (the Netherlands). The measurement site is completely surrounded by meadows, and it is mostly free from obstacles. Two fields (9B and 37B) of approximately 4 ha (in total) were used in this experiment. Slurry from the farm was applied into the fields on September 5, and the measurement period lasted for 4 days. Table 3.3 shows the results of the analysis performed for representative samples of the manure applied to the field. Also included in table 3.3 is the manure application rates used in the experiment. For meteorological information, the data from the meteorological station located south of field 15 (called “meteo veld”) was used.

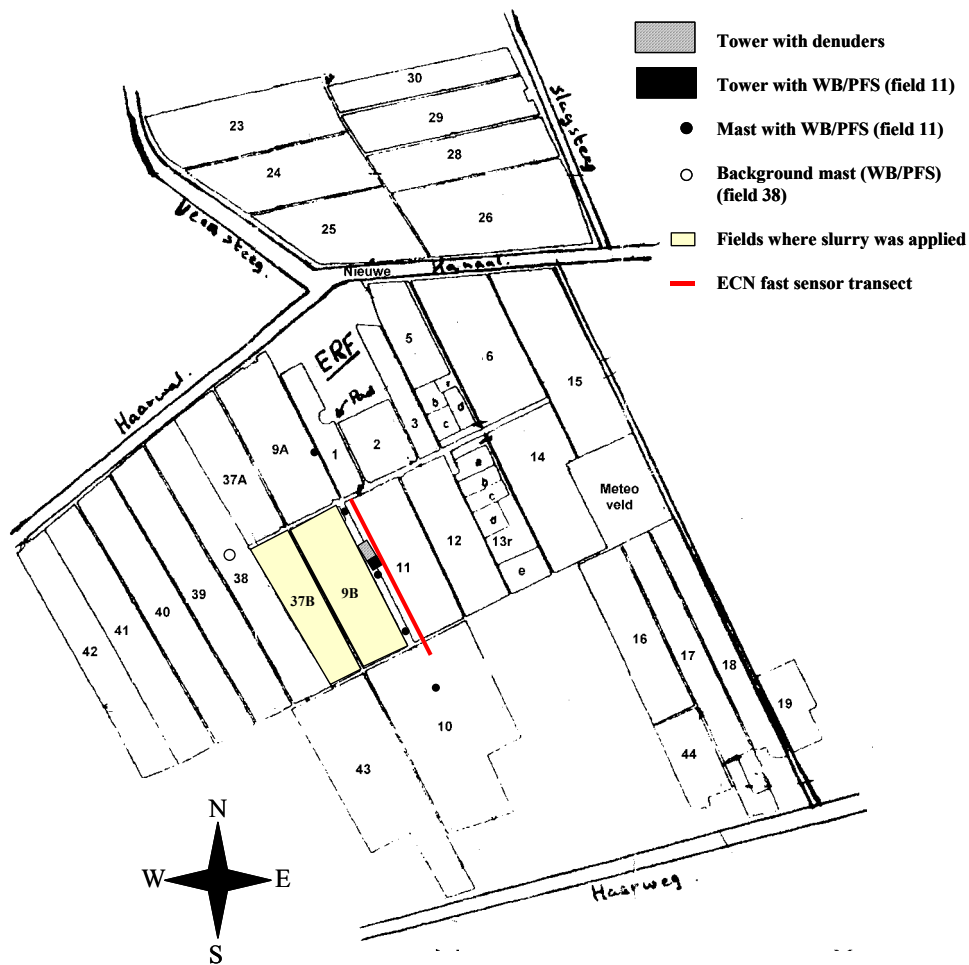


**Figure 3.6** Experimental station in Wageningen. WB=Willems badges. PFS=passive flux samplers

**Table 3.3** Slurry analyses and application rates (Wageningen).

	Field 9B	Field 37B
Ammonium-N (kg/ton product)	2.41	2.39
Slurry applied (ton)	42	25.5
Surface (ha)	2.3	1.7
Application rate ( $\text{m}^3 \text{ha}^{-1}$ )	18.3	15.0
Starting time (local time)	11:28	12:06
Final time (local time)	12:05	12:57

The experimental set-up in Wageningen included the following methods:

1. Flux frame approach.
  - A large mast (figure 3.7, height ~20 m) was used to measure ammonia concentrations at four different heights (1.3, 4.55, 8.55 and 19.35 m) using denuders (reference method).

- A 5 m height mast (figure 3.8) was provided with ammonia passive flux samplers and Willems badges, to measure directly, at four different heights (1.25, 2.45, 4.55 and 5 m), the horizontal ammonia flux and ammonia concentrations, respectively. The distance between this mast and the large mast was of approximately 2 m.
  - A set of short masts (figure 3.9, height ~1.2 m) was used to measure ammonia concentrations and horizontal ammonia fluxes by using Willems badges and ammonia passive flux samplers, respectively. One of the masts was located between the 5 m and the 20 m masts, and the distance between the short masts was 85 m.
2. Plume measurements.
- The NH<sub>3</sub> fast sensor (appendix F) and AMANDA (appendix F) were used by ECN to measure ammonia concentrations in the plume coming from the measurement field across the transect shown in figure 3.6. De AMANDA was located at about 15 m from the border of field 9B. The distance between the AMANDA system and the 20 m mast was of approximately 30 m.



**Figure 3.7** Experimental set-up in Wageningen: a) denuders (4 heights) in a large (20 m) mast configuration; b) ECN fast sensor (left) and AMANDA system (right).



**Figure 3.8** Experimental set-up in Wageningen: ammonia passive flux samplers and Willems badges in a 5 m height-mast configuration.



**Figure 3.9** Experimental set-up in Wageningen: ammonia passive flux samplers and Willems badges in a short-mast configuration.

Denuders, Willems badges and passive flux samplers were changed after pre-determined periods of 2, 5, 7.5, 22 and 44 hours after slurry application and were finally removed at 96 hours, to determine the cumulative losses and rates of loss of ammonia. Due to adverse meteorological conditions, only the first 44 hours were used. Ammonia concentrations from the denuders, Willems badges and passive flux samplers were determined using photometry, and were performed at the environmental laboratory of IMAG.

## 3.2 Ammonia emission from animal houses

### 3.2.1 Kootwijkerbroek (mechanically ventilated animal house)

Ammonia emission measurements took place in four different compartments (see figure 3.10) in an animal house (calves for meat) during two production periods between April 1995 and May 1996. All the animals were of the same age.

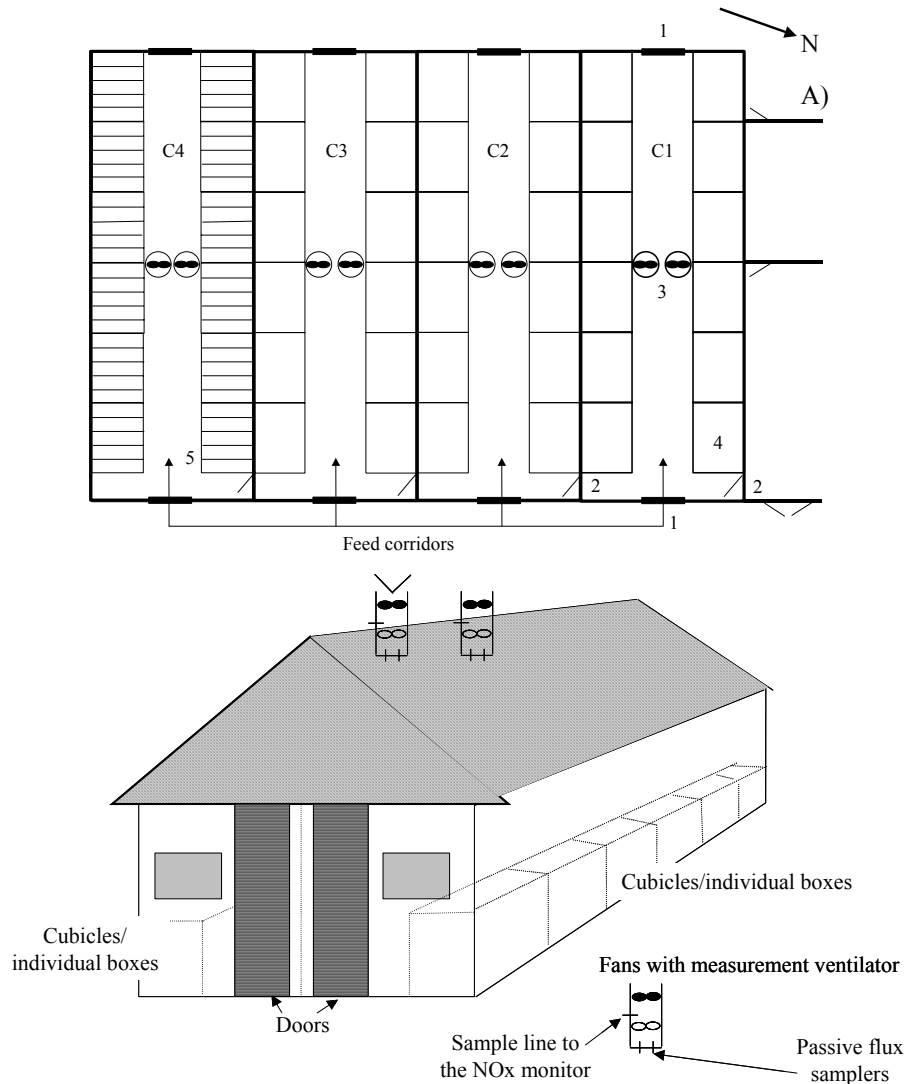


**Figure 3.10** Overview of the measurement site in Kootwijkerbroek.

A) Top view. The following notation has been used: C1, cubicles, flushing system; C2, cubicles, synthetic slatted floor; C3, cubicles, reference (traditional) house; C4, individual boxes, wooden slatted floor; 1, inlets; 2, connecting doors; 3, fans with a measurement ventilator; 4, cubicles for group accommodation; 5, boxes for individual accommodation; B) Front view of one of the four compartments of the animal house, showing the measurement set-up used for these measurements. Also shown the two ventilators, one with and one without a lid.

Three compartments (C1, flushing system; C2, synthetic slatted floor; and C3, reference) contained 60 animals in a collective accommodation, with cubicles (2.5m x 3 m) with space for 5 animals. The fourth compartment (C4, wooden slatted floor) had 44 animals in individual boxes (0.8 m x 1.8 m). The manure was collected in one canal at the end of the boxes. Each compartment had two rows of cubicles with a feeding area in the middle. The departments were connected through a walking area and swing doors perfectly closed.

Each compartment was mechanically ventilated with two fans in the top of the building with a diameter of 45 cm (total maximum capacity of 12000 m<sup>3</sup> h<sup>-1</sup>), without interference or effects in the ventilation of the other compartments. One of the two fans was continuously working, while the other one was switched on when the animal house temperature was above 10 °C. When the second ventilator was not operating it was closed with a “butterfly lid”. The ventilation was changed depending on the outside temperature, the health and the age of the animals (Hol and Groenestein, 1997).

Ammonia emission measurements were performed both in the door openings and beneath the ventilation shaft using passive flux samplers, as shown in figure 3.11, and the results compared with the reference method (ammonia emissions measured with the reference method are reported in Hol and Groenestein, 1997). Glass fibre paper inserts loaded with phosphoric acid were placed in the samplers. After a sampling time of 1 week, the samplers were transported to the IMAG laboratory for analysis using spectrophotometry.

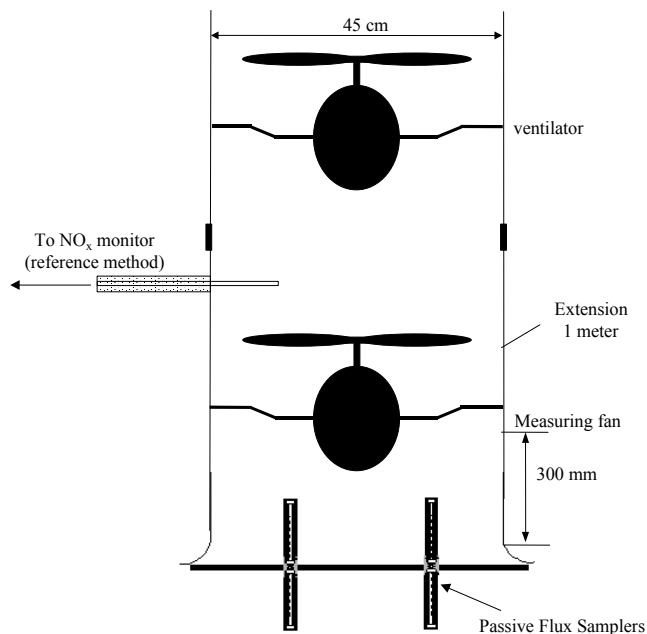


**Figure 3.11** Schematic representation of the sampling points (NO<sub>x</sub> monitor and passive flux samplers (PFS)) for NH<sub>3</sub> concentration measurements in the ventilation shafts of a mechanically ventilated animal house (diameter: 45 cm).

### 3.2.2 Barneveld (naturally ventilated poultry house)

To test the accuracy of the flux frame method (using passive flux samplers) to measure the ammonia emission from naturally ventilated animal houses, an experiment was performed at the location Barneveld (figure 3.12). The farm has three animal houses that are used for poultry breeding. At the moment of the experiment the houses were empty and completely clean, in preparation for a new operational period, which was planned to start in the last week of November 2002. Two set of experiments were performed on the 12<sup>th</sup> and 14<sup>th</sup> of November 2002. Because of its wide fetch area, which allows us to use the house for almost every wind direction range, the house in the middle was chosen for this experiment. The house has two compartments, each 40 m large and 10 m wide, separated by a distance of 6 m. Each compartment is provided with ventilation shafts on the roof, which were kept closed during the experiment in order to allow ammonia to leave only through the windows.

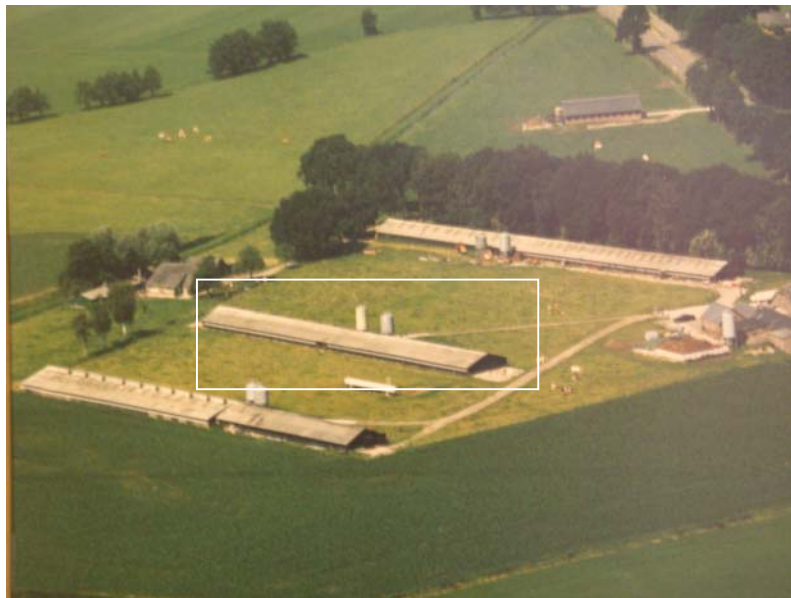


**Figure 3.12** Naturally ventilated poultry house in Barneveld.

In this experiment it was decided to simulate, as far as possible, the emission from the animal house under real conditions. Being an empty house, this means that we have to provide a method to mix properly the ammonia emitted in the animal house. In real conditions, this is achieved due to convection by the heat produced by the animals. To simulate this effect, a heater provided with a ventilator was used. The experimental set-up is schematically shown in figure 3.13a. Figure 3.13b shows the emission system as used in this experiment. For safety conditions, ammonia was pre-diluted to keep its concentration out of the range where ammonia in an air mixture is flammable.

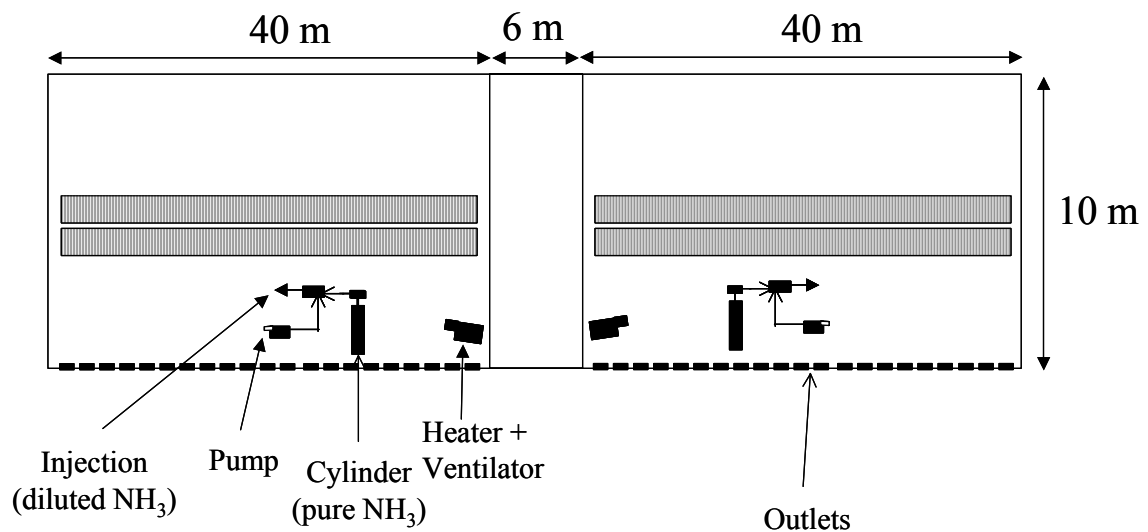


**Figure 3.13** Ammonia emission system used at the location Barneveld.

Since the weather forecast for the measurement period showed that the prevailing wind direction should be in the Z-ZW-W range, 4 masts were placed north of the animal house, along the axis of the building. On the first measurement day another mast was placed at the east side of the house. This mast was moved on the second measurement day to the west side of the house, in line with the other 4 masts (figure 3.14). To measure the ammonia emission from the animal house, each mast was equipped with passive flux samplers in a cross design (figure 3.15 and section 2.2), at four different heights (1.47, 2.89, 4.67 and 6.12 m for the 6 m mast, or 10 m for the 10 m mast). The flux frame method (section 2.3) was then used to calculate the ammonia emission from the two parts of the animal house.

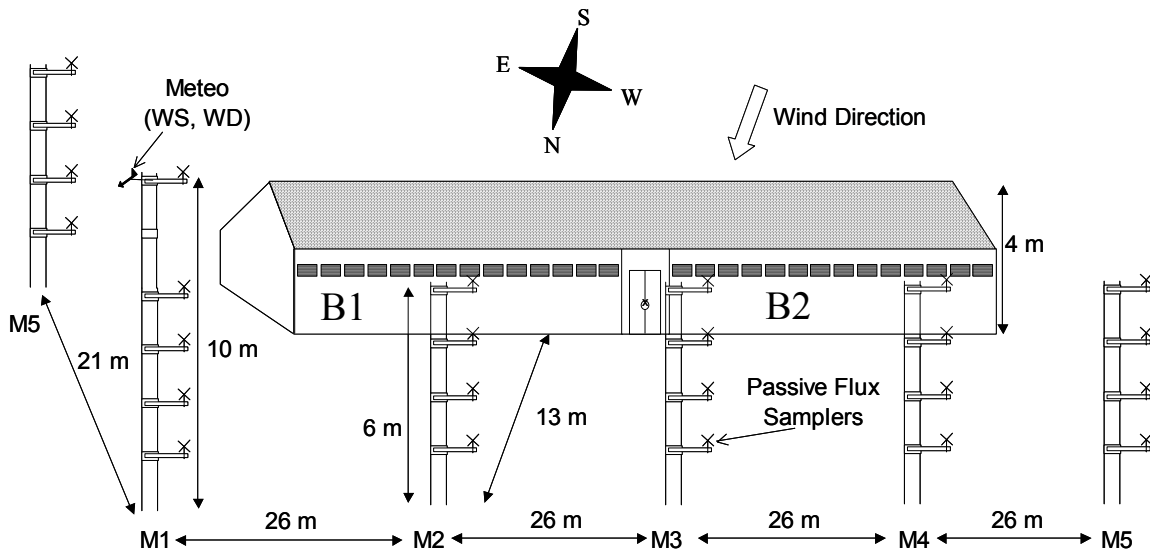


**Figure 3.14** Schematic representation of the measurement set-up in Barneveld.



**Figure 3.15** Passive flux samplers in a cross design as used in Barneveld.

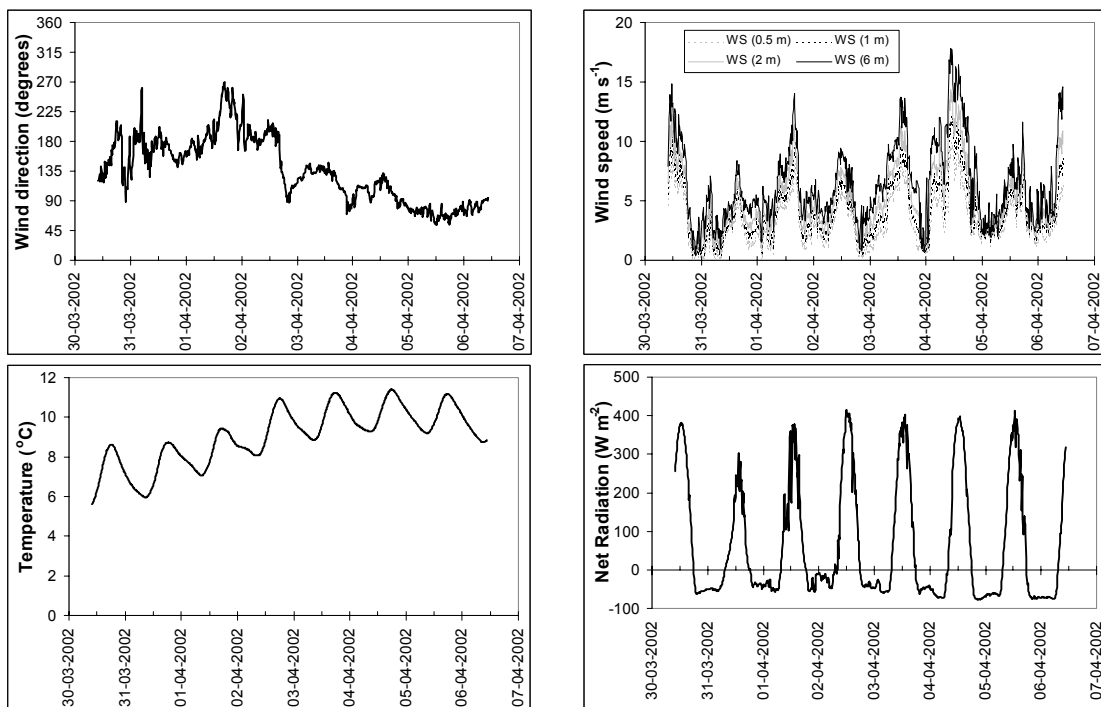
For meteorological information, a cup anemometer and a wind vane were placed at the mast “1” (figure 3.14), at a height of 2 m the first days, and at a height of 10 m the last measurement day. Besides, meteorological information from a meteorological station in Wageningen (19 km from the measurement site) was also collected. By comparing both meteorological data sets, it is possible to see whether or not the building affect the wind pattern in the area between the animal house and the measurement masts.

## 4 Ammonia emissions after field application of manure

### 4.1 Zegveld

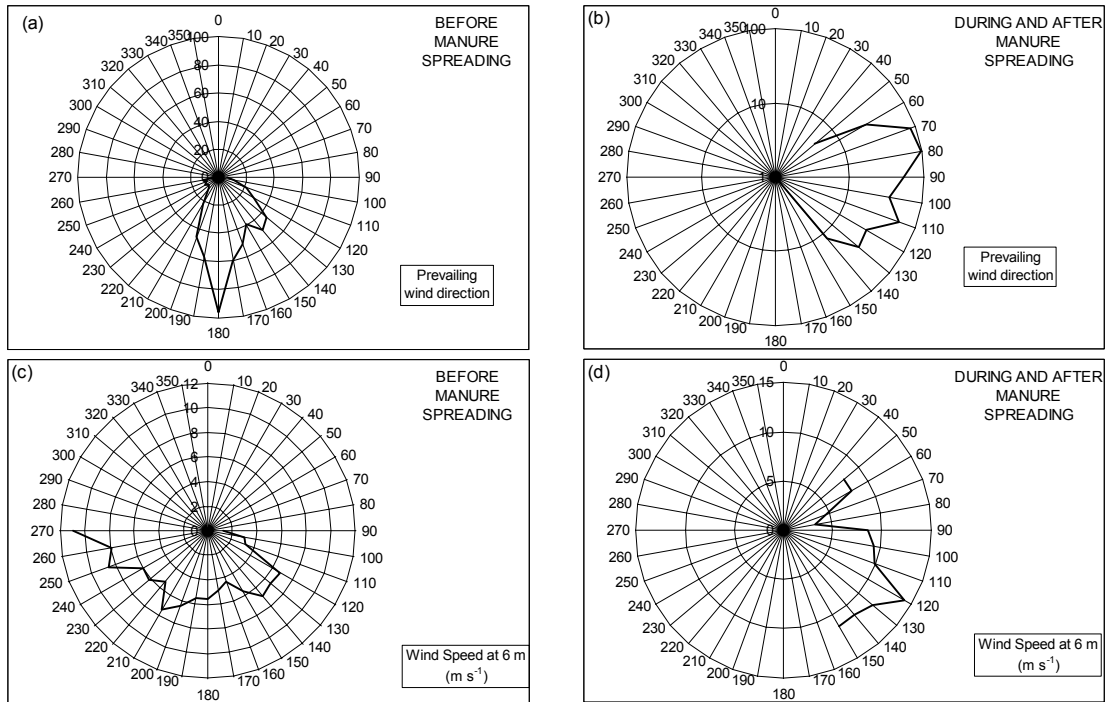
#### 4.1.1 Meteorological parameters

Figure 4.1 shows the time series (local time) of some meteorological parameters for the whole measurement period. An increase in temperature was observed throughout the measurement period, reaching a maximum of 11.4 °C, and a minimum of 5.6 °C at the beginning of the measurements. The average temperature was 9 °C (table 4.1). Wind direction was turning from South, to East (figure 4.2). During the period where manure spreading took place (including a 6-hours period after the event), wind direction was predominantly in the range 120-150. An average value of 136 degrees was obtained for the whole measurement period. Higher wind speed values were generally measured when the wind blew from the Southeast (figure 4.2).



**Figure 4.1** Meteorological parameters (wind direction, wind speed at four different levels, temperature and net radiation) over the period 30 March-6 April 2002 at the location Zegveld.

A diurnal pattern is observed for average wind speed and net radiation, as shown in figure 4.3 for the whole measurement period. This diurnal pattern shows a maximum value in daytime, with lower values during the night, the same pattern observed in the literature (Erisman and Wyers, 1993). This is clearly observed for net radiation, with changes from minimum values of  $-50 \text{ W}\cdot\text{m}^{-2}$  in nighttime, to maximum values up to  $400 \text{ W}\cdot\text{m}^{-2}$  during daytime.



**Figure 4.2** Sector dependence of prevailing wind direction (a, b) and average wind speed (c, d) over the period 30 March-6 April 2002 at the location Zegveld.

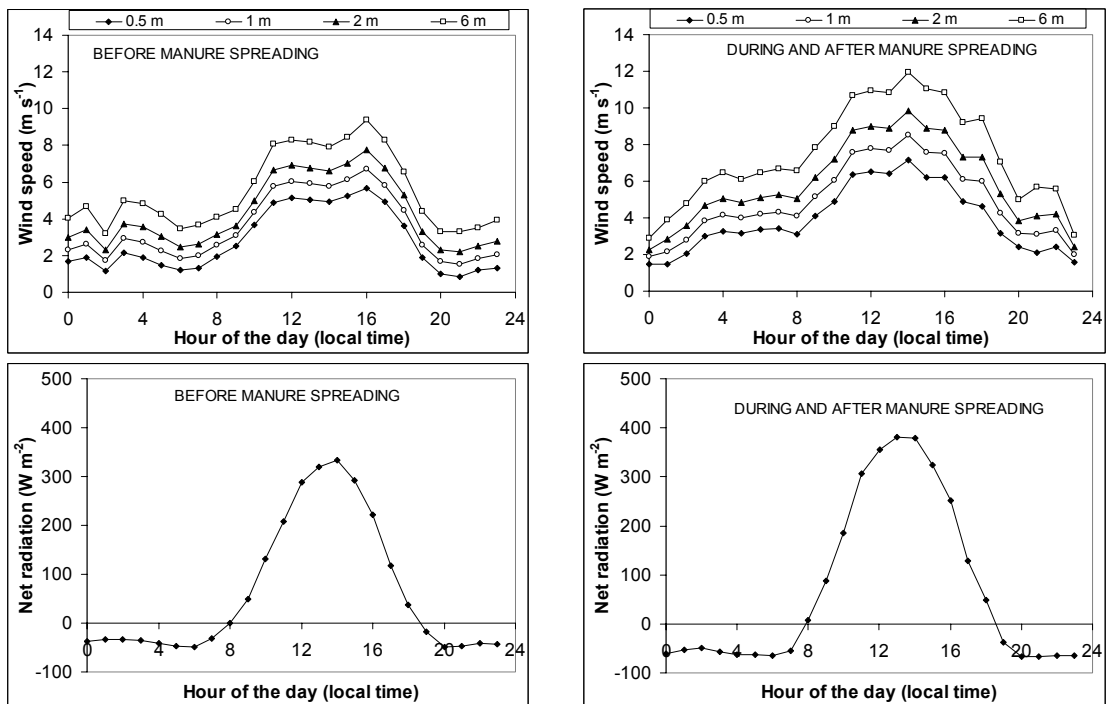


**Figure 4.3** Diurnal variation of some meteorological parameters (wind speed and net radiation) over the period 30 March-6 April 2002 at the location Zegveld.

**Table 4.1** Statistics of ammonia concentrations and some meteorological parameters measured at Zegveld during the period 30 March – 6 April 2002.

	MAX	MIN	MEAN	MEDIAN	STDV
Temperature (°C)	11.4	5.6	9.0	9.2	1.4
Wind speed, 0.5 m (m s <sup>-1</sup> )	9.9	-0.1	3.3	2.8	2.1
Wind speed, 1 m (m s <sup>-1</sup> )	12.1	0.4	4.2	3.5	2.4
Wind speed, 2 m (m s <sup>-1</sup> )	14.3	0.5	5.1	4.3	2.8
Wind speed, 6 m (m s <sup>-1</sup> )	17.9	0.4	6.5	5.7	3.4
Net radiation (W m <sup>-2</sup> )	415	-77	66	-21	155
Wind direction (degrees)	271	53	136	133	50
NH <sub>3</sub> (ppm, 0.5 m)	2.13	0.01	0.07	0.04	0.16
NH <sub>3</sub> (ppm, 1 m)	0.35	0.01	0.05	0.04	0.04
NH <sub>3</sub> (ppm, 2 m)	0.18	0.01	0.05	0.04	0.02
NH <sub>3</sub> (ppm, 6 m)	0.11	0.01	0.04	0.03	0.02

#### 4.1.2 Concentration measurements

Ammonia concentrations were measured at four different heights (0.5, 1, 2 and 6 (background) m) using converters to transform the NH<sub>3</sub> present in the sampled air to NO, and a NO<sub>x</sub> monitor. The results of these measurements are shown in figure 4.4 for the whole measurement period (local time is used; see table 4.1 for a statistical summary of both concentrations and meteorological conditions). The ammonia concentration pattern observed in figure 4.4a (highest concentration in the lowest level, lowest concentration in the highest level) reveals the ammonia emission that occurs directly after manure spreading. The emission decays exponentially with time, and after a few hours (dry period with strong wind speed) the concentrations reach values similar to the measured background level. After a few days the pattern reverses, showing the possibility of ammonia deposition into the field (figure 4.4b).

The ammonia concentrations measured in the field depend strongly on meteorological parameters such as wind speed and wind direction. When comparing the results shown in figure 4.5 for the ammonia concentrations measured in the field, with those presented in figure 4.2 (prevailing wind direction, and wind sector dependency of average wind speed), it is observed that, in general, higher concentration values are measured at lower wind speeds. Besides, higher concentrations are recorded when air is coming from a neighbouring source (i.e. after manure spreading into the same or neighbouring fields), which makes wind direction and wind speed measurements important for the analysis of the results obtained in the field.

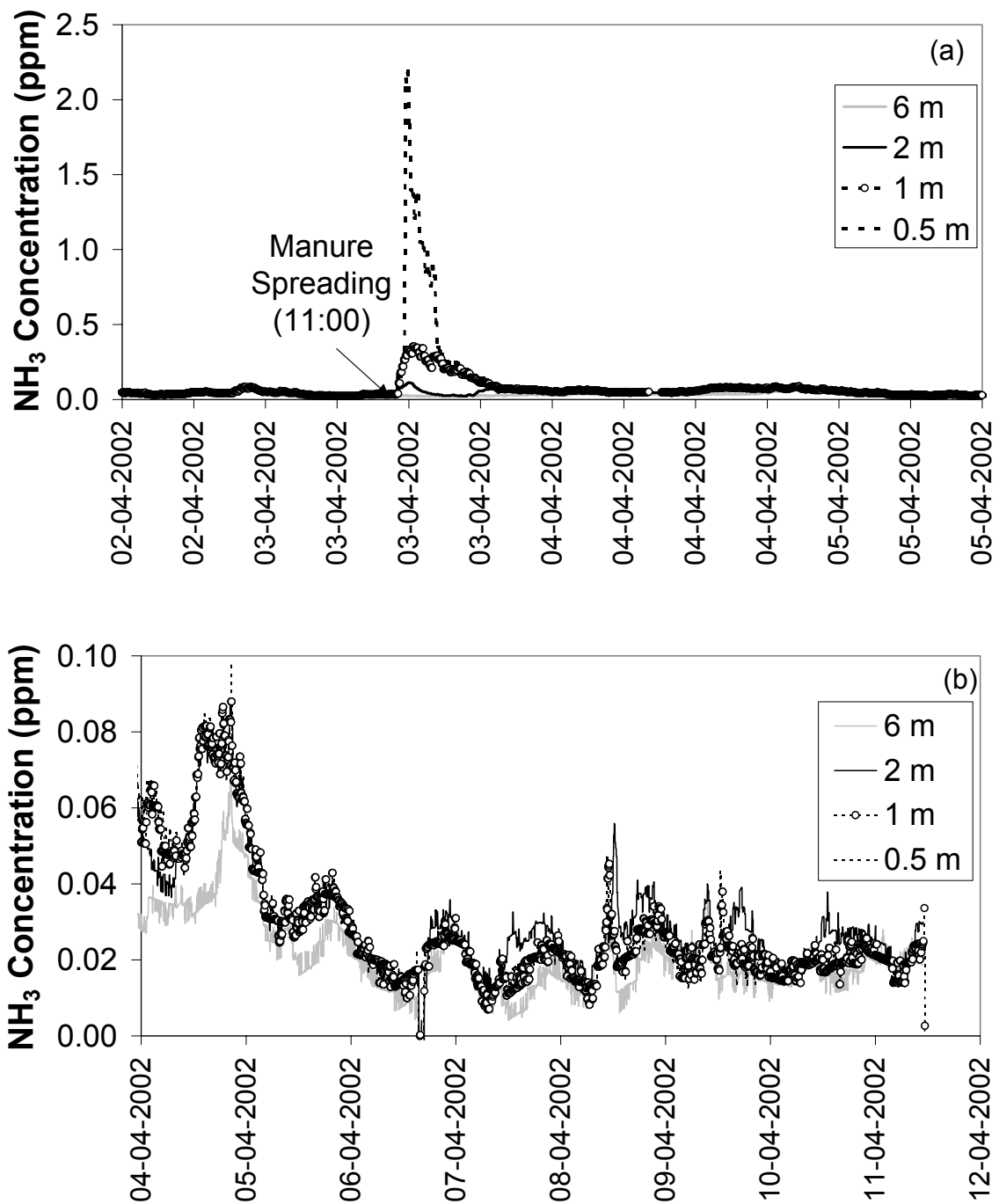


**Figure 4.4** NH<sub>3</sub> concentration profile as measured with the NO<sub>x</sub> monitor+NH<sub>3</sub> to NO converter system in Zegveld.

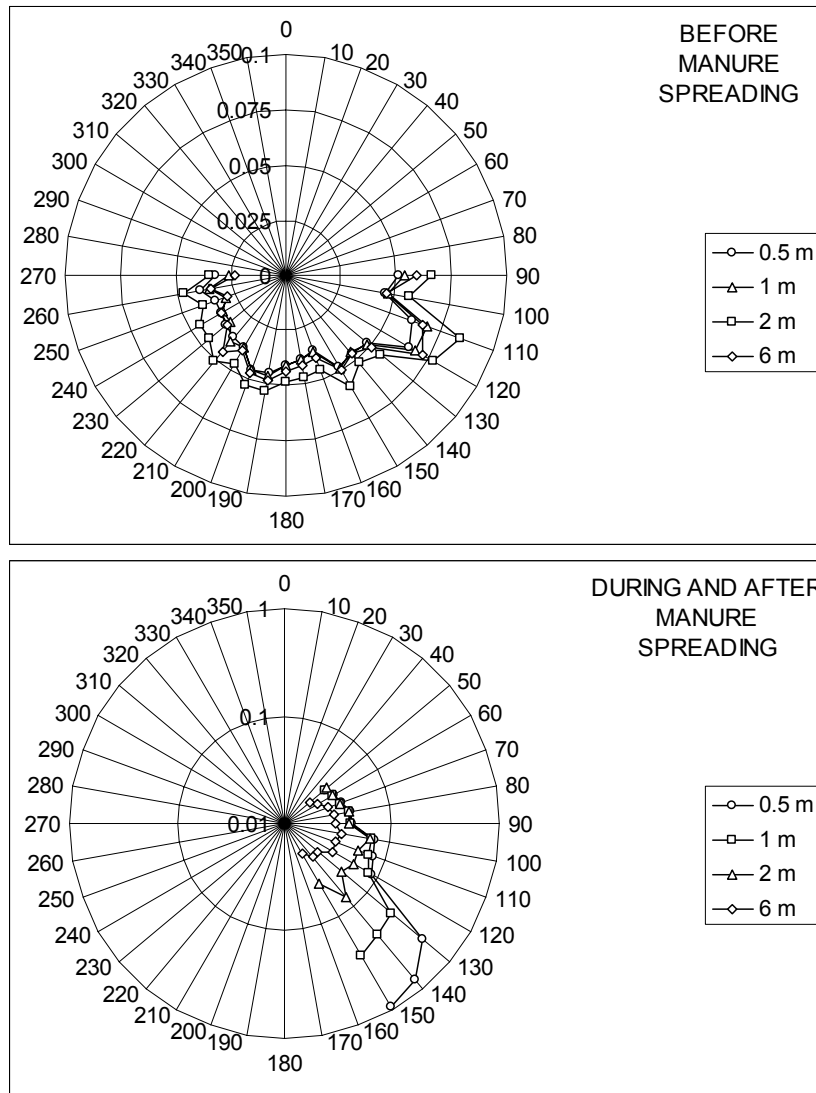


**Figure 4.5** Sector dependence of average  $\text{NH}_3$  concentrations (ppm) measured with the  $\text{NH}_3$  to  $\text{NO}$  converter and the  $\text{NO}_x$  monitor in Zegveld, during the period 30 March- 6 April 2002.

Average-integrated ammonia concentrations were also measured over specific periods of time (1.4, 4.5, 7.7, 24, 48 and 96 h), with active samplers (denuders, reference method), and passive samplers (Willems badges). Besides, passive flux samplers were also used at the same heights, which allows comparison of the “real” concentrations measured with denuders and Willems badges, with the “wind-averaged” concentrations calculated from the passive flux samplers. Figure 4.6 shows the comparison between the concentrations measured with the Willems badges and the denuder system. According to these results, Willems badges tend to underestimate the ammonia concentration in the air with respect to measurements performed with denuders, although a good agreement is observed between both measurement techniques. When comparing the ammonia concentration

measurements performed with the converters and the  $\text{NO}_x$  monitor, with the reference (denuder) system, we can see that the correlation is not so good as the one observed with the Willems badges (Figure 4.6). Because the converters were located close to the  $\text{NO}_x$  monitor, at a distance from the sampling point,  $\text{NH}_3$  was transported through the sampling line, instead of  $\text{NO}$ . And this increases the possibilities of absorption of  $\text{NH}_3$  through the sampling walls. For low ammonia concentrations, with a relatively constant concentration level, a small sampling flow is enough to transport all the ammonia to the detector, without having problems of absorption in the sampling line walls. In this case the agreement between both systems exists. However, for high ammonia concentrations, with strong fluctuations in concentration, the inner surface of the tubing and a possible water layer on it (although the tubing was slightly heated above ambient temperature to prevent condensation of water vapour) may act as a buffer, resulting in too low peak concentrations and increased low concentrations in between.

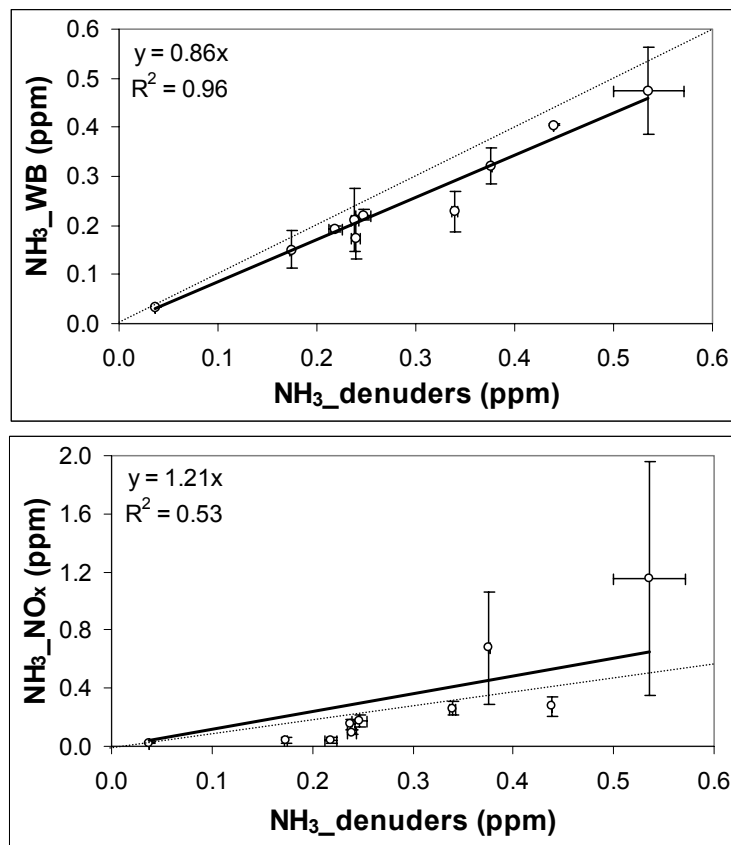


**Figure 4.6** Measured concentrations in Zegveld using passive samplers (Willems badges, WB) and the converters with the  $\text{NO}_x$  monitor, vs. the concentration measured with a reference method (denuders).

The dotted line represents the 1:1 relation between both methods. Error bars are also included.

Passive flux samplers, although they are used to measure directly the horizontal ammonia flux at different heights, can also be used to calculate the ammonia concentration at those heights (see section 2.2). Figure 4.7 shows that a good correlation can be obtained when comparing the ammonia concentrations calculated from the measurements performed with the passive flux samplers, and the ammonia concentration measured with the reference method (denuders). In general, passive flux samplers seem to overestimate the ammonia concentration measured with respect to the denuder system.

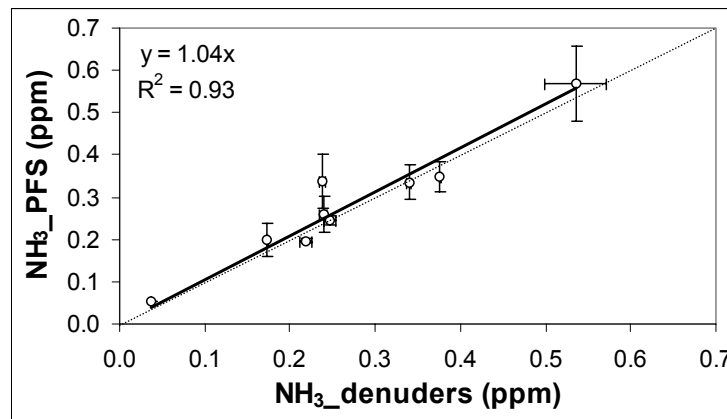


**Figure 4.7** Comparison between the concentrations calculated with the passive flux samplers (PFS) and the concentration measured with the reference method (denuders) in Zegveld.

The dotted line represents the 1:1 relation between both methods.

Figure 4.8 summarises the results of the ammonia concentration measurements for three different time intervals: I) 1.4 h after starting with manure spreading; II) 4.5 h after starting with manure spreading; III) 7.7 h after starting manure spreading, for the different measurement techniques at different heights. As shown previously, measurements performed with denuders (reference), Willems badges and passive flux samplers gave similar results, while the results with the NO<sub>x</sub> monitor were usually poorly correlated with any of the other techniques. All techniques showed a decrease in concentration with height for the three time intervals, reflecting the ammonia emission that occurs after the manure-spreading event. However, it looks like the NH<sub>3</sub> gradient is higher for the measurements performed with the NO<sub>x</sub> monitor than the one observed for the other techniques. The ammonia fluxes will be discussed in the next section.

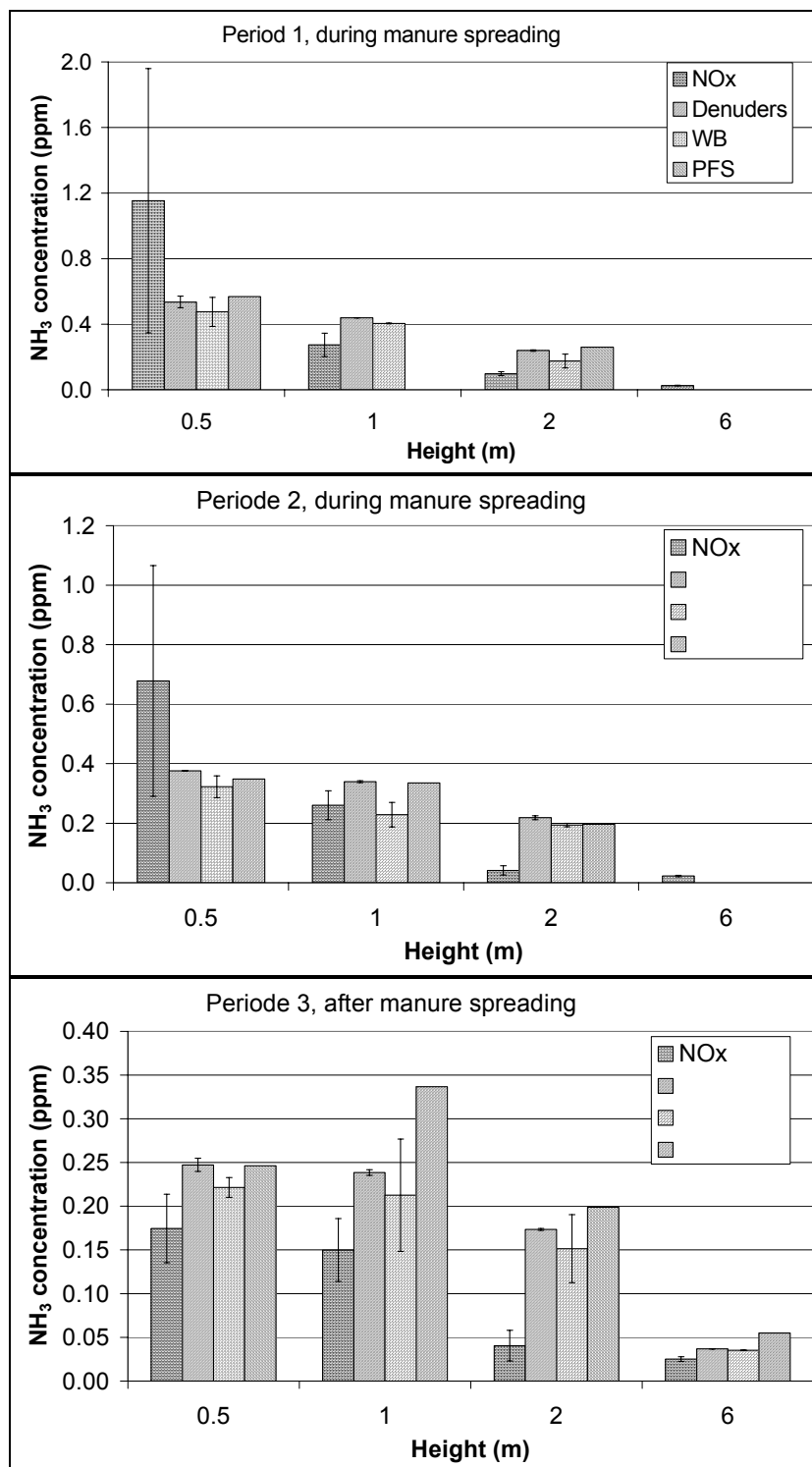


**Figure 4.8** Ammonia concentrations measured in Zegveld with denuders (reference), NO<sub>x</sub> monitor, Willems badges (WB) and passive flux samplers (PFS). Three sampling periods (1: 1.4 h after starting with manure spreading; 2: 4.5 h after starting with manure spreading; 3: 7.7 h after starting manure spreading) are considered.

### 4.1.3 Horizontal ammonia flux

The horizontal ammonia flux can be measured directly with passive flux samplers. The fixed system (cross, figure 3.4)) has the advantage that it is a simple set-up with no movable parts, but it is not always pointing directly to the wind direction. On the other hand, the windvane sampler (figure 3.5) has the advantage of always pointing at the wind direction, although it could have adjustment problems in periods with very low wind speeds. However, this can be considered of low relevance since the horizontal fluxes are also very low in these situations.

Figure 4.9 shows the comparison between the horizontal ammonia flux as measured with the fixed passive flux samplers (cross and windvane designs), and calculated using measurements of average horizontal wind speed, and ammonia concentration measurements using denuders (reference), Willems badges and converters together with the  $\text{NO}_x$  monitor. The horizontal ammonia flux is calculated as the product of the average horizontal wind speed, and the measured ammonia concentrations. This means that wind speed and concentration, both height-dependent, can influence the horizontal flux. Usually wind speed increases with height, while the concentration is usually higher at lower levels after a manure-spreading event. For this reason, the highest horizontal flux is not measured at the lowest (highest concentration) or highest (highest wind speed) level, but in an intermediate level, as shown in figure 4.9 for the different measurement techniques.

Besides, because the emission from the field decreases with time after manure spreading, the measured concentrations also decrease with time, and consequently the horizontal flux. We can also see that the passive flux samplers attached to the windvane do not always give the correct horizontal ammonia flux when compared with the passive flux samplers in the cross design, or the denuders (reference system). A possible explanation could be that the windvane was not reacting fast enough to changes in wind direction.

When comparing the horizontal ammonia flux measured with the fixed passive flux samplers, and calculated for the denuders, Willems badges and the system with the converters and the  $\text{NO}_x$  monitor, both figure 4.9 and figure 4.10 show a good correlation between passive flux samplers, Willems badges and denuders (reference method), while the system converters- $\text{NO}_x$  monitor usually shows a high deviation when compared to the other techniques.

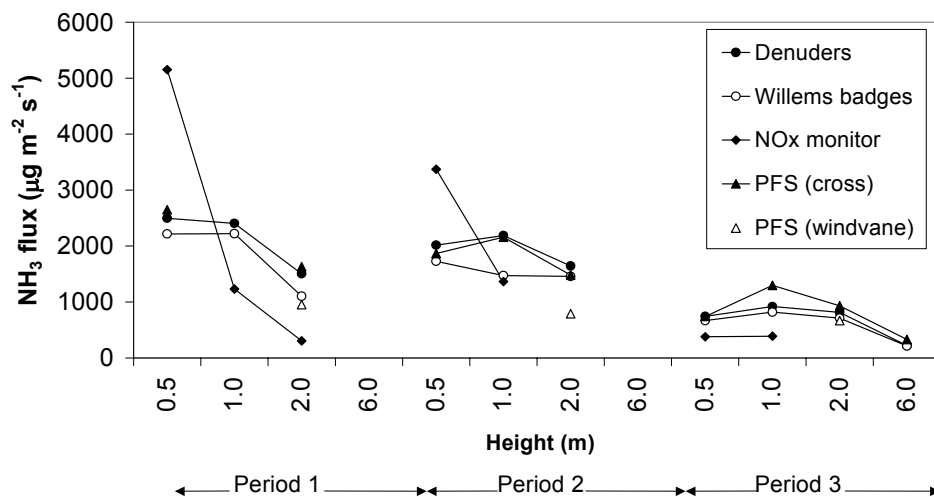


**Figure 4.9** Horizontal ammonia flux measured with fixed passive flux samplers (cross and windvane designs), and calculated for denuders, Willems badges, and the converters-NO<sub>x</sub> monitor system.

Measurements were performed at the site Zegveld during the following periods: 1) 1.4 hours; 2) 4.5 hours and 3) 7.7 hours after manure application into the field.

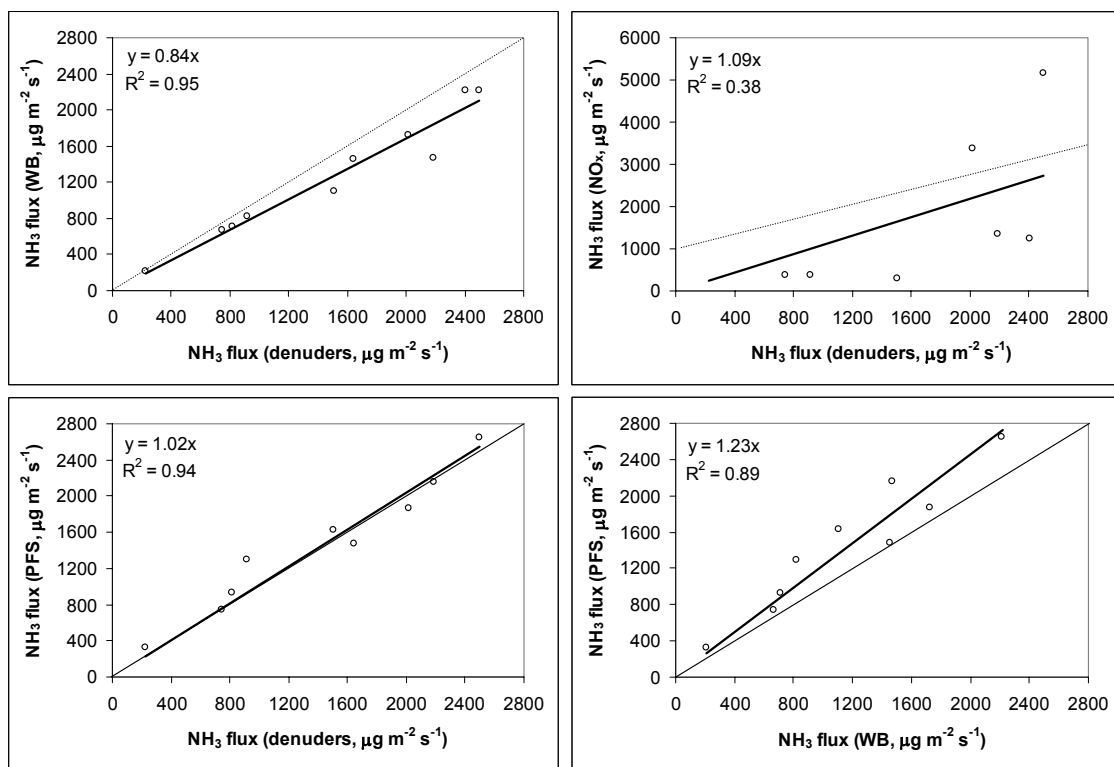


**Figure 4.10** Dispersion analysis showing the relation between the horizontal ammonia flux measured with fixed passive flux samplers (PFS), Willems badges (WB), converters-NO<sub>x</sub> monitor, and denuders, at the location Zegveld.

The dotted line represents the 1:1 relation between both methods.

#### 4.1.4 Vertical ammonia flux

One important question when trying to measure ammonia emissions from agricultural activities is which level of detail is required to get accurate and representative data on field emissions. The system with the converters and the  $\text{NO}_x$  monitor allows semi-continuous measurements of the concentrations and, in that way, monitoring of the ammonia flux (emission or deposition) in periods with and without manure spreading events. On the other hand, sometimes it is only necessary to know the ammonia emission on a weekly-, monthly-, or yearly basis. In this case, accumulation techniques such as denuders, Willems badges or passive flux samplers can be used instead of continuous monitoring. This section will show the suitability of these techniques to determine the ammonia emission after manure spreading into the field.

Ammonia exchange fluxes were calculated using the aerodynamic gradient method (section 2.1) using the ammonia concentration data available for four different heights, and meteorological parameters. A high emission peak is observed during and after the application of manure into the field (figure 4.11). Emission continues for some days (the duration of the emission depending, among others, from factors such as wind speed and temperature), and a second (smaller) peak is also observed the next day after manure spreading (figure 4.11).

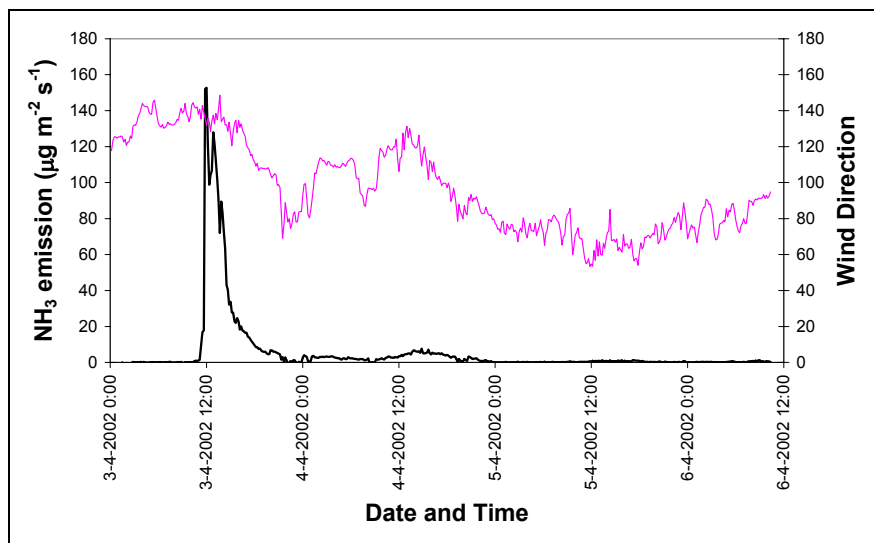


**Figure 4.11** Ammonia emission pattern in Zegveld calculated using the system with converters and the  $\text{NO}_x$  monitor. Also included in the figure the wind direction pattern during the first three days after the manure-spreading event.

Emission decays exponentially with time, therefore most of the emission is expected to occur in the first few hours after manure spreading. This can be seen in figure 4.12, where the accumulated  $\text{NH}_3$  emission is presented as a function of the time after the application of manure into the field. Figure 4.12 shows also almost no emission after 72

hours after the manure application event. In fact, more than 80% of the emission occurs in the first 10 hours, although emission continues for some days.

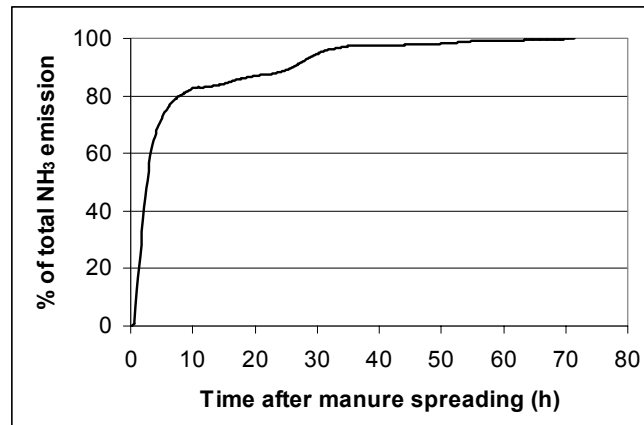


**Figure 4.12** Accumulated NH<sub>3</sub> emission at the site Zegveld, during the period 3-april-2002 to 6-april-2002, using a system with converters and the NO<sub>x</sub> monitor.

When we are interested only in average emission values, and not in the emission process itself, accumulation techniques (both active (denuders) and passive (Willems badges, passive flux samplers)) can be used. Figure 4.13 shows the comparison between the three integrating techniques, and the semi-continuous measurements using the system with the converters and the NO<sub>x</sub> monitor. It is shown that results with denuders, Willems badges and passive flux samplers agree both qualitatively and quantitatively. The NO<sub>x</sub> monitor, while showing the same trend in the ammonia emission as the accumulation techniques, differs significantly (factor 2 larger) in the measured values.

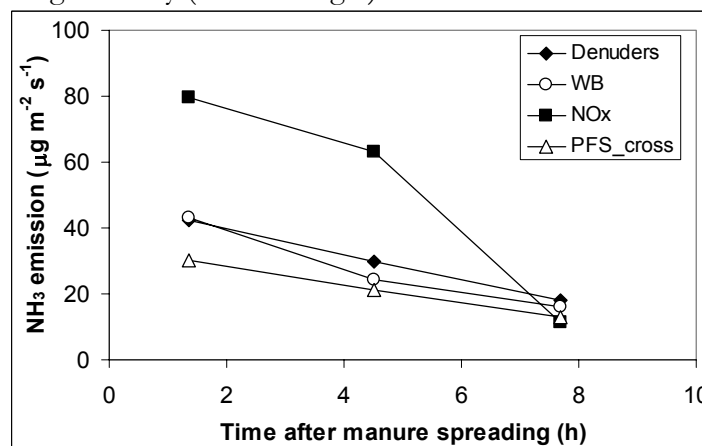


**Figure 4.13** Ammonia emission (vertical flux) after manure application into the field using integrating techniques (denuders, Willems badges, passive flux samplers) and a system with converters and a NO<sub>x</sub> monitor.

Measurements were performed at the site Zegveld during the following periods: 1) 1.4 hours; 2) 4.5 hours and 3) 7.7 hours after manure application into the field.

The accumulated ammonia emission from the field (figure 4.14) shows that, in general, passive techniques (Willems badges and passive flux samplers) underestimate the emission following the application of manure into the field, compared with denuders. On the other hand, the NO<sub>x</sub> monitor overestimates the emissions from the field. It is not yet clear what is the reason of this deviation with respect to accumulation techniques.

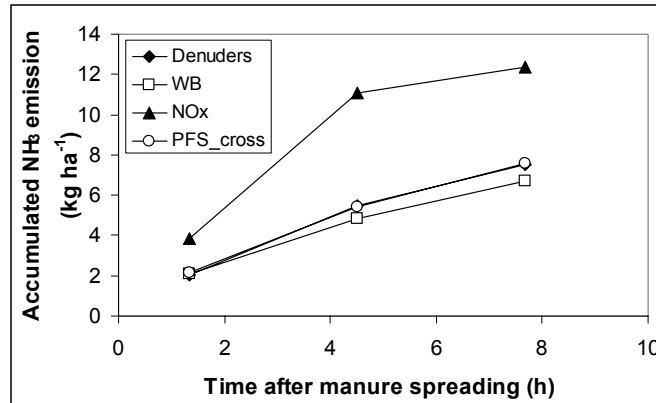


**Figure 4.14** Accumulated ammonia emission (vertical flux) after manure application into the field using integrating techniques (denuders, Willems badges (WB), passive flux samplers (PFS)) and a system with converters and a NO<sub>x</sub> monitor. Measurements were performed at the site Zegveld during the following periods: 1) 1.4 hours; 2) 4.5 hours and 3) 7.7 hours after manure application into the field.

Figure 4.14 shows that the NH<sub>3</sub> emission during the first 8 hours after manure application into the field varies between 6.7 and 7.5 kg NH<sub>3</sub>-N ha<sup>-1</sup> (WB, PFS, denuders), and 12.4 kg NH<sub>3</sub>-N ha<sup>-1</sup> according to NO<sub>x</sub> monitor. This represents a percentage of the total NH<sub>3</sub>-N applied into the field of:

- Denuders: 20%
- Willems badges: 18%
- Passive flux samplers: 14%
- NO<sub>x</sub> monitor: 33%

## 4.2 Wageningen

### 4.2.1 Meteorological parameters

Figures 4.15-4.17 show the meteorological conditions (local time) observed at the measurement site during the whole measurement period. During most of the measurement period, the prevalent wind direction was southwest-west-northwest. As in Zegveld, in Wageningen a diurnal pattern was observed for average wind speed, with low values (< 1 m s<sup>-1</sup>) usually measured during nighttime and in the first hours of the day, and the highest values around 14:00 h. Usually the highest wind speed values were observed for south-

westerly winds. The average temperature during the measurement period was 16.6 °C (table 4.2).

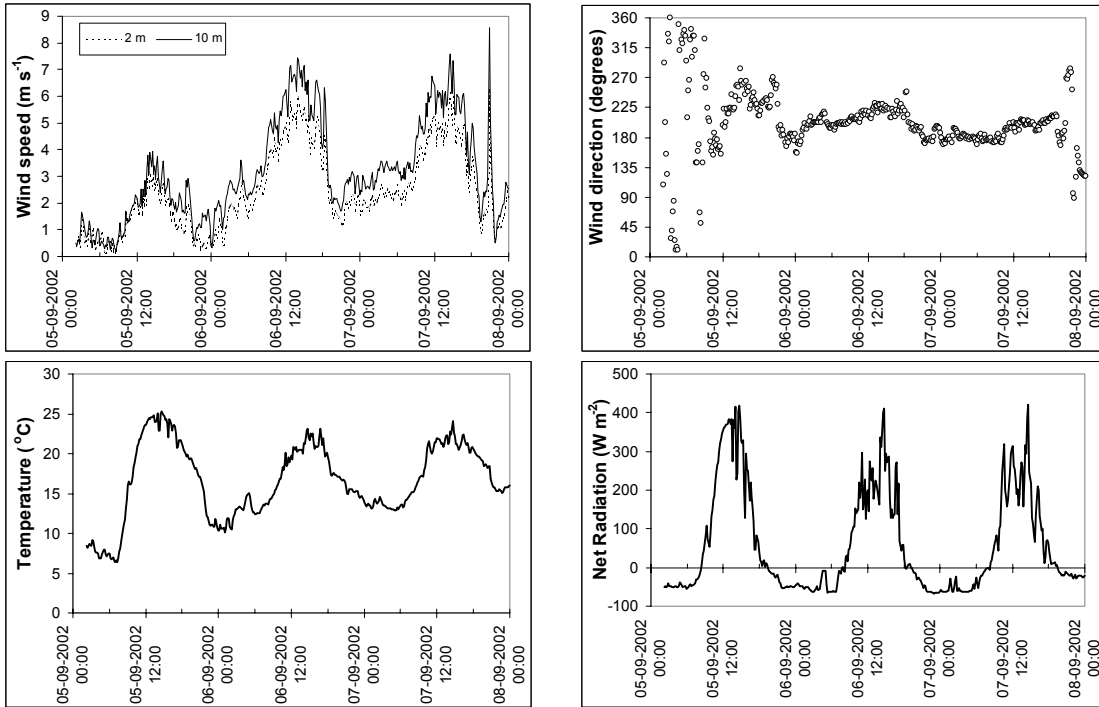


**Figure 4.15** Meteorological parameters (wind direction, wind speed, temperature and net radiation) measured at Wageningen over the period 5-9 september 2002.

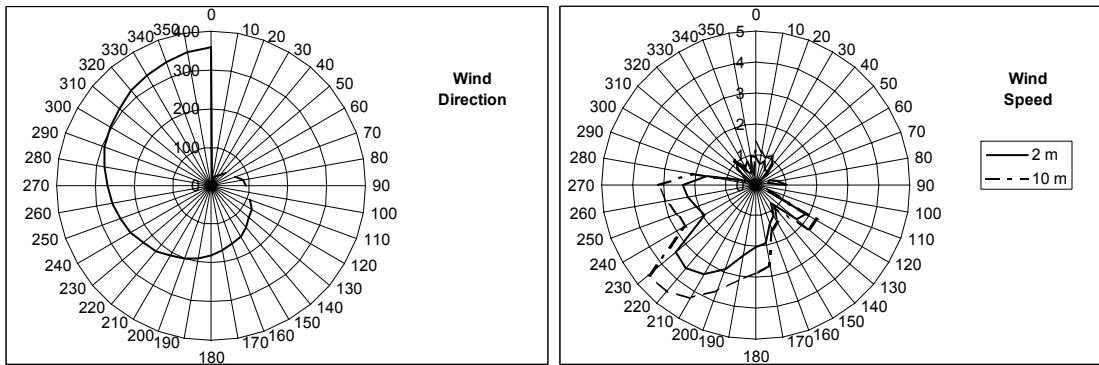


**Figure 4.16** Sector dependence of wind direction and wind speed over the period 5-9 september 2002 at the location Wageningen.

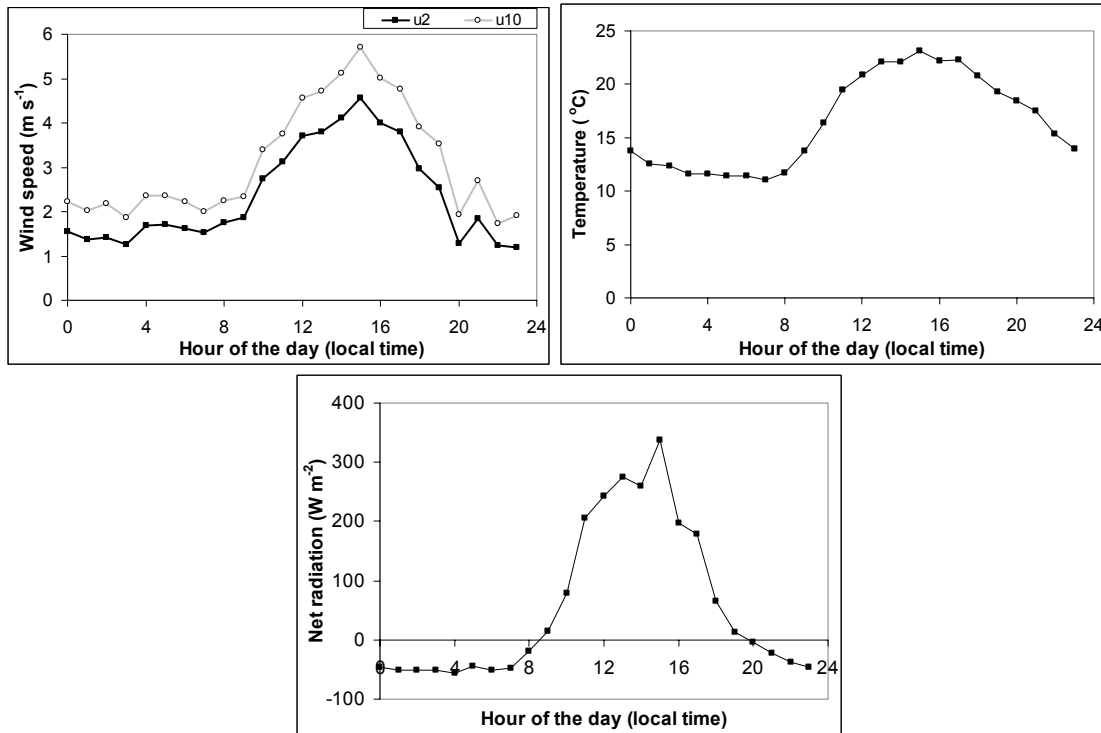


**Figure 4.17** Diurnal variation of wind speed, temperature and net radiation averaged over the period 5-8 september 2002 at the location Wageningen.

**Table 4.2** Statistics of some meteorological parameters measured at Wageningen during the period 5-8 September 2002.

	MAX	MIN	MEAN	MEDIAN	STDV
Temperature (°C)	25.3	6.3	16.6	16.3	4.7
Wind speed, 2 m (m s <sup>-1</sup> )	6.2	0.2	2.4	2.1	1.5
Wind speed, 10 m (m s <sup>-1</sup> )	8.6	0.2	3.1	2.8	1.8
Net Radiation (W m <sup>-2</sup> )	421	-67	60	-8	134
Wind direction (degrees)	359	10	202	200	47

#### 4.2.2 Ammonia concentrations

Figure 4.18 shows the comparison of the ammonia concentrations measured with the different averaging techniques (denuders, Willems badges and passive flux samplers) used in this experiment. It is important to note here that, in contrast with the measurements performed in Zegveld, the passive flux samplers were not used in the cross design, but as single samplers facing the wind. Only one of the measurement heights (4.55 m) is present in both the large mast (with the denuders), and the 5 m mast (with the ammonia passive flux samplers and the Willems badges). For that reason, the number of data points that can be used for comparison is small. Figure 4.18 shows that, as in the experiments in Zegveld (section 4.1), there is a good agreement between the concentrations measured with the

Willems badges (passive sampling) and the denuders (active sampling). In fact, the regression line is almost the same for both experiments. For the ammonia passive flux samplers, the results are not totally satisfactory. Although the regression line gives a good correlation between the concentrations measured with the passive samplers and the denuders, the passive samplers overestimate the ammonia concentrations up to a factor 2 when compared with the denuders.

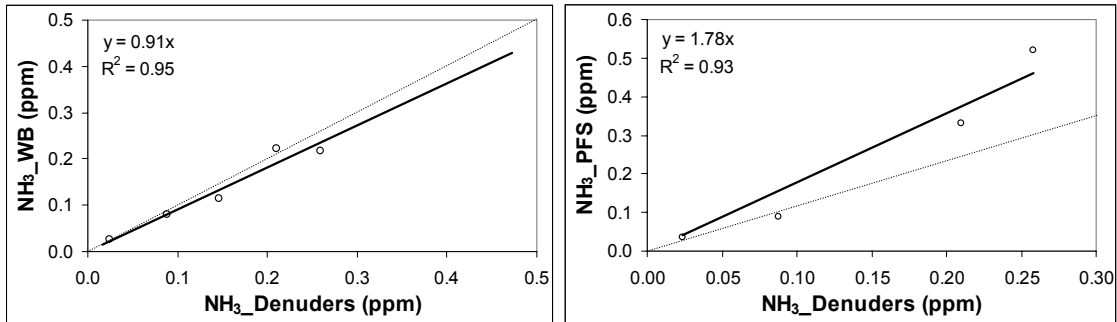


**Figure 4.18** Measured concentrations in Wageningen using passive samplers (Willems badges, WB; passive ammonia flux samplers, PFS) vs. the concentration measured with the denuders.

The dotted line represents the 1:1 relation between both methods.

This overestimation is explained from the cosine dependency of the samplers. Wind tunnel experiments (figure 4.19) showed that the maximum air velocities (maximum pressure drop) in the sampler are not found at 0 or 180°. At these angles the air velocity is approximately 95% of the maximum values. The maximum values are found at angles approximately 30° before and after the 0 and 180 degrees angles. Around the 90 and 270 degrees angles there is a serious instability. In this position the sampler is placed almost perpendicular to the direction of the airflow. The airflow through the sampler reverses at impact angles of 75, 95, 265 and 280 degrees. The pressure drop readings in this part of the graph have a much higher uncertainty. Between the impact angles 120 to 240 and 300 to 60 degrees there is little difference between the curves for the velocities applied.

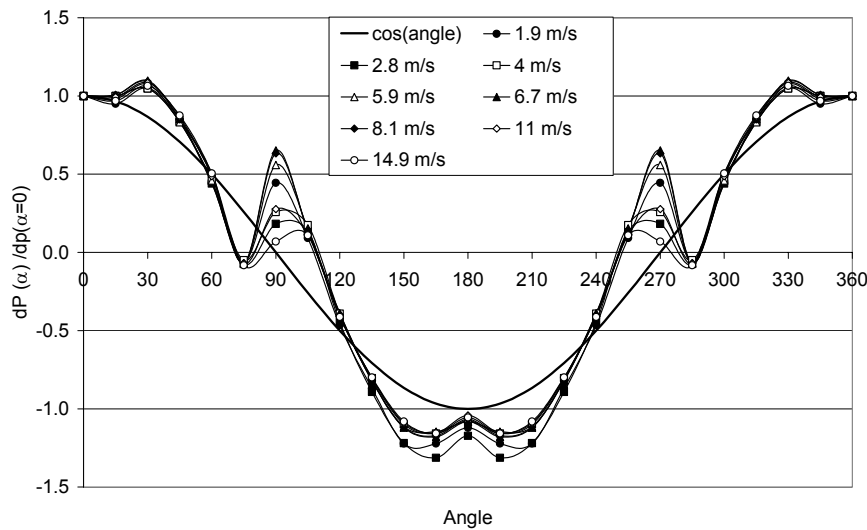


**Figure 4.19** Ratio of the pressure drop through the orifice against the angle of impact and the pressure drop at  $\alpha=0^\circ$ . Different wind speeds are considered. A theoretical cosine curve is also shown.

To minimise turbulence from the air flowing around the openings of the sampler both openings were equipped with a very smooth roundly sphere. The sphere was designed in such a way that turbulence caused by an airflow detaching from the sampler would not reach directly the opening of the sampler. Figure 4.20 shows that, after applying the spheres in the openings of the samplers, the disturbance was greatly reduced. The form of the curves for the different wind speeds applied closely resembles a cosine function. However, some of the peaks still remain. This requires further consideration. Due to the lack of enough spheres, they were used neither in Zegveld nor in Wageningen.

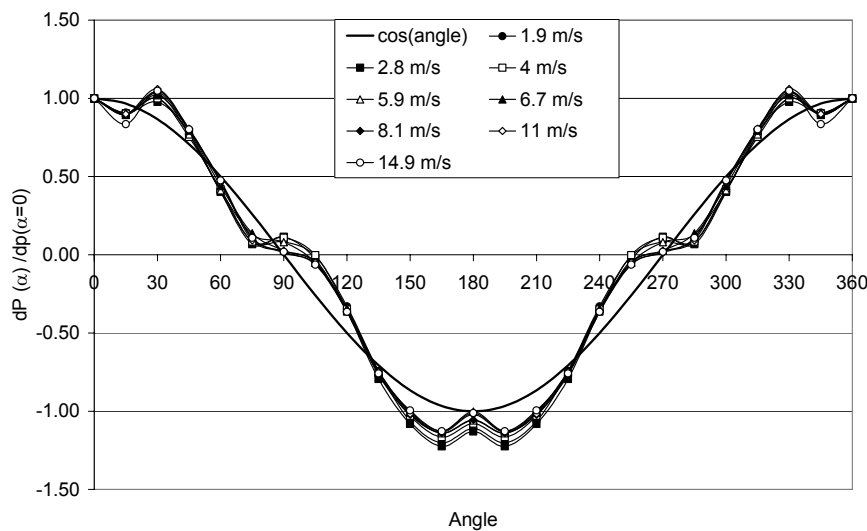


**Figure 4.20** Ratio of the pressure drop through the orifice against the angle of impact and the pressure drop at  $\alpha=0^\circ$ , for the straight sampler with spheres. Different wind speeds are considered. A theoretical cosine curve is also shown.

Ammonia concentrations were also measured semi-continuously by using the fast response sensor and AMANDA systems. Figure 4.21 shows, using the AMANDA system, the fast increase in concentration that occurs immediately after application of manure into the field. After that, the concentration decays exponentially with time, reaching background values after a period of approximately 1 day.

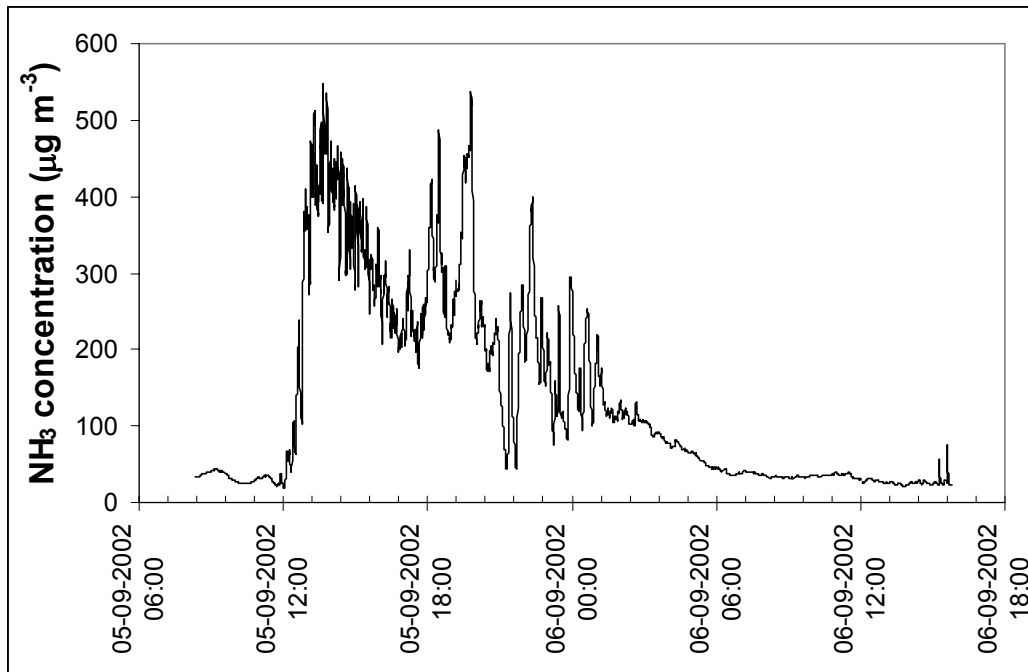


**Figure 4.21** Ammonia concentration measurements using the AMANDA system in Wageningen.

Because the fast response sensor does not measure absolute concentration values, it has to be calibrated before we can use those measurements. The procedure used is to compare the concentrations measured with the fast response sensor and the AMANDA, in the field, when both systems are located close to each other. Figure 4.22 shows the calibration curve (in the field) obtained for the experiments performed in Wageningen. Every point in the figure shows how the raw data from the fast response sensor (x-axis) relates to the simultaneous acquired AMANDA concentration levels. The fitting function can be used to calculate the corrected concentration level for all other positions of the fast response sensor. As an example, figure 4.23 shows the measured AMANDA concentrations, and the corrected concentrations measured with the fast response sensor, during the application of manure into the field. When the fast sensor moves out of the plume, as in the period around 13:10h shown in figure 4.23, different results can be obtained with both systems.

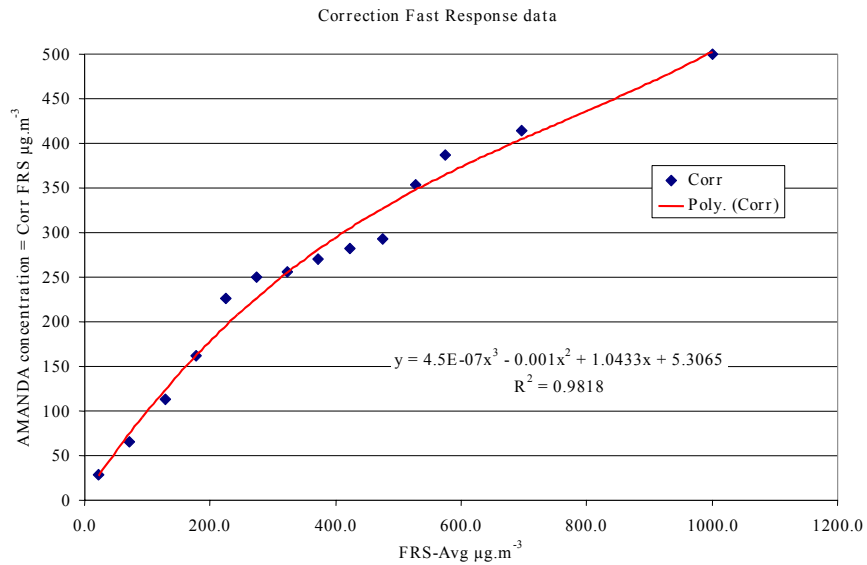


**Figure 4.22** Calibration curve (in the field) for the fast response sensor (FRS) using the AMANDA data as reference (Wageningen).

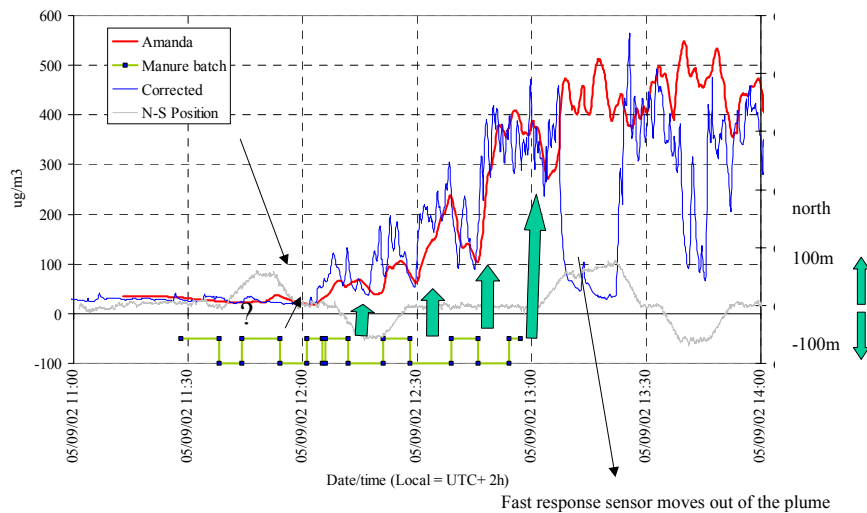
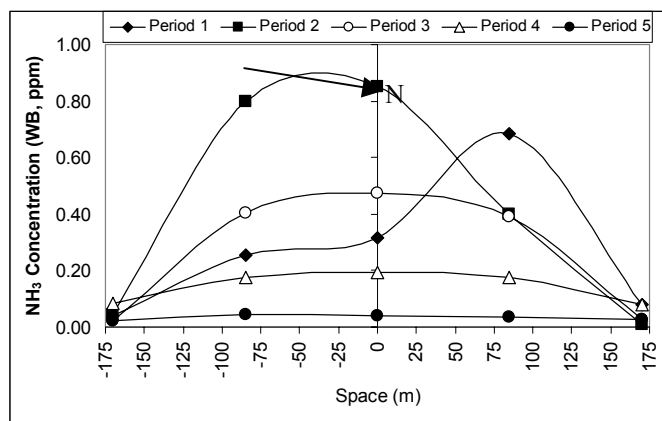


**Figure 4.23** Ammonia concentrations measured with the AMANDA, and corrected values of the concentrations measured with the fast response sensor, during the application of manure in Wageningen.

In this figure, the blocks show the periods where manure was applied in different part of the measurement field. The grey line gives the North-South coordinate of the fast sensor with respect to the AMANDA.

After the application of manure into the field, ammonia concentration plumes were observed, as shown in figures 4.24 and 4.25. Figure 4.24 shows the different average  $\text{NH}_3$  horizontal concentration profiles measured with the Willems badges for the five measurement periods considered in this analysis. In the first period, during manure

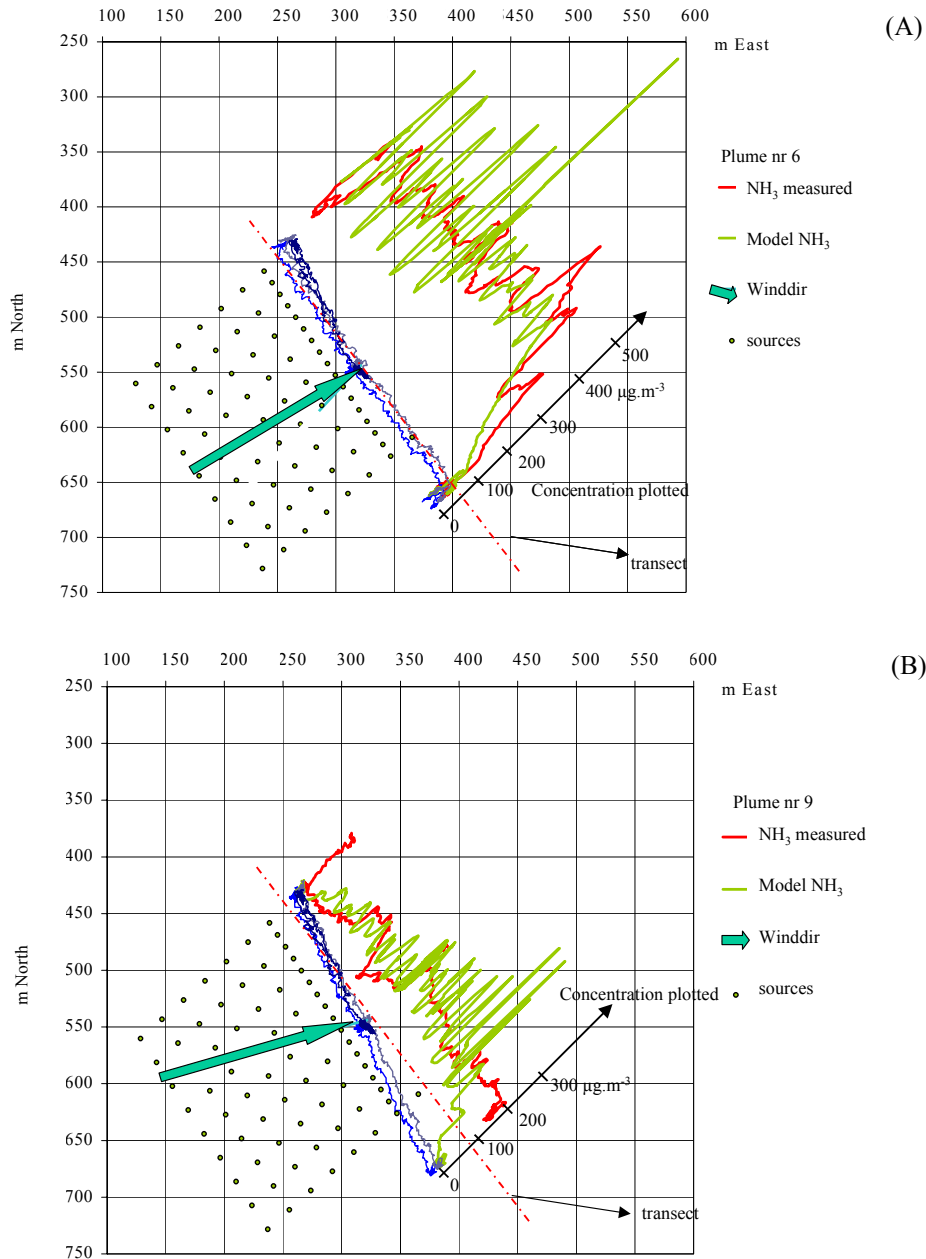
spreading, the wind direction was SSW. This explains the peak in concentration measured in the mast located in the northern part of the measurement site. As we walk south (left in the figure), the concentration decreases, getting a minimum value in the two measurement points outside the borders of the manured field. Wind direction changed from SSW to W at the end of period 1, and stayed in the W-SW are for periods 2 and 3, moving more to S-SW for periods 4 and 5. In these periods, a more uniform plume over the whole measurement field can be observed. Figure 4.24 also shows clearly the decrease in concentration with time after period 2. That the plume measured in period 2 has a higher concentration than the one measured in period 1 is explained by the fact that period 2 includes the emission from the 2 measurement fields, while part of period 1 comprises only the emission from 1 field.



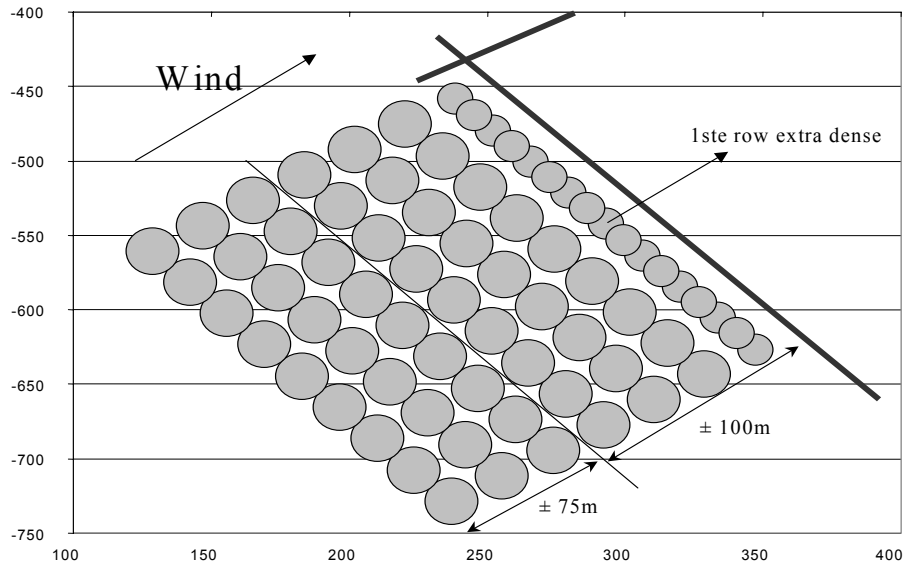
**Figure 4.24** Average ammonia plumes measured with the Willems badges in Wageningen, during the period 5-7 September 2002.

Figure 4.25 shows two examples of plumes measured with the fast response ammonia sensor. The results of the application of a gaussian plume model using the source configuration shown in figure 4.26 are also presented. In the first plume (figure 4.25a), the fast response sensor only stopped for a few minutes at the AMANDA site and then moved on along the measurement transect. Therefore the whole plume is acquired in a half hour time period where the concentration level over the whole plume changed only a little. However, the wind direction does change during this period. At the beginning of the experiment the wind direction is 244 degrees, explaining the position of the south edge of the plume. Going towards the AMANDA station the model shows an oscillating behavior, which is much stronger in the second part of the run, from the AMANDA further north. The reason is that we model the field with a limited number of emission points. Especially because the distance to the first emission points is only about 12 meter, avoiding this "spiky" pattern would require a lot more emission points. In the second part of the run the wind direction changed to 220 degrees, which apparently makes the wind coming over a line of sources, so the spikes and dips increase further. It looks then necessary to include more emission points in the model. Since this does not change the emission level estimate but only makes the model run look nicer, this was not done. It is clear that the very short distance between the model and the receptor in this measurement setup is not ideal,

inducing a larger uncertainty in the emission estimate. In the second plume (figure 4.25b), the wind direction is such that at the north end less and less area of the manured field is in the fetch of the measurement system, which explains the decrease in the concentration in that area, but not the high ammonia concentration peak measured at the north border of the field. Besides, a large difference is observed between the model and the measurements at the south border of the field.



**Figure 4.25** Two examples of plumes measured with the fast response sensor in Wageningen.



**Figure 4.26** Source distribution used in the Gaussian plume model (Wageningen).

Two of the measurement techniques applied in Wageningen (AMANDA, denuders) have been commonly used as a reference method in previous studies. Figure 4.27 shows the average ammonia concentrations as measured with the AMANDA and the denuders for the different measuring periods of this experiment. We can see that the concentration pattern measured with both techniques is the same. However, the absolute values measured with the denuders are systematically higher than the ones measured with the AMANDA. Different factors can be attributed to this systematic difference between both measuring techniques:

1. The denuder system was placed closer to the field than the AMANDA. That means that the influence of ammonia dispersion close to the source area and deposition will be smaller for the denuders in comparison with the AMANDA. And that will lead to higher ammonia concentrations in the denuders.
2. Besides, the denuders and the AMANDA were separated for a distance of approximately 30-40 m. Together with point 1, this means that the fetch area over the manured field for both measurement systems will not be the same for some particular wind directions. This is particularly important in the first measurement periods, when most of the emission occurs (and, therefore, higher concentrations can be measured).

These differences in the placement of both measurement methods makes it difficult to make a comparison between them. However, we have seen that both systems show the same concentration pattern versus time. Besides, the last measurement period (low concentrations) leads to a similar value for both techniques. Further experiments should be performed, with both techniques sharing the same conditions, in order to see if both techniques lead to the same final result.

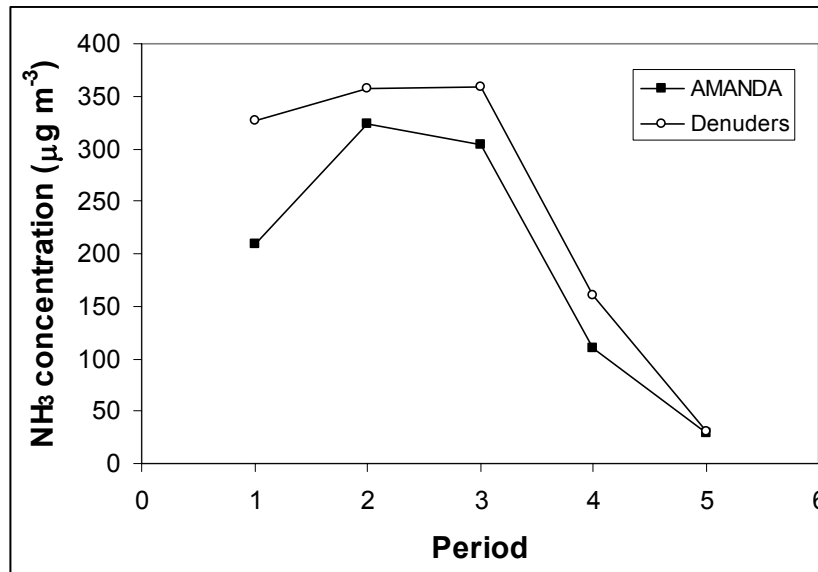


**Figure 4.27** Ammonia concentration versus time as measured with the denuders and the AMANDA in Wageningen.

#### 4.2.3 Horizontal Ammonia Flux

As for concentrations, when comparing the horizontal ammonia flux (figure 4.28) for the different techniques used in this experiment, the concentrations measured with the Willems badges and denuders show a good correlation, better than the one observed when comparing the concentrations measured with passive flux samplers and denuders. The cross design was not tested in Wageningen for the passive flux samplers, but simple samplers instead. The results are less satisfactory than the ones obtained with the cross design (Zegveld). Nevertheless, a good correlation is still observed.

When using both data sets (Zegveld and Wageningen), we can see (figure 4.29) that a good correlation is observed both for the Willems badges and the passive flux samplers, when compared with the reference system (denuders) and between them. Further improvements in the design and characterization of the ammonia passive flux samplers are necessary to make them suitable for the measurement of ammonia concentrations and fluxes after application of manure into the field. It is recommended to execute these improvements, because the passive flux samplers do not have the limitations of the denuders (electricity, flow measurements) or the Willems badges (necessary to measure the wind speed profile), especially for complex situations.

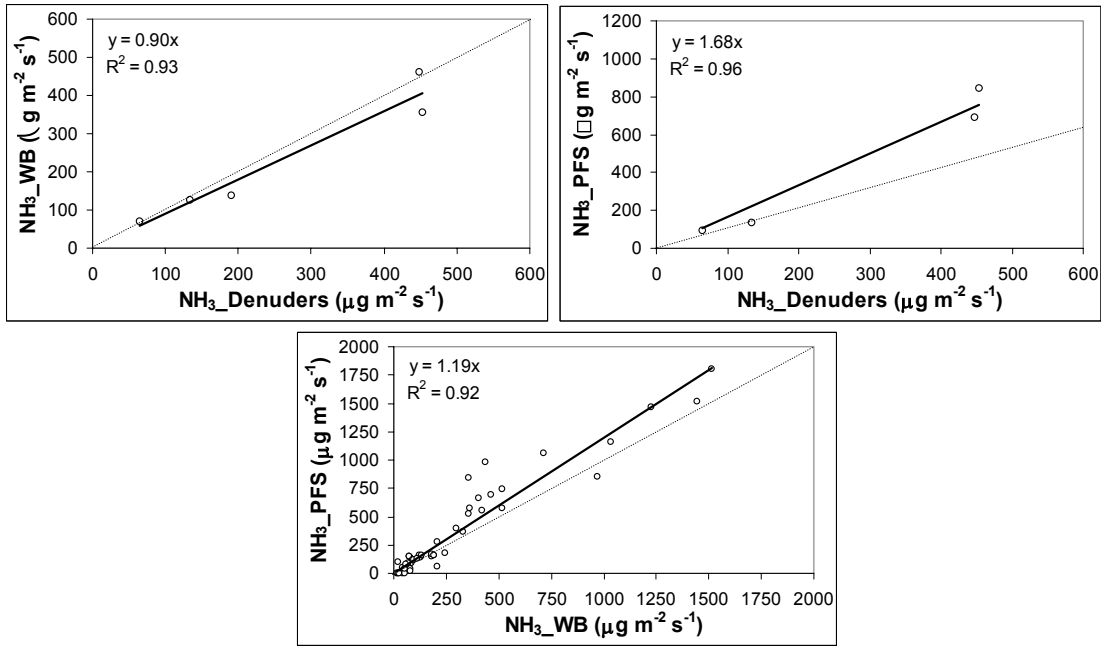


**Figure 4.28** Regression analysis showing the relation between the horizontal ammonia flux measured with fixed passive flux samplers (PFS), Willems badges (WB), and denuders, in Wageningen.

The dotted line represents the 1:1 relation between both methods.

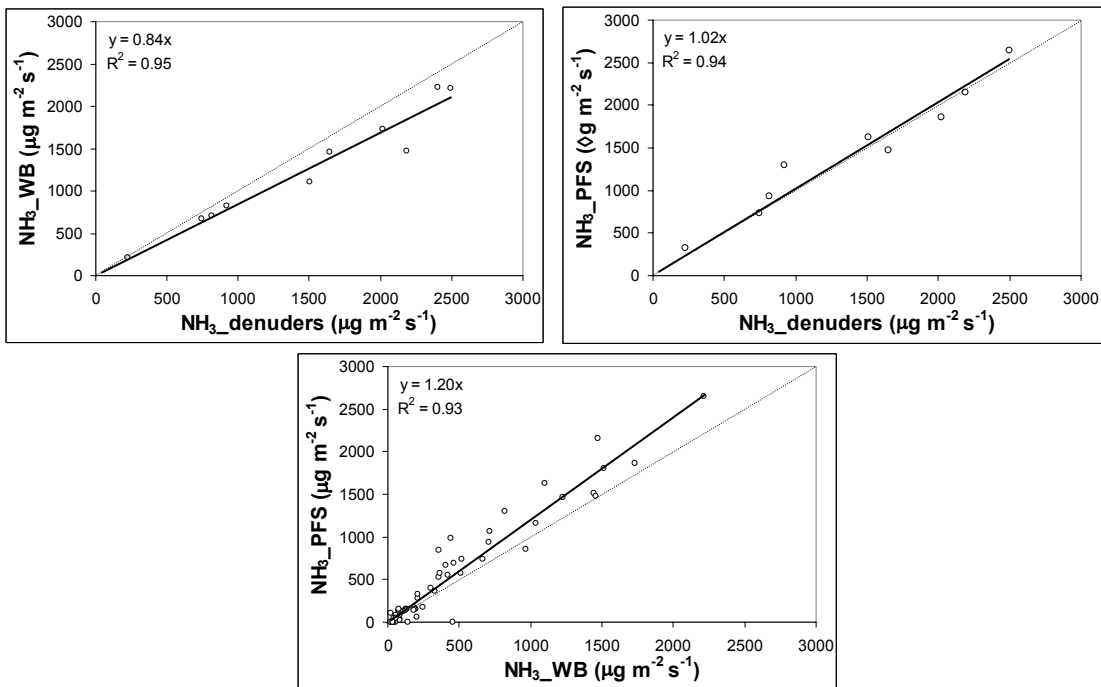


**Figure 4.29** Regression analysis showing the relation between the horizontal ammonia flux measured with fixed passive flux samplers (PFS), Willems badges (WB), and denuders for the data available both from Zegveld and Wageningen.

The dotted line represents the 1:1 relation between both methods.

#### 4.2.4 Vertical Ammonia Flux

To calculate the vertical ammonia flux, i.e. the emission from the field, for the averaging techniques (denuders, Willems badges and passive flux samplers) the following formula was used:

$$Q = \frac{A}{A_1} \cdot \int_{z=0}^{z=z_4} C(z) \cdot dz \cdot 1m \quad (4.1)$$

where  $A$  is the area of the field where manure application took place,  $A_1$  the footprint area (see figure 4.30),  $z_4$  the highest level where ammonia concentration measurements took place, and  $C(z)$  is the ammonia concentration profile with height. First the ammonia concentration profile was calculated (figure 4.31) as a function of the measurement height, using the concentration data from big mast (denuders) or the 5 m mast (passive flux samplers and Willems badges). Then the emission from the footprint area ( $A_1$ ) was determined, and the result scaled to the whole measurement field.

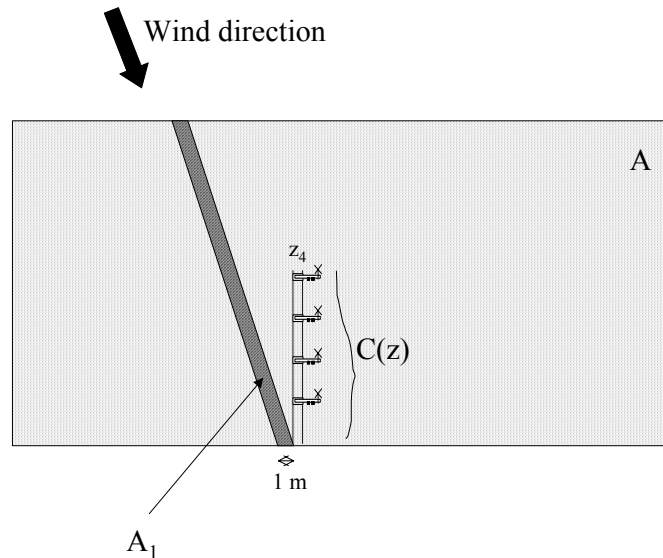


**Figure 4.30** Procedure used to calculate the ammonia emission from the field in Wageningen.

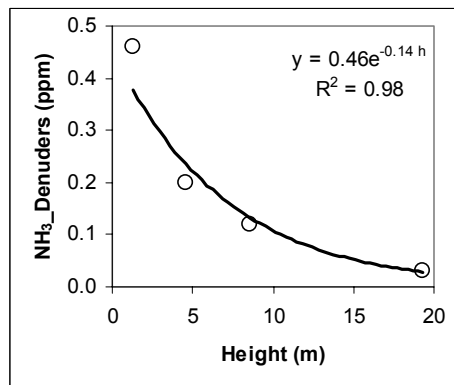


**Figure 4.31** Ammonia concentration profile calculated for the denuders for one of the measurement periods (Wageningen).

When comparing the different averaging techniques used to measure the ammonia emission after manure application into the field (figure 4.32), we can see that all techniques show an exponential decay of the emission with time. However, the emission levels differ between the different techniques during the first few hours after manure spreading, the period where most of the emission occurs. The denuder mast, being 20 m high, could capture more of the ammonia plume than the mast where both Willems badges and passive flux samplers were used (5 m high). In fact, when we compare the ammonia concentration measured at the highest level with the denuders, we see that we do not measure the background concentration, meaning that part of the plume is even not completely captured by that mast.

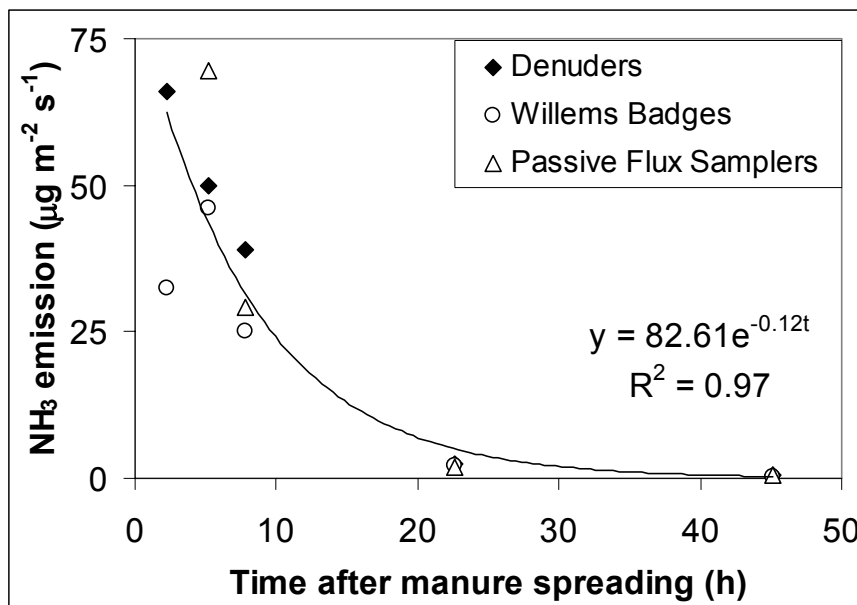


**Figure 4.32** Ammonia emission from the field as a function of time, using data from denuders, Willems badges, and passive flux samplers in Wageningen. The line represents the curve fit (exponential decay) using the denuder's data only.

Measurements with the denuders, passive flux samplers and Willems badges lead to an emission estimate (during the first 2 days after manure spreading into the field) of 16, 11.2 and 11.5 kg NH<sub>3</sub> ha<sup>-1</sup>, respectively (figure 4.33). This represents, respectively, 33%, 23% and 24% of the total NH<sub>3</sub> applied into the field. When using the information provided by the AMANDA system (figure 4.34), an emission estimate of 10.3 kg NH<sub>3</sub> ha<sup>-1</sup> is obtained. This represents 21% of the total NH<sub>3</sub> applied into the field. As we can see, the emission estimate obtained with the denuders is higher than the one measured with the other measuring techniques. This can be explained by the fact that measurements with denuders were performed up to a height of 20 m, while the other systems reach a maximum of 5 m. Therefore, a larger part of the plume can be measured with the denuders, in comparison to the other measurement techniques.

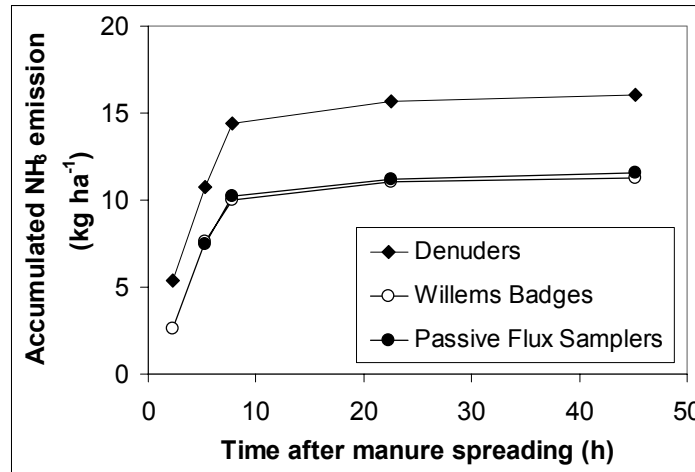


**Figure 4.33** Accumulated ammonia emission (vertical flux) after manure application into the field using denuders, Willems badges and passive flux samplers. Measurements were performed in Wageningen during the following periods: 1) 2 hours; 2) 5 hours; 3) 7.5 hours; 4) 22 hours and 5) 44 hours after manure application into the field.

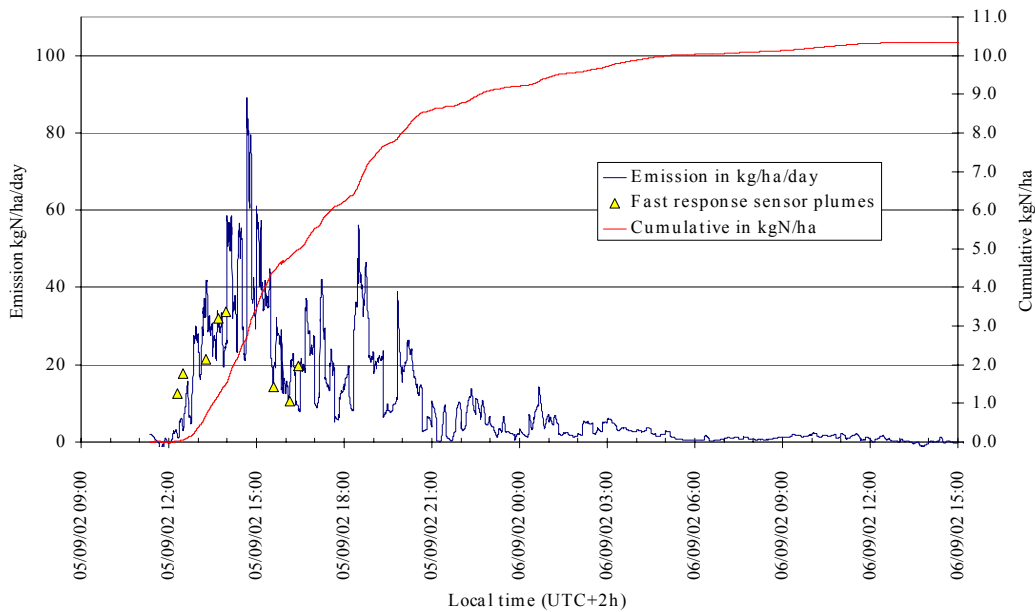


**Figure 4.34** Accumulated ammonia emission after manure application into the field using the AMANDA system (Wageningen).

When compared with the emission estimates obtained from the experiment in Zegveld (section 4.1), we can see that in Wageningen, both the total emission and the percentage of the total  $\text{NH}_3$  applied into the field that is emitted, are higher than the values measured in Zegveld. This can be explained by the fact that, during the measurement period in Wageningen, higher temperature and lower wind speed values were measured as compared with the measurement period in Zegveld. Higher temperature favors microbial activity, while low wind speeds allow the applied manure to dry slowly, and therefore both

situations are in favor of higher ammonia emissions. Besides, the slurry applied in Wageningen presented a higher ammonium-N content than the one applied in Zegveld. This will also lead to higher emissions.

## 5 Ammonia emissions from animal houses

### 5.1 Kootwijkerbroek: mechanically ventilated animal house

The measurements during the first few weeks, without mechanical ventilation, in the veal calves sheds showed clearly that the open ventilation shaft was the main exhaust opening the doors were relatively unimportant. Figure 5.1 shows the ammonia emission measured with the passive flux samplers (PFS) and calculated with the reference method, for the four different animal housing systems studied. As the animals increase in size and weight, an increase in ammonia emission is expected with time, which in fact is observed in all the different housing systems under consideration. The individual housing system seems to lead to smaller emissions when compared with the three group-housing systems. However, the number of animals in the individual housing system was also smaller than in the group-housing systems. In fact, when the emissions are normalised to emissions per animal, both the individual and the group-housing systems have a similar emission. For the synthetic-floor group-housing system, the one with highest emissions, a break-through of ammonia was observed for some of the samplers. These measurements are also reported here, although they are not used for the final interpretation of the results.

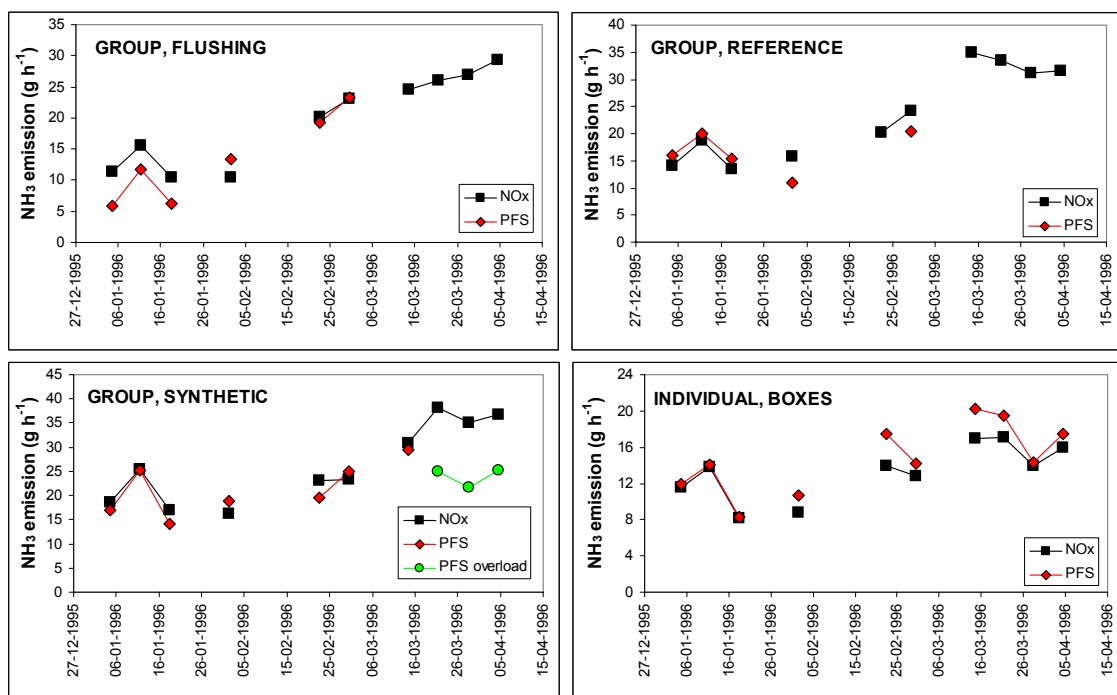


**Figure 5.1** Ammonia emission pattern ( $\text{g}\cdot\text{h}^{-1}$ ) as measured with passive flux samplers (PFS) beneath the ventilation shaft, and calculated with a reference method.

In general, for all the housing systems a good agreement is observed between the ammonia emission patterns calculated with the reference method and measured with the passive flux samplers (figure 5.2). This is reflected in an almost 1:1 line between both methods. However, a high variation in the data is also observed. For the group-housing system “synthetic”, a break-through of ammonia was observed in some samplers. This data is also shown in the figure, but not used for the comparison of both measuring techniques. A statistical test (t-test) was performed in order to see whether or not the difference between the measurements obtained with both methods (reference and passive flux samplers) was significant. The results of this analysis, summarised in table 5.1, show that the differences between both methods are not significant (at the 95% significance level) for the three group-housing systems. In the individual-housing system, the correlation between both methods is good but the differences are significant.

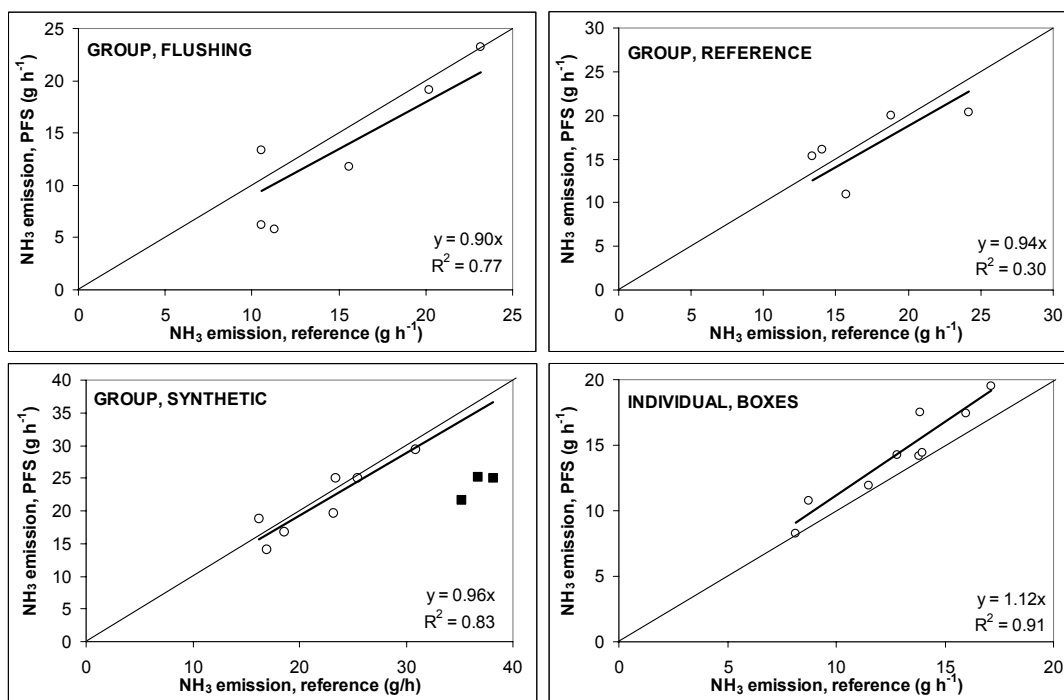


**Figure 5.2** Correlation between the NH<sub>3</sub> emission (g.h<sup>-1</sup>) measured with passive flux samplers (PFS) beneath the ventilation shaft, and calculated with the reference method. The squares represent observed overload of the passive flux samplers.

**Table 5.1** Statistical t-test (95% significance level) of the difference between the passive samplers and the reference system for each housing system.

Houses	Flushing	Synthetic	Reference	Boxes
Number of measurements	6	7	5	10
Average of  NOx - PFS	1.98	0.78	0.71	-1.54
Standard deviation	3.15	2.24	3.32	1.26
t	1.54	0.92	0.48	3.87
t (95%)	2.57	2.45	2.78	2.26

Figure 5.3 shows the results of combining the measurements performed in all different animal houses, but differentiating between measurements in the ventilation shaft with and without lid. As in figure 5.2, results where the break-through of ammonia was observed, are presented in the figure but not used for further calculations. Both in the ventilation shaft with lid and in the ventilation shaft without lid, both measurement techniques show similar results, but the data still shows a high variability. In this case, the statistical t-test (table 5.2) shows that the differences between both measurement techniques are not significant (95% significance level) for the ventilation shaft with lid. This is observed individually, for all the housing systems, and when we combine the data from all housing systems. For the ventilation shaft without lid, the combination of all data leads to the same results: no significant differences (95% significance level) between both measuring techniques. However, this is not the case for the group-housing system “synthetic”, and the individual (boxes) housing system.

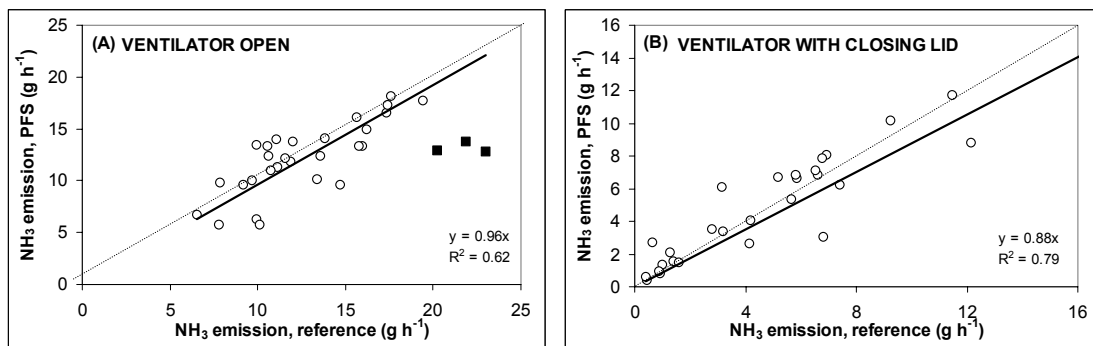


**Figure 5.3** Comparison between the reference method and the PFS for the two different ventilators present in the animal house.

The squares represent observed overload of the passive flux samplers.

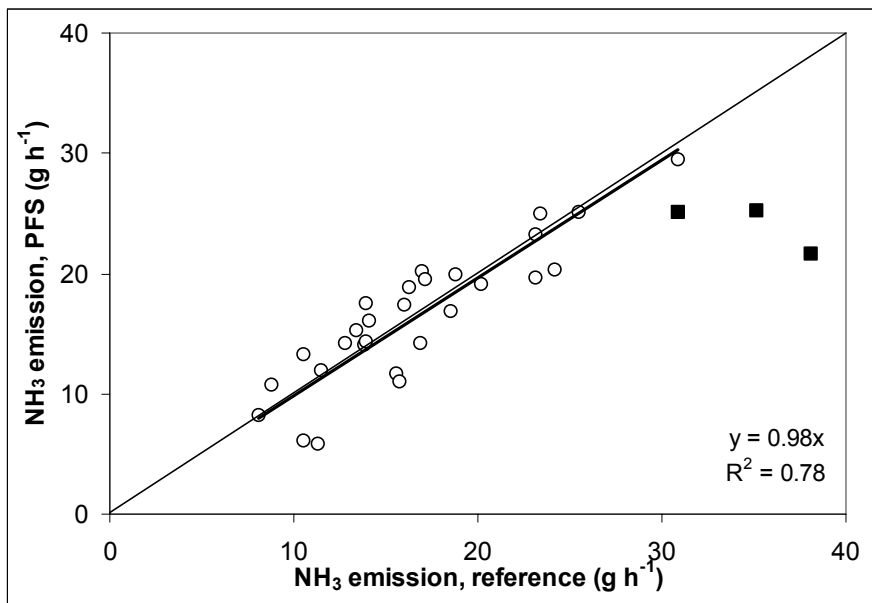
**Table 5.2** Statistical t-test (95% significance level) of the difference between the passive samplers and the reference system for the ventilation shafts with and without lid.

Shaft without lid	Flushing	Synthetic	Reference	Boxes	Total
Number of measurements	6	7	5	10	28
Average of $ \text{NOx}  -  \text{PFS} $	1.51	1.43	-0.01	-0.89	0.36
Standard deviation	2.52	1.51	3.22	0.94	2.17
$ t $	1.47	2.52	0.01	3.00	0.88
t (95%)	2.57	2.45	2.78	2.26	2.05

Shaft with lid	Flushing	Synthetic	Reference	Boxes	Total
Number of measurements	4	10	5	10	29
Average of $ \text{NOx}  -  \text{PFS} $	-0.17	0.79	0.71	-0.65	0.15
Standard deviation	0.45	2.52	1.93	0.92	1.82
$ t $	0.75	1.00	0.82	2.23	0.44
t (95%)	3.18	2.26	2.78	2.26	2.05

Figure 5.4 shows the result of combining all measurements (i.e., for all housing systems, and both for the ventilation shaft with lid and without lid). Once again, the points showing the breakthrough of ammonia in the sampler are also presented in the figure, but are not used in the linear regression. The statistical t-test (table 5.3) shows that, when combining all measurements, the differences between both methods are not significant at the 95% significance level. In this way, passive flux samplers offer a new way of measuring the ammonia emission from mechanically ventilated animal houses.



**Figure 5.4** Comparison between reference method and the new concept for measuring ammonia emissions ( $\text{g}\cdot\text{h}^{-1}$ ) from mechanically ventilated buildings. The squares represent observed overload of the passive flux samplers.

**Table 5.3** Statistical t-test (95% significance level) of the difference between the passive samplers and the reference system combining all measurements.

Houses	Total
Number of measurements	28
Average of $ \text{NO}_x  -  \text{PFS} $	0.20
Standard deviation	2.66
$ t $	0.39
$t$ (95%)	2.05

## 5.2 Barneveld: naturally ventilated poultry house

As discussed in section 3.2.2, wind direction (and wind speed) measurements were taken at the measurement site at two different heights: the first measurement day at a height of 2 m, and the second measurement day at a height of 10 m. Besides, data from a meteorological station in Wageningen (19 km from Barneveld) was also collected at a height of 10 m. Figure 5.5 shows the results of the comparison between both meteorological data sets. The first remarkable point is that both data sets are consistent (similar values) only in the last day (second measurement day), when meteorological measurements took place at the same height (10 m), well above the height of the building (4 m). The measurements in Barneveld, at a height of 2 m, clearly show the influence of the animal house in the wind pattern between the building and the meteorological mast. For winds in the East-South wind direction range, the two data sets (Wageningen and Barneveld) follow the same pattern. The small shift in the data observed between both data sets could be due to an error in the orientation of the windvane at the measurement site. In this wind sector range, measurements at the meteorological mast are not disturbed by the presence of the building.

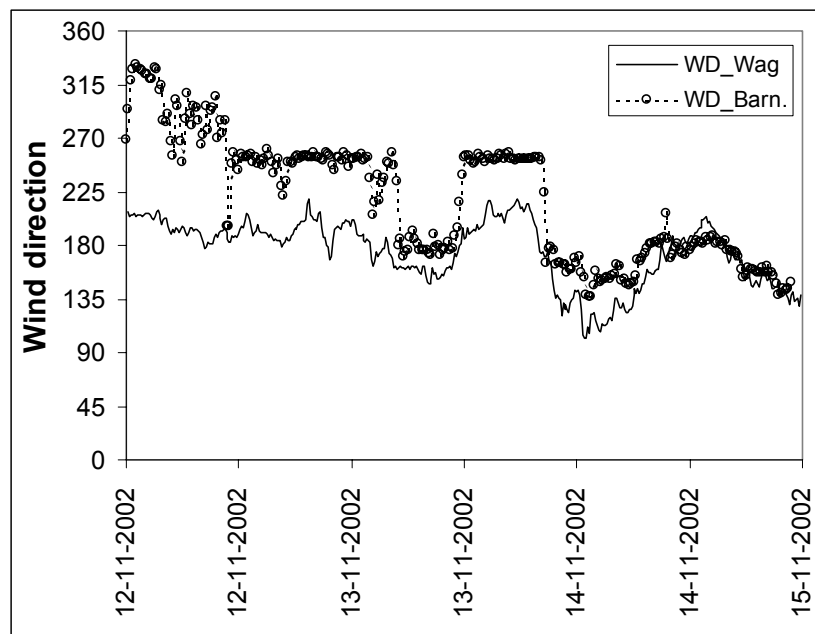


**Figure 5.5** Comparison of wind direction measurements at Barneveld and Wageningen.

However, for winds in the Southwest wind sector range, the building does affect the wind pattern at low heights. In this case, wind flows along the long axis of the building (Z-ZW, approximately  $240^\circ$ ), approximately the same angle that is measured at the meteorological mast at the height of 2 m. This also explains that, when looking at the amount of ammonia sampled in the four passive flux samplers (cross design, see section 2.2), this value is high not only in the two samplers oriented to the animal house, but also in a third sampler, oriented approximately to the West.

Figure 5.6 shows the horizontal ammonia flux measured with the passive flux samplers in a cross design, for each height and measurement mast, using the procedure described in section 2.2. In both measurement periods, wind was blowing (on average) from the Z-ZW wind sector range. When looking at the mast configuration, we can see the same pattern distribution for the measured horizontal ammonia flux in both periods: masts M1-M3 have the highest horizontal flux values, while M5 gives in general low values. Figure 5.6 also shows the dispersion of the emitted ammonia plume with height. As expected, since ammonia leaves the building at a height of approximately 2 m, the maximum horizontal fluxes are measured at the lowest levels, particularly at level 2 (height of 2.89 m). As the measurement height increases, the plume is increasingly dispersed, and a lower horizontal flux is measured.

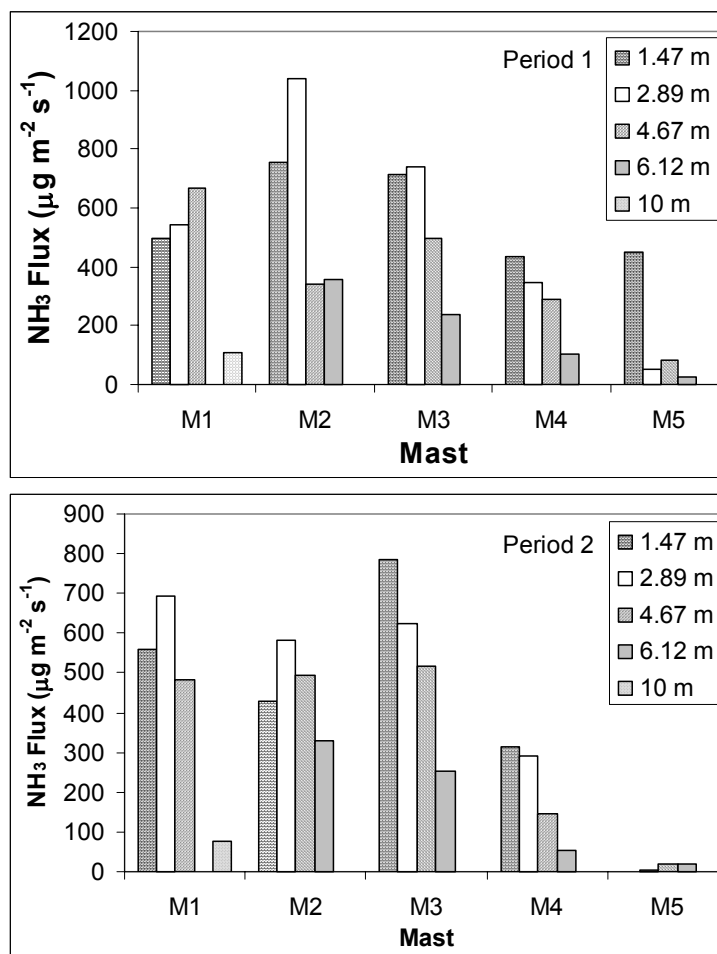


**Figure 5.6** Horizontal ammonia flux measured in Barneveld with the passive flux samplers in a cross design.

See figure 3.14 for a description of the different mast categories.

To calculate the ammonia emission from each part of the animal house, the following process was followed (figure 5.7):

1. The first step is to determine the average wind direction during the sampling period of the passive flux samplers. Besides, we should check whether or not the wind direction experienced large variations. For both measurement periods, the wind direction was rather constant (see table 5.4 for an overview): averages of 191° (data from Wageningen) and 181° (data from Barneveld) were obtained for periods 1 and 2, respectively.
2. The next step is to determine the representative emission area of the animal house for each mast. When part of this area lies outside the animal house, a correction factor (percentage of the representative emission area inside the animal house) should be applied. Figure 5.7 shows an example of how to calculate this emission area for a particular mast.
3. Assuming an undisturbed wind pattern, determine which mast would collect the ammonia emitted by each part of the animal house. In both periods, with winds in the Z-ZW wind sector range, ammonia emission from part B1 of the animal house will be mainly collected by masts M1 and M2. Correspondingly, ammonia emitted from part B2 of the animal house will be mainly collected by masts M3 and M4.
4. The emission from each part of the animal house can be then calculated by:

$$E_i = 10^{-6} \cdot \sum_{k=1}^m \left( \sum_{j=1}^n (F_j^k \cdot (h_j^k - h_{j-1}^k) \cdot \Delta t_j^k) \cdot d^k \cdot A^k \right) \quad (4.2)$$

where

- $i$  = part of the animal house being studied (1=B1; 2=B2)
- $j$  = measuring height in the mast (1=lowest level)
- $n$  = number of measuring levels (n=4 in this experiment)
- $k$  = mast being considered (M1-M5)
- $m$  = number of masts considered to be representative for each part of the house
- $\Delta t_j^k$  = sampling time interval for the samplers in mast  $k$  and height  $j$  (seconds)
- $h_j^k$  = representative height ( $j$ , meters) for the measurements at the mast  $k$  ( $h_0^k=0$ )
- $d^k$  = distance (meters) between two adjacent masts
- $A^k$  = correction factor (adimensional) to account for overestimation of the representative emission area in the animal house
- $F_j^k$  = horizontal ammonia flux ( $\mu\text{g m}^{-2} \text{s}^{-1}$ ) measured at height  $j$ , at the mast  $k$
- $E_i$  = amount of ammonia (grams) emitted by part  $i$  of the animal house

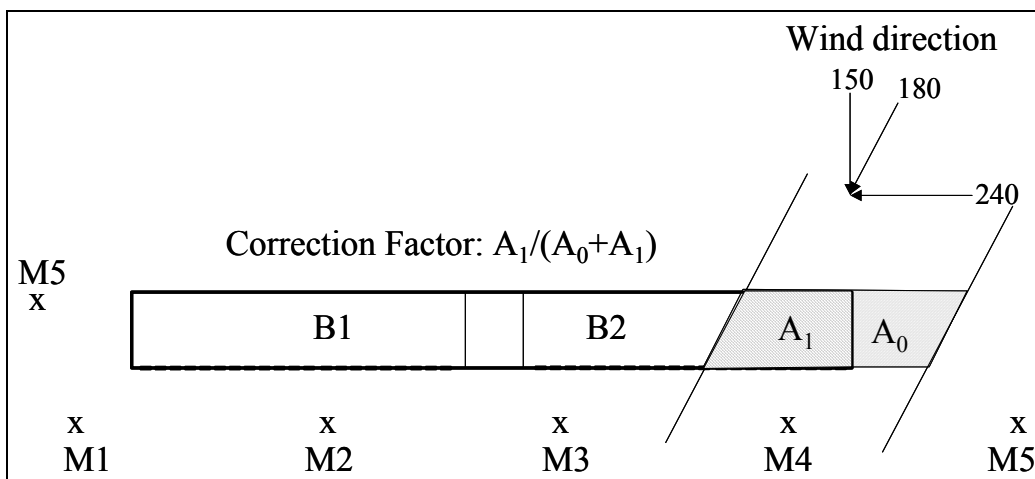


**Figure 5.7** Schematic representation of the method used to calculate the ammonia emission in Barneveld.

**Table 5.4** Statistical summary of the wind direction in Barneveld.

Period	Minimum	Maximum	Average	Median
1	178	207	191	190
2	172	188	181	182

Table 5.5 summarises the main results of this study. For the ammonia emitted from part B2 of the animal house, period 1 shows an underestimation of the emission, while period 2 shows an overestimation (6 %) of the emitted ammonia. In both cases, the differences between the applied and the measured ammonia are in the order of 10%. For part B1 of the animal house, a different analysis has to be done. As discussed above, the building was affecting the wind pattern between the animal house and the measuring masts. That means that masts M1 and M2, while in an undisturbed flow pattern will collect only ammonia coming from part B1, in this case they are also measuring part of the ammonia coming from part B2. When looking at the data presented in table 5.5, we can see that the percentage of the emission from part B2 collected by masts M1 and M2 is in the order of 57 % and 75 %, for periods 1 and 2, respectively.

**Table 5.5** Measured versus applied ammonia in the experiment in Barneveld.

Period/House part	Measured (gr NH <sub>3</sub> )	Applied (gr NH <sub>3</sub> )
Period 1/B1	2293	1150
Period 1/B2	1813	2000
Total Period 1	4106	3150
Period 2-B1	2252	1100
Period 2/B2	1649	1500
Total Period 2	3901	2600

## 6 Conclusions and recommendations

### 6.1 Ammonia emission after application of slurry into the field

1. Two of the measuring techniques (AMANDA, denuders) applied in the Wageningen experiment have been commonly used as a reference method for field emissions. Both techniques showed the same concentration pattern. However, the absolute values measured with the denuders were systematically higher than the ones measured with the AMANDA. A field comparison is needed in situations with rapid fluctuation in concentrations. For a constant concentration the comparison will be good. Different factors have been attributed to this systematic difference between both measuring techniques:
  - a) Ammonia deposition and less dilution of the emitted ammonia from the nearby field. Because the denuder system was placed closer to the field than the AMANDA, the influence of ammonia deposition and dilution will be smaller for the denuders in comparison with the AMANDA. This will lead to higher ammonia concentrations in the denuders.
  - b) Fetch area. The denuders and the AMANDA were separated for a distance of approximately 30-40 m. For some wind directions, the fetch area (representative emission area) will not be the same for both techniques. In general, for the prevailing winds during the experiment, the fetch area was higher for denuders than for the AMANDA, i.e. higher concentrations are expected to be measured with the denuders.
2. A thorough comparison should be made between the Amanda and the fast  $\text{NH}_3$  sensor in a situation with stable concentrations (laboratory) and fast changing situations. This because the response time of both systems is very different. This will shed light on the non-linear calibration curve to convert fast sensor data in absolute values with the aid of the AMANDA signal.
3. The  $\text{NO}_x$  monitor+converters system (Zegveld) shows an emission pattern that corresponds with what it is expected to occur in the field after manure spreading. However, a poor correlation is obtained when compared with the reference system (denuders). Absorption/desorption of ammonia through the sampling system could have an effect on this. The  $\text{NO}_x$  monitor+converters system cannot be used for low  $\text{NH}_3$  concentrations. Refrain from using a  $\text{NO}_x$  monitor for gradient measurements unless sampling lines are very short and ammonia concentrations high. For measurements in animal houses, where  $\text{NH}_3$  concentrations are usually high, this restriction does not apply.

4. Willems badges give, in general, better results (close to the reference system, denuders) than the passive flux samplers or the chemiluminescence NO<sub>x</sub> monitor+converters system. The results for the Willems badges are consistent in both locations studied (Zegveld and Wageningen), with a regression line (Willems badges vs. denuders) similar for both data sets. The following improvements are suggested:
  - a) Redesign of the entrance according to proposal made by Hofschreuder *et al* (1999). This reduces the external resistance resulting in an increase in sampled mass and less influence of external wind speed.
  - b) Use of a coating with more acid capacity (H<sub>2</sub>SO<sub>4</sub>) to maintain low equilibrium concentrations at the absorption surface even in situations with high ambient concentrations.
5. While the correlation between passive flux samplers and denuders is good both in the experiments in Zegveld and Wageningen, data from Wageningen show a factor-2 difference between both techniques. This suggests that the cross system, as used in Zegveld, should be used for further measurements. That the cross system leads to better results than the straight configuration could be due to the cosine dependency of the samplers. In the cross configuration, an average value (close to the cosine curve) is obtained, in the straight sampler there is more uncertainty for some angles (close to 90° and 270°). Using some cups/spheres in both openings of the sampler can make this uncertainty smaller. Optimisation of the sampler for low wind speeds is advised.
6. A bigger percentage of the NH<sub>3</sub> applied into the field is emitted in the experiments performed in Ossekampen when compared with Zegveld. Higher temperature, lower wind speed, and higher ammonium-N content in the slurry applied in Ossekampen are suggested as explanation of this effect. From the results of both experiments, it can be concluded that 15-40% of the inorganic N applied into the field is emitted during the first 48 hours. A percentage of 80-90% of the total emission was emitted during the first 8 hours after the application of manure.
7. When we are interested to show the dynamics with time of the ammonia emission after slurry application into the field, the AMANDA gradient system performs well. When the main question is to measure the ammonia emission for a specific period of time, accumulation techniques (denuders, Willems badges, passive flux samplers) in a flux frame or gradient approach are a good alternative. In particular for complex situations, use of passive flux samplers is recommended. Passive flux samplers are independent of electricity (denuders, AMANDA), airflow measurements (denuders), or wind speed profile measurements (Willems badges).

8. When gradient measurements are made to estimate the flux density of a field the height of masts is not an important factor, provided the fetch is large enough to get an accommodated surface layer up to the top of the mast. When the mass balance method is chosen, the mast should extend to about one fifth of the fetch of the field. This will be easily achieved by using pneumatic towers (commercially available up to 30 m).

## 6.2 Ammonia emission from mechanically ventilated animal houses

1. The use of ammonia passive flux samplers under the ventilation shafts of mechanically ventilated animal houses looks very promising as an alternative to the  $\text{NO}_x$  monitor (after conversion of  $\text{NH}_3$  to  $\text{NO}$ ), the reference method in the Netherlands to measure ammonia emissions from mechanically ventilated animal houses. One important point to consider here is the time scale of the measurements. The  $\text{NO}_x$  monitor measures  $\text{NH}_3$  concentrations semi-continuously, which makes it appropriate for process-level studies. On the other hand, passive flux samplers can be used for sampling periods of days to weeks, and are thus appropriate for estimates of the  $\text{NH}_3$  emission at this time scale.
2. Passive flux samplers seem to underestimate the ammonia emission when compared to the reference method ( $\text{NO}_x$  chemiluminescence monitor, after conversion of  $\text{NH}_3$  to  $\text{NO}$ ). However, a statistical t-test shows that the differences between both measuring techniques are not significant at the 95% significance level when combining all measurements.
3. The use of a lid in the ventilation shaft to regulate the temperature inside the animal house improves the correlation (less variation) between passive flux samplers and the reference method. The lid, when open, can force the airflow to be aligned with the samplers and, in this way, reduce the cosine dependency of the samplers. New measurements should be performed in order to see the influence of the lid in the constant factor  $K_s$  of the sampler.
4. Two aspects need further attention for general use of the passive flux sampler method:
  - a) The coating of the paper lining of the tubes should have more capacity to prevent overloading of the sampler. The use of  $\text{H}_2\text{SO}_4$  instead of phosphoric acid or tartaric acid should be investigated.
  - b) Flow distortion from obstacles in the ventilation duct (e.g. a closing lid) and the flow from below towards the samplers should get further attention. The effect of using flow-guiding inlets (spheres) in the openings of the samplers should be studied.

### 6.3 Ammonia emission from naturally ventilated animal houses

1. Currently, the method used by IMAG to measure the ammonia emission from naturally ventilated animal houses relies in ammonia concentration measurements inside the building, and the estimation of the ventilation rate by using a tracer gas. However, when mixing conditions are not good enough, the use of a tracer gas is not adequate. In these situations, measurements should be done outside the building. However, measurements outside the building suffer from flow distortion by the building and surrounding obstacles.
2. Results using the flux frame method with passive flux samplers to measure the ammonia emission from naturally ventilated animal houses are promising. Section 5.2 also shows the complexity of measuring the ammonia emission outside the animal house:
  - Close to the animal house, building effects are important, affecting the flow pattern between the house and the measuring equipment.
  - However, far from the animal house the measuring points should be placed at a higher level, to be sure that we are capturing the whole ammonia plume.
3. Recommendations for improvement of the measurement system are:
  - a) Explore other methods for interpretation of the obtained results.
  - b) Make an inventory of flows around obstacles (like it is done for the National Model) to design a better strategy for the measurements to be performed.
  - c) By using the fast response ammonia sensor, information about the width of the plume can be obtained. This information can be used to set up a flux frame measurement system wide and high enough to capture the whole plume. The plume method is not an alternative when measuring close to obstacles since the form and distribution of dilution factors within the plume are undefined.

## References

- Adema, E.H., Meijstrik, V. and Binek, B. (1991). The determination of NH<sub>3</sub> concentration gradients in a spruce forest in south Bohemia, CSSR, 1988, using a passive sampling technique. Agricultural University, Wageningen, *Report R-501*, 15 pp.
- Allen, A.G., Harrison, R.M. and Wake, M.T. (1988). A meso-scale study of the behaviour of atmospheric ammonia and ammonium. *Atmospheric Environment* **22**, 1347-1353.
- Aneja, V.P., Stahel, E.P., Rogers, H.H., Witherspoon, A.M. and Heck, W.W. (1978). Calibration and performance of a thermal converter in continuous atmospheric monitoring of ammonia. *Analytical Chemistry* **50**, 1705-1707.
- Anonymous (1996). Environmental balance 96 (in Dutch). Samson H.D. Tjeenk Willink bv, Alphen a/d Rijn, 142 pp.
- Asman, W.A.H. (1995). Ammonia and ammonium in the atmosphere: present knowledge and recommendations for further research. In *Acid Rain Research: do we have enough answers?* (ed. Heij, G.J. and Erisman, J.W.), pp. 55-70. Elsevier Science B.V., Amsterdam.
- Beljaars, A.C.M., Holtslag, A.A.M., Westrhenen, R.M. van (1989). Description of a software library for the calculation of surface fluxes. Technical report TR-112, Royal Netherlands Meteorological Institute (KNMI), De Bilt, The Netherlands.
- Binkley, D. and Richter, D. (1987). Nutrient cycles and H<sup>+</sup> budgets of forest ecosystems. *Adv. Ecol. Res.* **16**, 1-51.
- Black, A.S., Sherlock, R.R., Smith, N.P and Cameron, K.C. (1989). Ammonia volatilisation from urea broadcast in spring on to autumn-sown wheat. *NZ J. Crop. Hort. Sci.* **17**, 175-182.
- Blatter, A., Fahrni, M. and Neftel, A. (1992). A new generation of NH<sub>3</sub> passive samplers. In *Development of analytical techniques for atmospheric pollutants* (ed. Allegrini, I.), pp. 171-176. Air Pollution Research Report 41, Commission of the European Communities, Brussels.
- Bobbink, R., Boxman, D., Fremstad, E., Heil, G., Houdijk, A. and Roelofs, J. (1992). Critical loads for nitrogen eutrophication of terrestrial and wetland ecosystems based upon changes in vegetation and fauna. In *Critical loads for nitrogen* (Eds. Grennfelt, P. and Thörnelöf, E.), p.41. Nordic Council of Ministers, Copenhagen.
- Bouwman, A.F., Lee, D.S., Asman, W.A.H., Dentener, F.J., van der Hoek, K.W. and Olivier, J.G.J. (1997). A global high resolution inventory of ammonia emissions. *Global Biogeochemical Cycles* **11**, 561-587.
- Breitenbach, L.P. and Shelef, M. (1973). Development of a method for the analysis of NO<sub>2</sub> and NH<sub>3</sub> by NO-measuring instruments. *Journal of Air Pollution Control Association* **23(2)**, 128-131.
- Brunke, R. Alvo, P. Schuepp, P. and Gordon, R. (1988). Effect of meteorological parameters on ammonia loss from manure in the field. *J. Environ. Qual.* **17**, 431-436.

- Demmers, T.G.M., Burgess, L.R., Short, J.L., Phillips, V.R., Clark, J.A. and Wathes, C.M. (1999). Ammonia emissions from two mechanically ventilated UK livestock buildings. *Atmospheric Environment* **33**, 217-227.
- Denmead, O.T. (1983). Micrometeorological methods for measuring gaseous losses of nitrogen in the field. In *Gaseous Loss of Nitrogen from plant-soil systems* (eds. Freney, J.R. and Simpson, J.R.), pp. 133-157. Martinus Nijhoff/dr. W. Junk, The Hague.
- Droppo, J.G. Jr. (1985). Concurrent measurements of ozone dry deposition using eddy correlation and profile flux methods. *J. Geophys. Res.* **90**, 2111-2118.
- Dyer, A.J. (1974). A review of flux-profile relationships. *Boundary Layer Meteorology* **7**, 363-372.
- Dyer, A.J. and Hicks, B.B. (1970). Flux gradient relationships in the constant flux layer. *Q. J. Roy. Met. Soc.* **96**, 715.
- Erisman, J.W. and Bleeker, A. (1997). Emission concentration and deposition of acidifying substances. In *Studies in Environmental Research* **69** (eds. Hey, G.J. and Erisman, J.W.), pp. 21-82. Elsevier, Amsterdam.
- Erisman, J.W. and Wyers, G.P. (1993). Continuous measurements of surface exchange of SO<sub>2</sub> and NH<sub>3</sub>. Implications for their possible interaction in the deposition process. *Atmospheric Environment* **27A(13)**, 1937-1949.
- Erisman, J.W., Vermetten, A.W.M., Asman, W.A.H., Slanina, J. and Waijers-Ijpelaar, A. (1988). Vertical distribution of gases and aerosols: the behaviour of ammonia and related components in the lower atmosphere. *Atmospheric Environment* **22**, 1153-1160.
- Ferm, M. (1986). Concentration measurements and equilibrium studies of ammonium, nitrate and sulphur species in air and precipitation. Ph.D. thesis Dep. of Inorganic Chemistry, Chalmers Tekniska Högskola, Gothenburg, Sweden.
- Galloway, J.N. (1995). Acid deposition: perspectives in time and space. *Water, Air and Soil Pollution* **85**, 15-24.
- Ferm, M., Schjoerring, J.K., Sommer, S. G. and Nielsen, S. B. (1991). Field investigation of methods to measure ammonia volatilisation. In: *Odour and Ammonia Emissions from livestock Farming* (eds. V.C. Nielsen, J.H. Voorburg and P. l'Hermite), pp. 148-155. Elsevier Applied Science, Barking, Essex, UK.
- Fontijn, A., Sabadell, A.J. and Ronco, R.J. (1970). Homogeneous chemiluminescent measurement of nitric oxide with ozone. *Analytical Chemistry* **42**, 575.
- Galloway, J.N. (1995). Acid deposition: perspectives in time and space. *Water, Air and Soil Pollution* **85**, 15-24.
- Groenestein, C.M. (1993). Animal-waste management and emission of ammonia from livestock housing systems: field studies. In *Proceedings of the Fourth International Symposium "Livestock Environment IV, 6-9 July 1993"* (eds. E. Collins and C. Boon), pp. 1169-1175. American Society of Agricultural Engineers, Coventry, UK.
- Groenestein, C.M., Hol, J.M.G., Vermeer, H.M., Den Hartog, L.A. and Metz, J.H.M. (2001). Ammonia emission from individual- and group-housing systems for sows. *Netherlands Journal of Agricultural Science* **49**, 313-322.

- Groot Koerkamp, P.W.G., Metz, J.H.M., Uenk, G.H., Phillips, V.R., Holden, M.R., Sneath, R.W., Short, J.L., White, R.P., Hartung, J., Seedorf, J., Schröder, M., Linkert, K.H., Pedersen, S., Takai, H., Johnsen, J.O. and Wathes, C.M. (1998). Concentrations and emissions of ammonia in livestock buildings in Northern Europe. *Journal of Agricultural Engineering Research* **70**, 79-95.
- Gryning, S.E., Holtslag, A.A., Irwin, J.S. and Sivertsev, B. (1987). Applied dispersion modeling based on meteorological scaling parameters. *Atmospheric Environment* **21**, 79-89.
- Hansen, B., Nørnberg, P. and Rasmussen, K.R. (1998). Atmospheric ammonia exchange on a heathland in Denmark. *Atmospheric Environment* **32**, 461-464.
- Heij, G.J. and Schneider, T. (1995). Dutch Priority Programme on Acidification. Final report No. 300-05 (in Dutch). RIVM, Bilthoven, The Netherlands.
- Heil, G.W. and Bruggink, M. (1987). Competition for nutrients between *Calluna vulgaris* (L.) Hull and *Molinia caerulea* (L.) Moench. *Oecologia* **73**, 105-107.
- Hess, H.J. and Hügle, T. (1994). Vergleichende Messung zur NH<sub>3</sub>-emission. *Landtechnik* **49**, 362-363. SRI translation no. 51 New Series, 1995.
- Hicks, B.B., Matt, D.R., McMillen, R.T. (1989). A micrometeorological investigation of surface exchange of O<sub>3</sub>, SO<sub>2</sub> and NO<sub>2</sub>: a case study. *Boundary-Layer Meteorol.* **47**, 321-336.
- Hoff, J.D., Nelson, D.W. and Sutton, A.L. (1981). Ammonia volatilisation from swine manure applied to cropland. *J. Environ. Qual.* **10**, 90-95.
- Hofschreuder, P. (2002). Ontwikkeling van een meetmethode voor gasvormige emissies van oppervlaktebronnen op landbouwpraktijkschaal. *IMAG Rapport 2002-13*.
- Hofschreuder, P., van der Meulen, W., Heeres, P. and Slanina, J. (1999). The influence of geometry and draught shields on the performance of passive samplers. *J. Environ. Monit.* **1**, 143-147.
- Hol, J.M.G. and Groenestein, C.M. (1997). Praktijkonderzoek naar de ammoniakemissie van stallen XXXI. Verschillende huisvestingssystemen voor vleeskalveren. *IMAG rapport 97-1001*.
- Holtslag, A.A.M. and Bruijn, H.A.R. de (1988). Applied modeling of the nighttime surface energy balance over land. *J. Appl. Met.* **27**, 689-704.
- Hoy, S. (1995). Zur Anwendung des Multi-gas-monitoring unter tierhygienischen und umwelthygienischen aspekten. *Tierärztliche Umschau* **50**, 115-123.
- Hutchinson, G.L., Mosier, A.R. and Andre, C.E. (1982). Ammonia and amine emissions from a large cattle feed lot. *Journal of Environmental Quality* **11**, 288-293.
- Karlsson, S. (1994). Composting of deep straw manure. Report 94-C-092, presented at AgEng 94, Milano, Italy, 29 August-1 September.
- Karlsson, S. (1996). Measures to reduce ammonia losses from storage containers for liquid manure. Paper no. 96E-013, presented at AgEng 96, Madrid, Spain.

- Leuning, R., Freney, J.R., Denmead, O.T. and Simpson, J.R.A. (1985). Sampler for measuring atmospheric ammonia flux. *Atmospheric Environment* **19(7)**, 1117-1124.
- Ludwig, F.L., Gasiorek, L.S. and Ruff, R.E. (1977). Simplification of a Gaussian puff model for real-time minicomputer use. *Atmospheric Environment* **11**, 431-436.
- Matthews, R.D., Sawyer, R. and Schefer, R.W. (1977). Interference in chemiluminescent measurement of NO and NO<sub>2</sub> emission from combustion systems. *Environmental Science and Technology* **11**, 1092.
- Michorius, J.A.T. and Scholtens, R. (1995). Schatting van de ammoniakemissie van mechanisch geventileerde stallen met passieve flux-monsternemers (Estimating ammonia emission from force ventilated animal housing using passive flux samplers). IMAG-DLO rapport.
- Michorius, J.A.T., Hartog, K.D., Scholtens, R. and Harssema, H. (1995). Ammoniakemissiemeting aan stalcomplexen met de fluxraamethode en het Gaussisch pluimmodel: een haalbaarheidsstudie. Report 95-11, Instituut voor Milieu en Agritechniek, Wageningen (SRI translation no. 61 New Series, February 1997).
- Monteny, G.J., Hol, J.M.G., Wever, A.C. and Scholtens, R. (1999). Ammoniakemissie op gebiedsniveau binnen het Stikstofonderzoekprogramma (STOP). IMAG Rapport 99-16.
- Mosquera, J., Hofschreuder, P., Erisman, J.W., Mulder, E., Klooster, C.E. van 't, Ogink, N., Swierstra, D. and Verdoes, N. (2002). Meetmethoden gasvormige emissies uit de veehouderij. *IMAG Rapport 2002-12*.
- Ouwerkerk, E.N.J. van (ed.) (1993). Meetmethoden NH<sub>3</sub>-emissie uit stallen. Onderzoek inzake de mest- en ammoniak- problematiek in de veehouderij 16. Report 16, Agricultural Research Department, Wageningen, 178 pp.
- Pasquill, F. (1971). Atmospheric dispersion of pollution. *Journal of the Royal Meteorological Society* **97**, 369-395.
- Pasquill, F. and Smith, F.B. (1983). Atmospheric diffusion (3<sup>rd</sup> edition). Ellis Horwood Limited, New York.
- Pearson, J. and Stewart, G.R. (1993). The deposition of atmospheric ammonia and its effects on plants. *New Phytol.* **125**, 283-305.
- Pérez-Soba, M., Stulen, I. and van der Eerden, L.J.M. (1994). Effects of atmospheric ammonia on the nitrogen metabolism of Scots pine (*Pinus sylvestris*) needles. *Physiol. Plant.* **90**, 629-636.
- Perry, H., Green, D.W. and Maloney, J.O. (1985). *Perry's chemical engineers' Handbook*, 6<sup>th</sup> edn. McGraw-Hill, Singapore.
- Phillips, V.R., Sneath, R.W., Williams, A.G., Welch, S.K., Burgess, L.R., Demmers, T.G.M. and Short, J.L. (1997). Measuring emission rates of ammonia, methane and nitrous oxide from full-sized slurry and manure stores. Proceedings of the International Symposium 'Ammonia and odour control from animal production facilities', Vinkeloord, Netherlands, 6-10 October, vol. 1, pp. 197-208.

- Phillips, V.R., Holden, M.R., Sneath, R.W., Short, J.L., White, R.P., Hartung, J., Seedorf, J., Schröder, M., Linkert, K.H., Pedersen, S., Takai, H., Johnsen, J.O., Groot Koerkamp, P.W.G., Uenk, G.H., Metz, J.H.M. and Wathes, C.M. (1998a). The development of robust methods for measuring concentrations and emission rates of gaseous and particulate air pollutants in livestock buildings. *Journal of Agricultural Engineering Research* **70**, 11-24.
- Phillips, V.R., Bishop, S.J., Price, J.S. and You, S. (1998b). Summer emissions of ammonia from a slurry-based, UK, dairy cow house. *Bioresource Technology* **65**, 213-219.
- Plantaz, M.A.H.G. (1998). Surface-atmosphere exchange of ammonia over grazed pasture. Ph. D. thesis.
- RIVM and CBS (2001). Milieucompendium 2001: het milieu in cijfers. Centraal Bureau voor de Statistiek CBS), Voorburg/Heerlen en Rijksinstituut voor Volksgezondheid en Milieu (RIVM), Bilthoven.
- Schade, G.W. and Crutzen, P.J. (1995). Emission of aliphatic amines from animal husbandry and their reactions: potential source of N<sub>2</sub>O and HCN. *Journal of Atmospheric Chemistry* **22**, 319-346.
- Schimmel, D.S., Parton, W.J., Adamsen, F.J., Woodmansee, R.G., Senft, R.L. and Stillwell, M.A. (1986). The role of cattle in the volatile loss of nitrogen from a shortgrass steppe. *Biogeochemistry* **2**, 39-52.
- Schjoerring, J.K. (1995). Long-term quantification of ammonia exchange between agricultural crop land and the atmosphere-I. Evaluation of a new method based on passive flux samplers in gradient configuration. *Atmospheric Environment* **29**, 885-893.
- Schjoerring, J. K., Sommer, S. G. and Ferm, M.A. (1992). Simple passive sampler for measuring ammonia emission in the field. *Water, air, and soil Pollution* **62**, 13-24.
- Scholtens, R. (1990). Ammoniakemissionsmessungen in zwangsbeluften Ställen (Measurement of ammonia emissions from mechanically ventilated housing systems). In: Ammoniak in der Umwelt (ammonia in the environment), Proceedings Symposium, Braunschweig, KTBL, Darmstadt, Beitrag-Nr. 20, pp 9.
- Scholtens, R. (1993). NH<sub>3</sub>-converter + NO<sub>x</sub>- analyser. In *Meetmethoden NH<sub>3</sub>-emissie uit stallen. Onderzoek inzake de mest- en ammoniak-problematiek in de veehouderij 16* (eds E.N.J. van Ouwkerk). DLO, Wageningen, p. 19-22.
- Scholtens, R. (1996). Werkwijze en inrichting voor het meten van de emissie van een gas, deeltjes of aerosols (Mode of operation and layout for measuring emissions of gases, particles and aerosols), Het Bureau I.E., Patent nr. OA 1003272 Ned, Den Haag, pp 13.
- Schulze, E.D., de Vries, W., Hauhs, M., Rosén, K., Rasmussen, L., Tamm, S.O. and Nilsson, J. (1989). Critical loads for nitrogen deposition on forest ecosystems. *Water Air Soil Pollut.* **48**, 451-456.

- Sharan, M., Yadav, A.K. and Singh, M.P. (1995). Comparison of sigma schemes for estimation of air pollution dispersion in low winds. *Atmospheric Environment* **29(6)**, 2051-2059.
- Sherlock, R.R., Freney, J.R., Smith, N.P. and Cameron, K.C. (1989). Evaluation of a sampler for assessing ammonia losses from fertilised fields. *Fertilizer Research* **21**, 61-66.
- Sliggers, J. (ed.) (2001). Op weg naar duurzame niveaus voor gezondheid en natuur. Overzichtspublicatie thema verzuring en grootschalige luchtverontreiniging. Rapport VROM 010344/h/10-01 17529/187, Ministerie van Volksgezondheid, Ruimtelijke Ordening en Milieubeheer, Den Haag, oktober 2001, 229 pp.
- Sommer, S.G., Sibbesen, E., Nielsen, T., Schjoerring, J.K. and Olesen, J.E.A. (1996). Passive flux sampler for measuring ammonia volatilization from manure storage facilities. *Journal of Environmental Quality* **25(2)**, 241-247.
- Stull, R.B. (1988). An introduction to Boundary-layer meteorology. Kluwer Academic Publishers, Dordrecht, the Netherlands.
- Sutton, M.A., Pitcairn, C.E.R. and Fowler, D. (1993). The exchange of ammonia between the atmosphere and plant communities. *Adv. Ecol. Res.* **24**, 301-391.
- Svensson, L. and Ferm, M. (1993). Mass transfer coefficient and equilibrium concentration as key factors in a new approach to estimate ammonia emission from livestock manure. *Journal of Agricultural Engineering Research* **56**, 1-11.
- Tamminga, S. (1992). Nutrition management of dairy cows as a contribution to pollution control. *Journal of dairy Science* **75**, 345-357.
- Thom, A.S. (1975). Momentum, mass and heat exchange of plant communities. In *Vegetation and Atmosphere* (ed. Monteith, J.L.), pp. 58-109. Academic Press, London.
- Turner, D.B. (1994). Workbook of atmospheric dispersion estimates (2<sup>nd</sup> edition). CRC Press, Inc. Boca Raton.
- Van Breemen, N. and van Dijk, H.F.G. (1988). Ecosystem effects of atmospheric deposition of nitrogen in the Netherlands. *Envir. Pollut.* **54**, 249-274.
- Van Breemen, N., Burrough, P.A., Velthorst, E.J., Dobben, H.F. van, Wit, T. De, Ridder, T.B. and Reinders, H.F.R. (1982). Soil acidification from atmospheric ammonium sulfate in forest canopy throughfall. *Nature* **299**, 548-550.
- Van Dam, D., van Dobben, H.F., ter Braak, C.F.J. and de Wit, T. (1986). Air pollution as a possible cause for the decline of some phanerogamic species in the Netherlands. *Vegetatio* **65**, 47-52.
- Van der Hoek, K.W. (1994). Berekeningsmethodiek ammoniakemissie in Nederland voor de jaren 1990, 1991, en 1992, (Calculation of ammonia emissions for the years 1990, 1991 and 1992), RIVM report nr. 773004003, Bilthoven, 1994, pp 51.
- Van Dijk, H.F.G. and Roelofs, J.G.M. (1988). Effects of excessive ammonium deposition on the nutritional status and condition of pine needles. *Physiol. Plant.* **73**, 494-501.

- Vertregt, N. and Rutgers, B. (1988). Ammonia volatilisation from urine patches in grassland. In *Volatile emissions from livestock farming and sewage operation* (eds. Nielsen, V.C., Voorburg, J.H. and L'Hermitte, P.), pp. 85-91. Elsevier Applied Science, London.
- Wesely, M.L. and Hicks, B.B. (1977). Some factors that affect the deposition rates of sulfur dioxide and similar gases on vegetation. *J. Air Pollut. Control Assoc.* **27**, 1110-1116.
- Willems, J.J.H. and Hofschreuder, P. (1990). A passive monitor for measuring ammonia. In *Field Intercomparison Exercise on Ammonia and Ammonium Measurement* (eds. Allegrini, I., Febo, A. and Perrino, C.), pp. 113-121. Air Pollution Research Report 37, Commission of the European Communities, Brussels.
- Wyers, G.P., Otjes, R.P. and Slanina, J. (1993). A continuous-flow denuder for the measurement of ambient concentrations and surface exchange fluxes of ammonia. *Atmospheric Environment* **27A**, 2085-2090.
- Zannetti, P. (1990). Air pollution modelling. Van Nostrand Reinhold, New York.
- Zeller, K.W., Massman, D., Stocker, D.G., Stedman, D., Hazlett, D. (1989). Initial results from the Pawnee eddy correlation system for dry acidic deposition research. U.S.D.A. Forest Service Research Paper RM-282.



## Summary

In areas with intensive agricultural activities, deposition of ammonia and ammonium poses a serious threat to the environment. It contributes not only to soil acidification, but it also leads to disruption of the nutrient cycle and disappearance of sensitive natural ecosystems. Recent estimates suggest that approximately 94% of the Dutch ammonia emissions originate from agriculture. Governmental policies and measures have been developed that are aimed to reduce the emission of ammonia. However, a large uncertainty still exists in the ammonia emission, concentration and deposition estimates. New measurement methods are needed, which allow monitoring the ammonia emission from a larger number of locations.

Financed by the Ministerie van Landbouw, Visserij en Natuurbeheer (LNV), different studies have been performed to review the measurement methods and techniques available to quantify ammonia emissions from agriculture. Based on this work, a selection of methods was applied and compared based on their suitability to estimate the ammonia emission from various agricultural activities (slurry application into the field, mechanically ventilated animal houses, naturally ventilated animal houses). This report summarises the results of this study.

First of all, a description of the selected measurement techniques (chapter 2) and the measurement locations (chapter 3) is given. For surface sources (ammonia emission during and after slurry application into the field, chapter 4), both the AMANDA and denuder systems have been used up to now as reference methods. Willems badges and passive ammonia flux samplers in a flux frame approach are a good alternative. In particular for complex situations, use of passive ammonia flux samplers is recommended, because they do not have limitations on electricity (denuders, AMANDA), airflow measurements (denuders), or wind speed profile measurements (Willems badges). For mechanically ventilated animal houses (chapter 5), the current method used in the Netherlands relies on the  $\text{NO}_x$  monitor (after conversion of  $\text{NH}_3$  to  $\text{NO}$ ). The use of passive ammonia flux samplers under the ventilation shafts of the animal houses gives promising results as an alternative method. For naturally ventilated animal houses (chapter 5), the current method used by IMAG relies upon ammonia concentration measurements inside the building, and the estimation of the ventilation rate by using a tracer gas. However, when mixing conditions are not good, the use of a tracer gas is not adequate. In these situations, measurements should be done outside the building. Results using the flux frame method with passive ammonia flux samplers are promising. Conclusions and recommendations for future developments are given in chapter 6.



## Appendix A: aerodynamic gradient method

The vertical flux and the gradient of a property are assumed to be related by a turbulent diffusion coefficient, the diffusivity  $K$ , which can be defined as the ratio of the property flux through the medium to its concentration gradient (in the same direction) at that point. The vertical flux of momentum is equal in magnitude to the shearing stress  $\tau$ , which is the drag force per unit area of level ground caused by horizontal air motion (Thom, 1975). Unlike the sign convention for fluxes,  $\tau$  is usually denoted positive for downward transport of momentum. The flux towards or away from the surface is found as the product of this gradient and the diffusivity.

- For the momentum flux ( $\tau$ ): 
$$\tau = K_m(z) \frac{\partial(\rho u)}{\partial z} \quad (\text{A1})$$

- For sensible heat flux ( $H$ ): 
$$H = K_h(z) \frac{\partial(\rho_a c_p \theta)}{\partial z} \quad (\text{A2})$$

- For pollutant mass flux ( $F$ ): 
$$F = K_c(z) \frac{\partial c}{\partial z} \quad (\text{A3})$$

where  $u$  is the wind speed,  $z$  the vertical distance and  $c$  the pollutant concentration. Fluxes directed towards the earth are defined negative. The approximate similarity of:

$$K_m \approx K_h \approx K_c \quad (\text{A4})$$

appears to be valid in neutral and stable conditions (Thom, 1975; Droppo, 1985). In unstable conditions, experiments showed that the equality of  $K_h$  and  $K_c$  with  $K_m$  does not hold (Droppo, 1985), although  $K_h$  and  $K_c$  were also similar in these conditions (Droppo, 1985; Hicks *et al.*, 1989; Zeller *et al.*, 1989).

The shearing stress, or momentum flux  $\tau$ , is defined as the drag force per unit area of a horizontal plane caused by horizontal air motion (Thom, 1975).  $\tau$  is related to the air density and the effectiveness of vertical turbulent exchange in the air flow over the surface:

$$\tau = \rho_a u_*^2 \quad (\text{A5})$$

where  $u_*$  is the *eddy velocity* or friction velocity associated with the momentum flux. The term  $u_*$  may be defined in terms of gradient theory, such that:

$$u_* = l \frac{\partial u}{\partial z} \quad (\text{A6})$$

where  $l$  is the mixing length for momentum, or rather the effective eddy size, at level  $z$ . Under neutral conditions,  $l$  is proportional to height ( $l = k \cdot z$ ). However, in a non-neutral atmospheric stability may reduce or enlarge the vertical eddy size. In general, the value for  $l$  may be given by:

$$l = \frac{\kappa (z - d)}{\phi_m} \quad (\text{A7})$$

where  $\kappa$  is the Von Karman constant, established experimentally to be about 0.41.  $\phi_m$  is the empirically estimated dimensionless correction for stability effects upon this ratio, while  $d$  is the zero displacement height.

The eddy diffusivity  $K_m$  is described by

$$K_m = \frac{\kappa (z - d) u_*}{\phi_m} \quad (\text{A8})$$

This equation may be used to estimate  $K_c$ , given the similarity between  $K_m$ ,  $K_h$  and  $K_c$ . For  $K_c$ ,  $\phi_h$  is used rather than  $\phi_m$ . Thus, given the equality of  $\phi_h$  and  $\phi_c$ :

$$K_c = \frac{\kappa (z - d) u_*}{\phi_h} \quad (\text{A9})$$

which may be substituted into the mass flux (eqn. A3), yielding:

$$F = \frac{\kappa (z - d) u_*}{\phi_m} \frac{\partial c}{\partial z} \quad (\text{A10})$$

$u_*$  is derived from eqn. A1 and eqn. A2:

$$u_* = \frac{\kappa (z - d)}{\phi_m} \frac{\partial u}{\partial z} \quad (\text{A11})$$

This expression can be integrated to give the expression:

$$\bar{u} = \left( \frac{u_*}{\kappa} \right) \ln \left( \frac{z - d}{z_0} \right) \quad (\text{A12})$$

Similarly, the eddy concentration can be defined as:

$$c_* = \frac{\kappa (z - d)}{\phi_h} \frac{\partial c}{\partial z} \quad (\text{A13})$$

and thus the mass flux becomes:

$$F = u_* c_* \quad (\text{A14})$$

As a result, the flux of a pollutant may be derived from information on the wind profile, the concentration gradient and the effect of stability. The stability function is a correction for the departure of the neutral profile. Therefore under neutral conditions  $\phi_m = \phi_h = \phi_c = 1$ . The stability correction is a function of height.

- Under stable conditions: 
$$\phi_m = \phi_h = \phi_c = 1 + 5.2 \frac{(z-d)}{L} \quad (\text{A15})$$

- Under unstable conditions: 
$$\phi_m^2 = \phi_h = \phi_c = \left[ 1 - 16 \frac{(z-d)}{L} \right]^{-0.5} \quad (\text{A16})$$

A summary of  $\phi$  forms can be found in Dyer (1974).  $L$  is the Monin Obukhov length used as stability parameter ( $0 < L < 100$  m, stable;  $-100 < L < 0$  m, unstable;  $|L| \rightarrow \infty$  neutral), given as:

$$L = - \frac{T \rho_a c_p u_*^3}{\kappa g H} \quad (\text{A17a})$$

where  $T$  is the absolute potential temperature and  $g$  the acceleration of gravity. The sensible heat flux  $H$  and  $u_*$  can be derived from sonic anemometer measurements or calculated from the net radiation. However, according to Wesely and Hicks (1977):

$$L = - \frac{T \rho_a c_p u_*^3}{(\kappa g H + L_w E)} \quad (\text{A17b})$$

where  $L_w E$  is the latent heat of evaporation.

Integration of eqn. A11 and eqn. A13 between the roughness length  $z_0$  and  $z$  yields:

$$u_* = \frac{\kappa u(z)}{\ln\left(\frac{z-d}{z_0}\right) - \psi_m\left(\frac{z-d}{L}\right) + \psi_m\left(\frac{z_0}{L}\right)} \quad (\text{A18})$$

$$c_* = \frac{\kappa c(z)}{\ln\left(\frac{z-d}{z_0}\right) - \psi_h\left(\frac{z-d}{L}\right) + \psi_h\left(\frac{z_0}{L}\right)} \quad (\text{A19})$$

where

$$\begin{aligned}
\psi_m\left(\frac{z-d}{L}\right) &= 2 \ln\left(\frac{1+x}{2}\right) + \ln\left(\frac{1+x^2}{2}\right) \\
&\quad - 2 \arctan(x) + \frac{\pi}{2} \\
\psi_h\left(\frac{z-d}{L}\right) &= 2 \ln\left(\frac{1+x^2}{2}\right) \\
x &= \left[1 - 16\left(\frac{z-d}{L}\right)\right]^{0.25}
\end{aligned} \tag{A20}$$

for unstable conditions (Dyer and Hicks, 1970), and

$$\begin{aligned}
\psi_m\left(\frac{z-d}{L}\right) &= \psi_h\left(\frac{z-d}{L}\right) \\
&= -5.2\left(\frac{z-d}{L}\right)
\end{aligned} \tag{A21}$$

for stable conditions (Dyer and Hicks, 1970).

In some cases, some slightly adapted parameterisations are used for the stability functions under stable conditions (Holtslag and De Bruijn, 1988; Beljaars *et al.*, 1989; Plantaz, 1998):

$$\begin{aligned}
\psi_m\left(\frac{z-d}{L}\right) &= -0.7\left(\frac{z-d}{L}\right) \\
&\quad - 0.75\left(\frac{z-d}{L} - 14.29\right) \exp\left(-0.35\left(\frac{z-d}{L}\right)\right) - 10.72 \\
\psi_h &= \psi_m
\end{aligned} \tag{A22}$$

$\psi_m((z-d)/L)$  and  $\psi_h((z-d)/L)$  are the integrated stability corrections for momentum and heat. If the reference height is sufficiently larger than  $z_0$  ( $z \gg z_0$ ), the values of the  $\psi$ -functions for  $z_0/L$  are small compared to those for  $z/L$  and can be neglected.

A different approximation is found in Wesely and Hicks (1977) for the  $\psi$ -functions:

$$\text{for } 0 < z/L < 1, \quad \psi_H = \psi_w = \psi_M = -5\left(\frac{z}{L}\right) \tag{A23}$$

$$\begin{aligned}
& \text{for } 0 > z/L > -1 \\
& \psi_H = \psi_W = e^{[0.598+0.39\ln(-z/L)-0.090(\ln(-z/L))^2]} \\
& \psi_m = e^{[0.032+0.448\ln(-z/L)-0.132(\ln(-z/L))^2]}
\end{aligned}
\tag{A24}$$

The roughness length  $z_0$  values are commonly derived from measurements of the wind profile (Thom, 1975). In neutral conditions, where the stability correction is negligible, a linear fit of  $\ln(z)$  against  $u(z)$  can provide information on  $z_0$ . Empirically,  $z_0$  may be approximated as  $0.1h$  (Stull, 1988), where  $h$  is the height of the receptor surface.



## Appendix B: denuders

The denuder (figure B1) is usually an active sampler utilising a pump to pull a known flow of air through a cylindrical tube treated with an acidic substance, which reacts with  $\text{NH}_3$ . Air is sucked through the denuder for a certain period and the sample volume is measured by a gas meter or estimated from sample time and flow, the latter being controlled by a critical orifice. After sampling, the coating of the denuder is extracted and analysed for the compound of interest. Denuder systems can distinguish between compounds in gaseous and particulate form. Gases, due to their large diffusion velocity compared to aerosols, can reach the walls of the tube and be absorbed by the coating. Aerosols pass the denuder without touching the walls, as their diffusion is very slow.

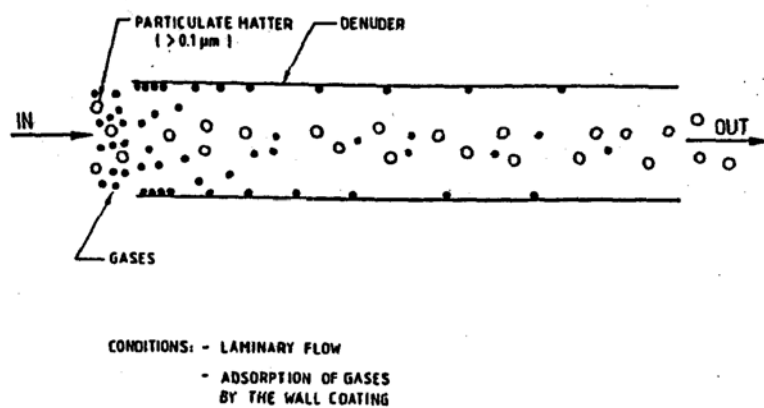


**Figure B1** Principle of the denuder technique.

Active denuders collect ammonia by using gaseous diffusion from a laminar flow of air. In an active denuder the air is drawn at a known and controlled flow rate through the absorption tube, which has an internal absorbing surface. The concentration in the air ( $C$ ) can be calculated as follows:

$$C(\mu\text{g}/\text{m}^3) = \frac{Q(\mu\text{g})}{F(\text{ml}/\text{min}) \cdot t(\text{s})} \cdot 60 \cdot 10^6 \quad (\text{B1})$$

where  $C$  =  $\text{NH}_3$  concentration ( $\mu\text{g m}^{-3}$ )

$Q$  = amount of  $\text{NH}_3$  absorbed on the filter ( $\mu\text{g}$ )

$F$  = flow rate ( $\text{ml min}^{-1}$ )

$t$  = exposure time (s)



## Appendix C: Willems badges

The Willems badge (figure C1) is a passive sampling technique for gas concentrations that uses the principle of gas diffusion. When the badge is exposed the reaction filter coated with acid is exposed to the air. Ammonia in the air diffuses into the badge to the reagent and binds with acid in the form of ammonium ions. Several authors have described this type of devices (Willems and Hofschreuder, 1990; Adema *et al.*, 1991; Blatter *et al.*, 1992; Svensson and Ferm, 1993). Depending on the geometry of the sampler, low or high wind speeds can be a problem (Willems and Hofschreuder, 1990).

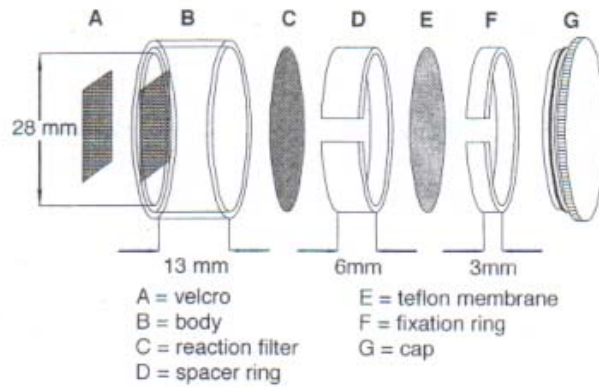


**Figure C1** Schematic representation of the Willems badges.

After initial exposure, the badge is suspended from the sampling points of the masts with the opening downwards, in order to reduce the influence of rain and aerosol deposition. After a given sampling time the badge is sealed with the lid. The concentration in the sampled air ( $C$ ) is calculated as follows:

$$C = \frac{Q \cdot R_t}{A \cdot t} \quad (C1)$$

where  $C$  =  $\text{NH}_3$  concentration ( $\mu\text{g m}^{-3}$ )

$Q$  = amount of  $\text{NH}_3$  absorbed on the filter ( $\mu\text{g}$ )

$R_t$  = total resistance ( $\text{s m}^{-1}$ )

$A$  = area of the badge ( $\text{m}^2$ )

$t$  = exposure time (s)

or

$$C = \frac{Q \cdot Z \cdot f \cdot p \cdot 293.2}{D \cdot A \cdot t \cdot 101.3 \cdot (T + 273.2)} \cdot 10^6 \quad (C2)$$

where	C =	NH <sub>3</sub> concentration (µg m <sup>-3</sup> )
	Q =	amount of NH <sub>3</sub> absorbed on the filter (µg)
	Z =	diffusion length (0.2 cm)
	f =	resistance factor (~4.9)
	p =	atmospheric pressure (kPa)
	101.3 =	standard atmospheric pressure (kPa)
	T =	temperature during sampling (°C)
	293.2 =	standard temperature in Kelvin at 20 °C
	D =	diffusion coefficient of NH <sub>3</sub> in the air (0.228 cm <sup>2</sup> s <sup>-1</sup> )
	A =	area of the badge (m <sup>2</sup> )
	t =	exposure time (s)

The total resistance  $R_t$  can be calculated as:

$$R_t = R_d + R_f + R_e \quad (C3)$$

where  $R_d$  is the resistance against uptake of the pollutant by the sampler,  $R_f$  is an additional resistance due to the introduction of a draught screen in the sampler, and  $R_e$  accounts for the resistance to uptake of the pollutant due to the development of a stagnant layer of air in front of the draught screen that can appear at low wind speeds.

The resistance against uptake of the pollutant within the sampler is defined by (Hofschreuder *et al.* (1999)

$$R_d = \frac{L}{D} \quad (C4)$$

where  $L(m)$  is the diffusion length within sampler and  $D$  is the diffusion coefficient (m<sup>2</sup> s<sup>-1</sup>). The resistance of the draught shield can be approximated by the equation (Hofschreuder *et al.* (1999)

$$R_f = \frac{e}{D \cdot P} \quad (C5)$$

where  $e$  is the thickness of the draught shield (m) and  $P$  the porosity. For a filter, the thickness and porosity should be derived from data from the manufacturer. Typical values for  $R_f$  for a glass fibre filter and a membrane filter are 15-20 s m<sup>-1</sup> ( $e=0.35$  mm,  $P=0.9$  mm), and 1-4 s m<sup>-1</sup> ( $e=0.025-0.075$ ,  $P=0.85$ ) respectively.

A value for the external boundary layer resistance ( $R_e$ ) is difficult to estimate. This resistance will be very dependent on sampler geometry and meteorological conditions. Values of  $R_e$  are summarised in table C1 for different wind speeds (Hofschreuder *et al.*, 1999).

**Table C1**  $R_e$  values for situations with different wind speeds (Hofschreuder *et al.*, 1999).

$R_e$ (s m <sup>-1</sup> )	Wind speed (m s <sup>-1</sup> )						
	0.1	0.2	0.5	1.0	2.0	4.0	10.0
	131	114	95	83	72	63	52



## Appendix D: chemiluminescence (NO<sub>x</sub> monitor)

This method is commonly used in the Netherlands for continuous measurement of NH<sub>3</sub> concentrations in livestock buildings, and is described in detail in Ouwerkerk (1993) and Groot Koerkamp *et al.* (1998). A chemiluminescence detector can be used to measure ammonia concentrations, provided ammonia is first oxidised to nitric oxide (NO). The prior oxidation of ammonia to nitric oxide can be achieved (Aneja *et al.*, 1978) using a stainless-steel catalytic converter in the form of a long tube of 5 mm i.d., at a temperature of 750 °C. At this temperature not only ammonia, but also organic nitrogen-containing compounds (e.g. trimethylamine and dimethylamine), nitric acid (HNO<sub>3</sub>), nitrogen dioxide (NO<sub>2</sub>) and ammonium-containing aerosols are formed. The concentration of all these latter compounds in the air in animal houses is expected to be negligible in comparison with ammonia. Nitrous oxide (N<sub>2</sub>O) is converted to NO only to a negligible degree.

Loss of ammonia by adsorption on to the walls of the gas handling parts (e.g. lines and vacuum pump) and by solution in water is possible, but these risks were minimised by the use of FEP-Teflon and by preventing water condensation by trace heating. Another possibility is to place the converters as close as possible downstream of each sampling point. In this way the less adsorptive gas NO, rather than NH<sub>3</sub>, is transported through the main lengths of the lines.

Commonly, the conversion of ammonia to nitric oxide has an efficiency of around 95%. The minimum lifespan of the catalyst is at least 6 months. The converter can be integrated in a NO<sub>x</sub>-analyser or be used as a separate instrument. A potential problem is the long response time of converters to a change in ammonia concentration, up to 30 minutes for a change from 17 mg m<sup>-3</sup> to 0.1 mg m<sup>-3</sup>. Due to the long response time of the converter the use of a separate converter for each sampling point is recommended (Scholtens, 1990).

Following conversion, the concentration of nitric oxide is measured with a chemiluminescence NO<sub>x</sub>-analyser. The analyser operates on the principle that the reaction of nitric oxide with ozone produces nitrogen dioxide in an excited state. The nitrogen dioxide molecules return to a lower energy state by releasing photons. The response time of the analyser to changes in nitric oxide concentration is relatively short (10-20 s). With excess ozone, the intensity of this radiation is proportional (Fontijn *et al.*, 1970; Breitehbach and Shelef, 1973; Matthews *et al.*, 1977; Scholtens, 1993) to the concentration of NO.



## Appendix E: passive flux samplers

Leuning *et al.* (1985) reported the first form of passive flux sampler based on an internal (oxalic) acid coating to capture any ammonia in air flowing at a controlled rate through the sampler. Leuning's sampler has vanes and pivots to keep it pointing always upwind. This is an advantage when carrying out plot experiments, but makes the device less applicable to studies on manure stores and less applicable again to studies on buildings. They give only a measurement of the average flux over the time of exposure: a suitable time of exposure depends on the conditions. Sherlock *et al.* (1989) reported a detailed experiment to test the accuracy of this type of flux sampler for measuring ammonia loss rates from fertilised plots of land. They found only 1.5% difference between the results from flux samplers and from a reference micrometeorological method in which acid bubblers were used to measure ammonia concentration and cup anemometers to measure wind speeds.

A simpler, and far cheaper, passive flux sampler, originally developed by Ferm (1986), was subsequently reported by Schjoerring *et al.* (1992). As with Leuning's sampler, the principle was to capture ammonia from air flowing through the sampler, quantitatively, in an oxalic acid coating. The sampler (now commonly known as the 'Ferm tube', Figure E1) has been widely used, mainly for measuring fluxes from non-point sources such as areas of crop or land spread with manure, but also, less widely, for fluxes from manure heaps (Karlsson, 1994; Phillips *et al.*, 1997) and slurry stores (Hess and Hügler, 1994; Karlsson, 1996; Sommer *et al.*, 1996; Phillips *et al.*, 1997), and, less widely again, for fluxes from livestock buildings, both force-ventilated (Michorius *et al.*, 1995) and naturally ventilated (Phillips *et al.*, 1998b).

Figure E1 shows a schematic drawing of the sampler as designed by Ferm (1986). This flux sampler consists of a pair of two connected tubes (A1 + B1 and A2 + B2) coated with oxalic acid with an orifice placed on one side. The oxalic acid on the walls of the tubes captures the ammonia from the air flowing through the sampler. Sampler tubes facing upstream are exposed to ammonia first and should capture all ammonia passing through them. Opposite tubes measure advective tubes from opposite airflow's. The average amount of ammonia captured by the combination of tubes A1+A2 and B1+B2 are used to calculate fluxes from either side of the flux plane. This is done to correct for differences between air velocities generated in tubes facing upstream with or without an orifice. Air passing the sampler should induce a linear proportional airflow through the coupled tubes, depending on the orifices used. In fact there is, according to literature (Ferm, 1986; Ferm *et al.*, 1991), a cosine dependency between wind direction and air collected by the PFS. In this way passive flux samplers incorporate in one instrument measurement of concentration, wind speed and wind direction without the use of any power supply. After a certain exposure time the amount of gas (ammonia) captured by the sampler is analysed. From this the flux of ammonia through a plane perpendicular to the sampler is calculated. For a flux measurement at one location a pair of these samplers is installed with orifices at opposite

sides. From practical experiments Ferm (1986) concluded that an average flux value from the two tubes at each side gave the best results:

$$F_{hz} \cdot \Delta t = \int_{t_1}^{t_2} U \cdot \cos \alpha \cdot [NH_3] \cdot dt \approx \frac{1}{0.77} \cdot \left( \frac{A_1 + A_2}{2 \cdot \pi \cdot r^2} - \frac{B_1 + B_2}{2 \cdot \pi \cdot r^2} \right) \quad (E1)$$

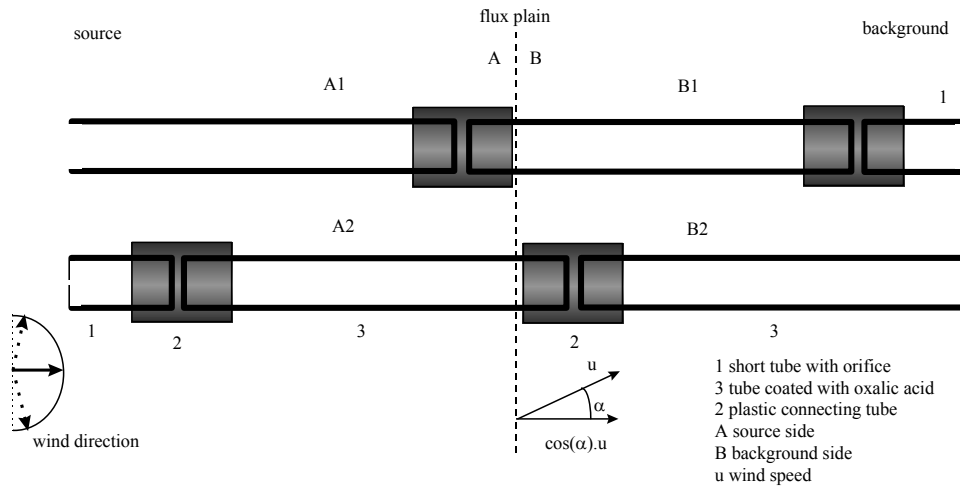


**Figure E1** Schematic drawing of flux sampler proposed by Ferm (1986).

Hansen *et al.* (1998) used a modified type of Ferm tube, mounted on a wind vane, when studying fluxes from heathland. They thus achieved a simpler, cheaper directional flux sampler than Leuning's, although as stated above, directional flux samplers are generally less applicable to studies on buildings or manure stores than are fixed ones.

All the above types of sampler, as well as any other type based on an acid absorbent, will register, as well as ammonia, any other alkaline gas that may be present. In practice, this means mainly various amines, but their concentrations relative to that of ammonia are normally small (Hutchinson *et al.*, 1982; Hoy, 1995). It can be deduced from figures given by Schade and Crutzen (1995), and by Bouwman *et al.* (1997), that, globally, total amine emissions are less than 1% of total ammonia emissions.

Scholtens (1996) describes a patent for a new passive flux sampler design, based on the passive flux sampler for ammonia proposed by Ferm (1986). In the improved sampler the orifice is placed in the middle of the sampler, connecting two absorption chambers. This symmetrical design minimises the number of analysis but more importantly it greatly improved and simplified validation procedures. The main role of the orifice in a passive flux sampler is to regulate the amount of air flowing through the sampler, but having the orifice in the centre of the sampler, well shielded from turbulence, means it can also be used as a flow meter. For test purposes the sampler can be equipped with pressure points (radius pressure taps located at a distance from the orifice plate of approximately  $\frac{1}{2} D_o$  (orifice diameter)). In the chambers a specific gas or type of gases can be bound to a gas-

absorbing agent. Acid loaded glass fibre paper inserts are placed having a higher binding capacity than an oxalic acid coating on the wall of a tube of similar size. It is essential that the flow resistance is not significantly increased by the introduction of the absorbing agent in the chambers of the sampler. Figure E2 shows a schematic drawing of the simple design based on this new concept.

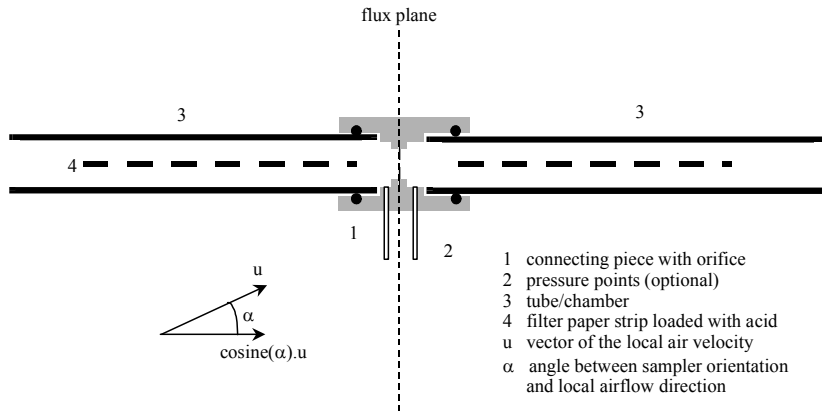


**Figure E2** Schematic drawing of the improved sampler.

The working of a passive sampler is based on the following two basic principles. Firstly an airflow passing an object results in an under pressure downstream of this object. This under pressure can be described by the following equation (Perry *et al.*, 1985).

$$P_D = \frac{F_D}{A_p} = C_D \cdot \frac{1}{2} \rho \cdot v_m^2 \quad (\text{E2})$$

- with:  $P_D$  = under pressure downstream of object [Pa]  
 $F_D$  = drag force [N]  
 $C_D$  = drag coefficient []  
 $\rho$  = air density [ $\text{kg}\cdot\text{m}^{-3}$ ]  
 $v_m$  = air velocity [ $\text{m}\cdot\text{s}^{-1}$ ]  
 $A_p$  = projected area of the object in the air flow [ $\text{m}^2$ ]

Secondly, the airflow through an orifice meter depends on the pressure drop over the orifice meter, as shown in Perry *et al.* (1985).

$$P_o = \frac{(1-B^4)}{Y C^2} \cdot \frac{1}{2} \rho v_o^2 = C_o \cdot \frac{1}{2} \rho v_o^2 \quad (\text{E3})$$

- with:  $P_o$  = pressure drop over the orifice meter [Pa]  
 $B$  = ratio orifice diameter ( $D_o$ ) to channel diameter ( $D_2$ )

$C$	=	coefficient of discharge []
$Y$	=	expansion factor []
$v_o$	=	air velocity through orifice [m.s <sup>-1</sup> ]
$C_o$	=	orifice meter constant []

Both equations show a square root dependency between air velocity and pressure drop. In the first equation the pressure drop is caused by the air velocity, in the second equation the pressure drop induces airflow through the orifice meter. Under normal atmospheric conditions both equations can be combined to the following equation (assuming  $P_D=P_O$ )

$$v_o = \sqrt{\frac{C_D}{C_o}} \cdot v_m = K_s \cdot v_m \quad (E4)$$

where  $K_s$  is the sampler constant.

This shows theoretically the desired linear relationship. With the improved sampler it is simple to establish the sampler constant ( $K_s$ ) under practical conditions for different sampler designs. It is not necessarily to use an artificial ammonia source under field conditions or in a wind tunnel.

The relationship between air velocity and pressure drop over the orifice meter was tested in a wind tunnel. The sampler (7 mm internal diameter) was placed horizontally in the wind tunnel. A range of air velocities was applied (0 -15 m.s<sup>-1</sup>) and the pressure drop (corrected after calibration with the calibration pressure meter “DIGIMA >>premo<<”) over the orifice meter (1 mm diameter) in the sampler recorded. The measured air velocities were corrected using the Lambrecht correction:

$$V_L(real) = (C_5 \cdot V_{meas}^5 + C_4 \cdot V_{meas}^4 + C_3 \cdot V_{meas}^3 + C_2 \cdot V_{meas}^2 + C_1 \cdot V_{meas}^1 + C_0)$$

where:

	$V_{meas} < 2.1 \text{ m.s}^{-1}$	$V_{meas} > 2.1 \text{ m.s}^{-1}$
$C_0$	-0.00499786	0.649231389500
$C_1$	1.2399491	0.372856651700
$C_2$	-1.141792948	0.247812975900
$C_3$	1.885757356	-0.03212594340
$C_4$	-1.166629163	0.00173713950
$C_5$	0.242920864	-0.0000330851



**Figure E3** Picture of the wind tunnel used in the measurements.

A linear regression on the results gave the  $C_D$  value for this sampler design. The regression line was forced through zero (figure E4).

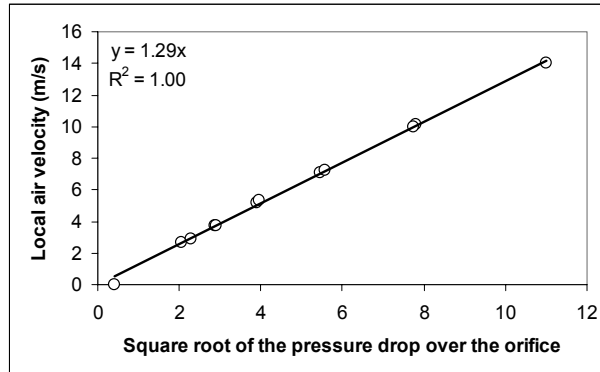


**Figure E4** Relation between the outside local air velocity ( $\text{m s}^{-1}$ ) and the square root of the pressure drop over the orifice in the sampler ( $\sqrt{\text{Pa}}$ ).

The relationship between air velocity through the orifice meter and the pressure drop over the orifice meter was measured using a soap bubble meter. A range of pressure drops (0-120 Pa) was applied and the airflow registered. In this case the pressure is measured directly, therefore no corrections are needed. The internal diameter of the orifice meter was used to calculate the air velocity. From the results a linear regression was used to calculate the orifice meter constant  $C_O$  (figure E5).

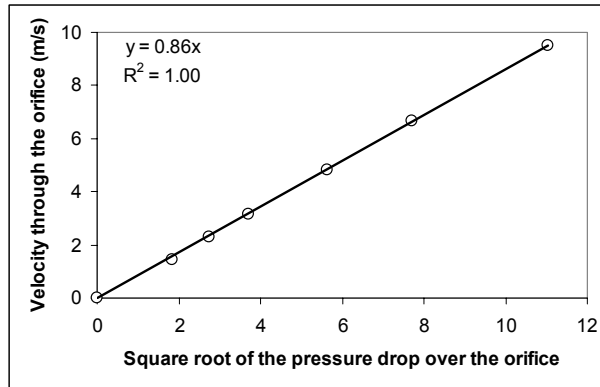


**Figure E5** Relation between the air velocity through the orifice ( $\text{m s}^{-1}$ ) and the square root of the pressure drop over the orifice in the sampler ( $\sqrt{\text{Pa}}$ ).

The sampler constant was calculated using equation leading to the following linear proportional relation between local air velocity and air velocity in the sampler (figure E6):

$$V_o = 0.67 \cdot V_L$$

with:  $V_L$  : local air velocity, air velocity outside the sampler ( $\text{m.s}^{-1}$ )  
 $V_o$  : air velocity through the orifice ( $\text{m.s}^{-1}$ )

or

$$V_L = 74 \cdot V_s$$

with:  $V_L$  : local air velocity, air velocity outside the sampler ( $\text{m.s}^{-1}$ )  
 $V_s$  : air velocity inside the sampler ( $\text{m.s}^{-1}$ )

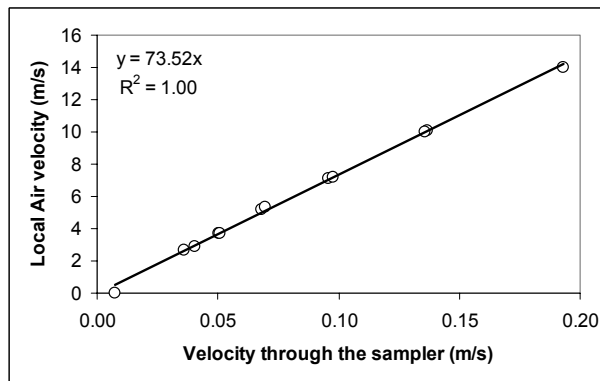


**Figure E6** Relation between the outside local air velocity ( $\text{m s}^{-1}$ ) and the velocity through the sampler ( $\text{m s}^{-1}$ ).

The amount of ammonia captured by the sampler, assuming that the wind direction is parallel to the sampler, can be described as:

$$S_{NH_3} = K_s \cdot A_o \int_{t_1}^{t_2} v(t) \cdot C_{NH_3}(t) dt \quad (E5)$$

with:  $A_o$  = surface area of hole in orifice [ $m^2$ ]  
 $S_{NH_3}$  = amount of ammonia captured [mg]  
 $C_{NH_3}$  = ammonia concentration [ $mg \cdot m^{-3}$ ]  
 $t$  = time of day  
 $t_1$  = start of exposure  
 $t_2$  = end of exposure

With equation (E5) the horizontal ammonia flux is calculated from the amount of ammonia captured:

$$F_{NH_3} = \frac{S_{NH_3}}{K_s \cdot A_o \cdot (t_2 - t_1)} \quad (E6)$$

with:  $F_{NH_3}$  ammonia flux [ $mg \cdot m^{-2} \cdot s^{-1}$ ]  
 $t_2 - t_1$  exposure time [s]

And the emission through a ventilation shaft can be calculated as:

$$E_{NH_3} = F_{NH_3} \cdot A_{VS} \quad (E7)$$

with:  $E_{NH_3}$  ammonia emission [ $mg \cdot s^{-1}$ ]  
 $A_{VS}$  surface area of the ventilation shaft [ $m^2$ ]



## Appendix F: AMANDA and fast sensor

The AMANDA system is a continuous flow denuders developed by ECN for ammonia measurements (Wyers *et al.*, 1993). The working principle of this instrument is illustrated in figure F1. Ambient air is pumped through an annular denuder using a sample flow of  $30 \text{ l min}^{-1}$ . The denuder is rotated around its axis at a speed of  $30 \text{ rotations min}^{-1}$ . Ammonia is collected in  $9 \text{ ml}$  of a  $3.6 \text{ mM}$   $\text{NaHSO}_4$  absorption solution, covering the walls of the annular space in the rotating denuder. The absorption solution is continuously pumped into and out of the denuder by two peristaltic pumps, in counterflow with the sampled air. The resistance of the solution film inside the denuder is measured with two Pt-electrodes and used to adjust the flow rate of absorption solution into the denuder to keep the volume of solution inside the annulus at a constant level and compensate for evaporation losses.

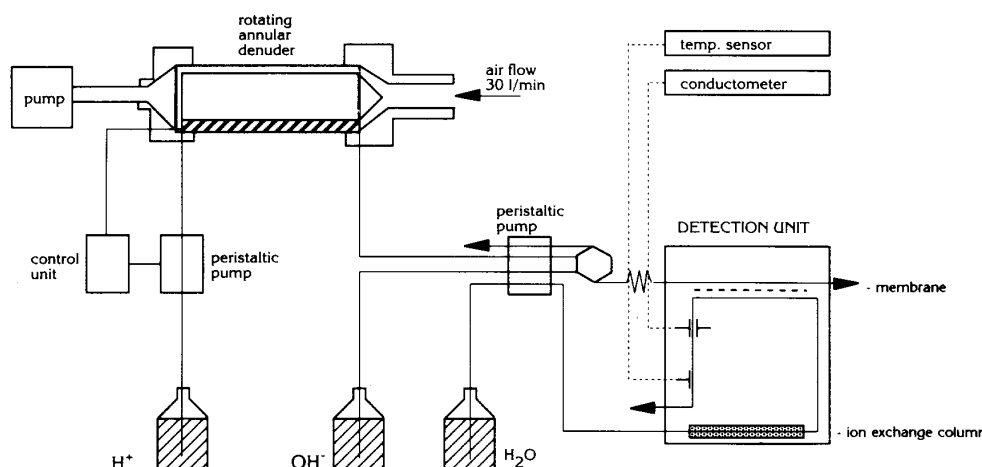


**Figure F1** Continuous flow denuder system (AMANDA) for ammonia measurements.

The solution is pumped out of the denuder at a fixed but adjustable rate of  $0.5\text{--}4 \text{ ml min}^{-1}$ . Downstream of the denuder a  $0.5 \text{ M}$   $\text{NaOH}$  solution containing  $60 \text{ ppb}$   $\text{NH}_4^+$ , is merged with the absorption solution in a mixing chamber/debubbler at a rate of  $0.08 \text{ ml min}^{-1}$ , causing a shift of the  $\text{NH}_4^+/\text{NH}_3$  equilibrium towards  $\text{NH}_3$ , which is separated from the solution by diffusion through a semi-permeable membrane. Approximately 30% of the ammonia permeates the membrane and is dissolved in a stream of double-demineralised water ( $0.08 \text{ ml min}^{-1}$ ), from which all traces of (bi)carbonate have been previously removed on an ion exchange column. The ammonium concentration in the water stream is determined conductimetrically and compared with calibration standards. The temperature of the stream is measured by a thermistor and used to correct the analysis for temperature

effects. The instrument cannot be used at ambient temperatures below the freezing point, unless special precautions are taken.

The detector is calibrated with solutions containing typically 50 and 500 *ppb*  $\text{NH}_4^+$  and a blank solution. The detector response is a square-root function of the ammonium concentration in the absorption solution. Deviations from this behaviour in the low concentration range are due to a decrease in the hydronium concentration, which has a higher ion-specific conductivity than ammonium, but can be avoided by addition of a 60 *ppb* background  $\text{NH}_4^+$  concentration to the absorption solution flow. The instrument has a compact design and is fully automated. Figure F2 shows a photograph of the continuous-flow denuder as it is used for field measurements.

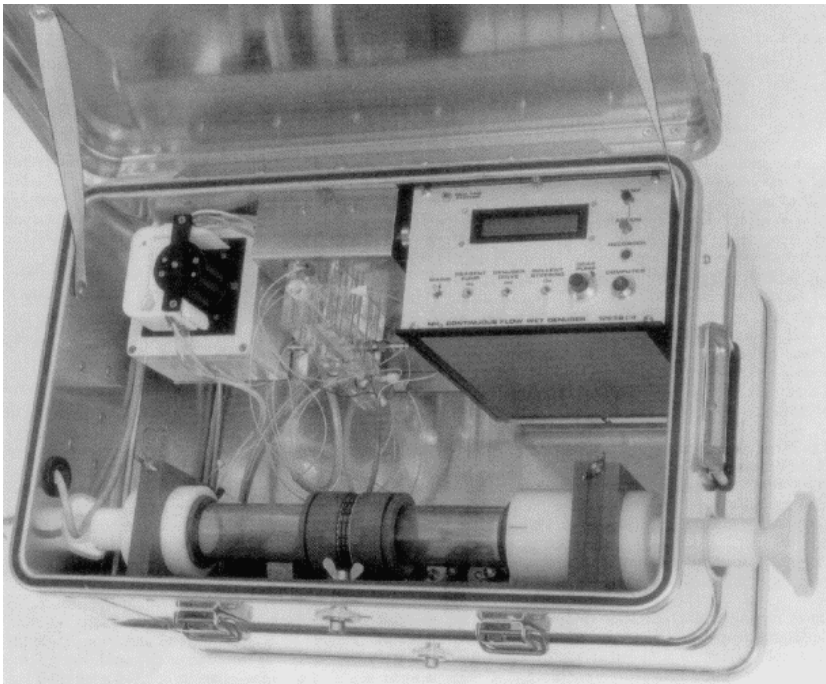


**Figure F2** Photograph showing the continuous-flow denuder. Size of the aluminium box: 60x39x32 cm.

The detection limit of the continuous-flow denuder is  $6 \text{ ng NH}_3 \text{ m}^{-3}$ , and can measure concentrations up to  $1000 \text{ } \mu\text{g m}^{-3}$ . The AMANDA provides data with a time resolution of 5 seconds. The response time of the system is approximately 1 minute.

The fast response sensor consists of a vertical denuder (20 cm) and has a response time of approximately 1 minute. The denuder and other accessories are mounted in a handcart provided with a 100 m spool.

## List of figures

<b>Figure 2.1</b> Schematic drawing of a sample arrangement (fixed PFS, cross design) for non point source measurements.	16
<b>Figure 3.1</b> Experimental station at Zegveld.	22
<b>Figure 3.2</b> Experimental set-up for ammonia concentration/flux measurements (Zegveld).	24
<b>Figure 3.3</b> Experimental set-up in Zegveld: denuders and Willems badges in the right tower.	25
<b>Figure 3.4</b> Experimental set-up in Zegveld: ammonia passive flux samplers (cross), and sample line going to the NH <sub>3</sub> to NO converter + NO <sub>x</sub> monitor system, in the right tower.	25
<b>Figure 3.5</b> Experimental set-up in Zegveld: ammonia passive flux samplers attached to the wind vane in the left tower.	26
<b>Figure 3.6</b> Experimental station at Ossekampen.	27
<b>Figure 3.7</b> Experimental set-up in Ossekampen: a) denuders (4 heights) in a large (20 m) mast configuration; b) ECN fast sensor (left) and AMANDA system (right).	28
<b>Figure 3.8</b> Experimental set-up in Ossekampen: ammonia passive flux samplers and Willems badges in a 5 m height-mast configuration.	29
<b>Figure 3.9</b> Experimental set-up in Ossekampen: ammonia passive flux samplers and Willems badges in a short-mast configuration.	29
<b>Figure 3.10</b> Overview of the measurement site in Kootwijkerbroek.	30
<b>Figure 3.11</b> Schematic representation of the sampling points (NO <sub>x</sub> monitor and PAF) for NH <sub>3</sub> concentration measurements in the ventilation shafts of a mechanically ventilated animal house (diameter: 45 cm).	31
<b>Figure 3.12</b> Naturally ventilated poultry house in Barneveld.	32
<b>Figure 3.13</b> Ammonia emission system used at the location Barneveld.	33
<b>Figure 3.14</b> Schematic representation of the measurement set-up in Barneveld.	34
<b>Figure 3.15</b> Passive flux samplers in a cross design as used in Barneveld.	34
<b>Figure 4.1</b> Meteorological parameters (wind direction, wind speed at four different levels, temperature and net radiation) over the period 30 March-6 April 2002 at the location Zegveld.	35
<b>Figure 4.2</b> Sector dependence of prevailing wind direction (a, b) and average wind speed (c, d) over the period 30 March-6 April 2002 at the location Zegveld.	36
<b>Figure 4.3</b> Diurnal variation of some meteorological parameters (wind speed and net radiation) over the period 30 March-6 April 2002 at the location Zegveld.	36
<b>Figure 4.4</b> NH <sub>3</sub> concentration profile as measured with the NO <sub>x</sub> monitor+NH <sub>3</sub> to NO converter system in Zegveld.	38
<b>Figure 4.5</b> Sector dependence of average NH <sub>3</sub> concentrations (ppm) measured with the NH <sub>3</sub> to NO converter and the NO <sub>x</sub> monitor in Zegveld, during the period 30 March- 6 April 2002.	39
<b>Figure 4.6</b> Measured concentrations in Zegveld using passive samplers (Willems badges, WB) and the converters with the NO <sub>x</sub> monitor, vs. the concentration measured with a reference method (denuders).	40

<b>Figure 4.7</b> Comparison between the concentrations calculated with the passive flux samplers (PFS) and the concentration measured with the reference method (denuders) in Zegveld.	41
<b>Figure 4.8</b> Ammonia concentrations measured in Zegveld with denuders (reference), NO <sub>x</sub> monitor, Willems badges (WB) and passive flux samplers (PFS).	42
<b>Figure 4.9</b> Horizontal ammonia flux measured with fixed passive flux samplers (cross and windvane designs), and calculated for denuders, Willems badges, and the converters-NO <sub>x</sub> monitor system.	44
<b>Figure 4.10</b> Dispersion analysis showing the relation between the horizontal ammonia flux measured with fixed passive flux samplers (PFS), Willems badges (WB), converters-NO <sub>x</sub> monitor, and denuders, at the location Zegveld.	44
<b>Figure 4.11</b> Ammonia emission pattern in Zegveld calculated using the system with converters and the NO <sub>x</sub> monitor. Also included in the figure the wind direction pattern during the first three days after the manure spreading event.	45
<b>Figure 4.12</b> Accumulated NH <sub>3</sub> emission at the site Zegveld, during the period 3-april-2002 to 6-april-2002, using a system with converters and the NO <sub>x</sub> monitor.	46
<b>Figure 4.13</b> Ammonia emission (vertical flux) after manure application into the field using integrating techniques (denuders, Willems badges, passive flux samplers) and a system with converters and a NO <sub>x</sub> monitor.	46
<b>Figure 4.14</b> Accumulated ammonia emission (vertical flux) after manure application into the field using integrating techniques (denuders, Willems badges (WB), passive flux samplers (PFS)) and a system with converters and a NO <sub>x</sub> monitor.	47
<b>Figure 4.15</b> Meteorological parameters (wind direction, wind speed, temperature and net radiation) measured at Wageningen over the period 5-9 september 2002.	48
<b>Figure 4.16</b> Sector dependence of wind direction and wind speed over the period 5-9 september 2002 at the location Wageningen.	48
<b>Figure 4.17</b> Diurnal variation of wind speed, temperature and net radiation averaged over the period 5-8 september 2002 at the location Wageningen.	49
<b>Figure 4.18</b> Measured concentrations in Wageningen using passive samplers (Willems badges, WB; passive ammonia flux samplers, PFS) vs. the concentration measured with the denuders.	50
<b>Figure 4.19</b> Ratio of the pressure drop through the orifice against the angle of impact and the pressure drop at $\alpha=0^\circ$ . Different wind speeds are considered. A theoretical cosine curve is also shown.	51
<b>Figure 4.20</b> Ratio of the pressure drop through the orifice against the angle of impact and the pressure drop at $\alpha=0^\circ$ , for the straight sampler with spheres. Different wind speeds are considered. A theoretical cosine curve is also shown.	51
<b>Figure 4.21</b> Ammonia concentration measurements using the AMANDA system in Wageningen.	52
<b>Figure 4.22</b> Calibration curve (in the field) for the fast response sensor (FRS) using the AMANDA data as reference (Wageningen).	53
<b>Figure 4.23</b> Ammonia concentrations measured with the AMANDA, and corrected values of the concentrations measured with the fast response sensor, during the application of manure in Wageningen.	53
<b>Figure 4.24</b> Average ammonia plumes measured with the Willems badges in Wageningen, during the period 5-7 september 2002.	54

<b>Figure 4.25</b> Two examples of plumes measured with the fast response sensor in Wageningen.	55
<b>Figure 4.26</b> Source distribution used in the Gaussian plume model (Wageningen).	56
<b>Figure 4.27</b> Ammonia concentration versus time as measured with the denuders and the AMANDA in Wageningen.	57
<b>Figure 4.28</b> Regression analysis showing the relation between the horizontal ammonia flux measured with fixed passive flux samplers (PFS), Willems badges (WB), and denuders, in Wageningen.	58
<b>Figure 4.29</b> Regression analysis showing the relation between the horizontal ammonia flux measured with fixed passive flux samplers (PFS), Willems badges (WB), and denuders for the data available both from Zegveld and Wageningen.	58
<b>Figure 4.30</b> Procedure used to calculate the ammonia emission from the field in Wageningen.	59
<b>Figure 4.31</b> Ammonia concentration profile calculated for the denuders for one of the measurement periods (Wageningen).	59
<b>Figure 4.32</b> Ammonia emission from the field as a function of time, using data from denuders, Willems badges, and passive flux samplers in Wageningen.	60
<b>Figure 4.33</b> Accumulated ammonia emission (vertical flux) after manure application into the field using denuders, Willems badges and passive flux samplers.	61
<b>Figure 4.34</b> Accumulated ammonia emission after manure application into the field using the AMANDA system (Wageningen).	61
<b>Figure 5.1</b> Ammonia emission pattern ( $\text{g}\cdot\text{h}^{-1}$ ) as measured with passive flux samplers (PFS) beneath the ventilation shaft, and calculated with a reference method.	63
<b>Figure 5.2</b> Correlation between the $\text{NH}_3$ emission ( $\text{g}\cdot\text{h}^{-1}$ ) measured with passive flux samplers (PFS) beneath the ventilation shaft, and calculated with the reference method.	64
<b>Figure 5.3</b> Comparison between the reference method and the PFS for the two different ventilators present in the animal house.	65
<b>Figure 5.4</b> Comparison between reference method and the new concept for measuring ammonia emissions ( $\text{g}\cdot\text{h}^{-1}$ ) from mechanically ventilated buildings.	66
<b>Figure 5.5</b> Comparison of wind direction measurements at Barneveld and Wageningen.	67
<b>Figure 5.6</b> Horizontal ammonia flux measured in Barneveld with the passive flux samplers in a cross design.	68
<b>Figure 5.7</b> Schematic representation of the method used to calculate the ammonia emission in Barneveld.	70
<b>Figure B1</b> Principle of the denuder technique.	91
<b>Figure C1</b> Schematic representation of the Willems badges.	93
<b>Figure E1</b> Schematic drawing of flux sampler proposed by Ferm (1986).	100
<b>Figure E2</b> Schematic drawing of the improved sampler.	101
<b>Figure E3</b> Picture of the wind tunnel used in the measurements.	103
<b>Figure E4</b> Relation between the outside local air velocity ( $\text{m s}^{-1}$ ) and the square root of the pressure drop over the orifice in the sampler ( $\sqrt{\text{Pa}}$ ).	103
<b>Figure E5</b> Relation between the air velocity through the orifice ( $\text{m s}^{-1}$ ) and the square root of the pressure drop over the orifice in the sampler ( $\sqrt{\text{Pa}}$ ).	104

<b>Figure E6</b> Relation between the outside local air velocity ( $\text{m s}^{-1}$ ) and the velocity through the sampler ( $\text{m s}^{-1}$ ).	104
<b>Figure F1</b> Continuous flow denuder system (AMANDA) for ammonia measurements.	107
<b>Figure F2</b> Photograph showing the continuous-flow denuder. Size of the aluminium box: 60x39x32 cm.	108

## List of tables

<b>Table 1.1</b> NH <sub>3</sub> emissions from animal husbandry in the Netherlands in the year 2000, expressed in % (Sliggers, 2001).	8
<b>Table 3.1</b> Slurry analyses (Zegveld).	23
<b>Table 3.2</b> Application rates of cattle slurry to grassland (Zegveld).	23
<b>Table 3.3</b> Slurry analyses and application rates (Ossekampen).	27
<b>Table 4.1</b> Statistics of ammonia concentrations and some meteorological parameters measured at Zegveld during the period 30 March – 6 April 2002.	37
<b>Table 4.2</b> Statistics of some meteorological parameters measured at Wageningen during the period 5-8 September 2002.	49
<b>Table 5.1</b> Statistical t-test (95% significance level) of the difference between the passive samplers and the reference system for each housing system.	64
<b>Table 5.2</b> Statistical t-test (95% significance level) of the difference between the passive samplers and the reference system for the ventilation shafts with and without lid.	65
<b>Table 5.3</b> Statistical t-test (95% significance level) of the difference between the passive samplers and the reference system combining all measurements.	66
<b>Table 5.4</b> Statistical summary of the wind direction in Barneveld.	70
<b>Table 5.5</b> Measured versus applied ammonia in the experiment in Barneveld.	70
<b>Table C1</b> Re values for situations with different wind speeds (Hofschreuder <i>et al.</i> (1999)).	95